Tu-Pos219

SPERMIDINE RELEASE FROM XENOPUS OOCYTES: ELECTRODIFFUSION THROUGH A MEMBRANE CHANNEL. ((Sha, Q., Lopatin, A.N. and C.G. Nichols)) Department of Cell Biology and Physiology, Washington University School of Medicine, St. Louis, MO 63110

The release of ^{3}H-spermidine from *Xenopus* oocytes was examined under different ionic conditions, and under voltage-clamp. In normal solution (2 mM [K^+]), the efflux rate is less than 1% per hour, and is stimulated ~ 2-fold by inclusion of Ca^{2+} (1 mM) in the incubation medium. Spermidine efflux is stimulated ~10-fold in high [K^+] (100 mM K^+) solution. In high [K^+] solution, efflux is strongly inhibited by divalent cations (K_i for Ba^{2+} block of spermidine efflux is ~ 0.1 mM), but not by tetraethylammonium ions or verapamil. Spermidine efflux rates were not different between control oocytes and those expressing HRK1 or IRK1 inward rectifier K^+ (Kir) channels. When the membrane potential was clamped, either by changing external [K^+] in oocytes expressing HRK1, or by 2-microelectrode voltage-clamp, spermidine efflux was shown to be strongly dependent on voltage, as expected for a simple electrodiffusive process, where spermidine^{3+} is the effluxing species. This result argues against spermidine diffusing out as an uncharged species, or in exchange for similarly charged counterions, and is consistent with efflux occurring through a membrane channel. These results are the first conclusive demonstration of a simple electrodiffusive pathway for spermidine efflux from cells.

Tu-Pos220

A SIMPLE BARRIER MODEL IS SUFFICIENT TO EXPLAIN 'CROSSOVER' EFFECT AND CORRECT SHIFT OF INWARD RECTIFICATION INDUCED BY MULTIVALENT POLYAMINES. ((A.N. Lopatin, E.N. Makhina and C.G. Nichols)) Department of Cell Biology and Physiology, Washington University School of Medicine, St. Louis, MO 63110

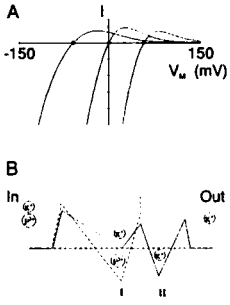

Fig. 1A. "Crossover" and shift of rectification for model in B in the presence of spermidine^{3+} at K_{OUT} = 15, 150 and 1500 mM, K_{IN} = 150 mM.

Inward rectification induced by multivalent polyamines (spermine^{4+}, spermidine^{3+}, putrescine^{2+}) is relieved by external [K^+], shifting strictly with E_K (Lopatin & Nichols, 1995, *J. Phys.* abstr.). We have sought to explain these results in terms of a single file pore containing multiple ion binding sites. It has been reported that the effects of 'crossover', and shift of rectification with E_K is not reproducible with blocking particles of valency > 1 (Hille & Schwartz, 1978, *J. Gen. Phys.* 72, 409-442). However, this is not an 'intrinsic" problem of the barrier model, and even a simple 2-site, 3-barrier scheme with a single polyamine binding site (Fig. 1) can reproduce the observed behavior if one assumes strong binding of K^+ ions in the selectivity filter, and electrostatic interaction between polyamines and K^+ ions inside the pore.

Tu-Pos221

A STOCHASTIC MODEL OF CELL-SUBSTRATE DETACHMENT VIA CENTRIFUGATION. ((C. Zhu, J.W. Piper, and R.A. Swerlick*)) School of Mechanical Engineering, Georgia Institute of Technology, Atlanta, GA, 30332; *Department of Dermatology, Emory School of Medicine, Atlanta, GA 30322

Cell-substrate adhesion and detachment are integral components of many physiological processes. A mathematical model has been developed to describe cell-substrate detachment in a commonly used centrifugation assay. The model treats the detachment of a cell as a stochastic event which is capable of occurring at any force with a certain probability. Using an exponential relationship between binding affinity and bond force, we explored different representations and determined that Bell's formulation (Bell, Science, vol. 200, p.618-627, 1978) described our data better than the formulation of Dembo et al. (Proc. R. Soc. Lond., vol. 234, p.55-83). Using this approach to determine bond formation and dissociation of the cell population, the fractions of the population adherent by any number of bonds in equilibrium were solved in closed form. The model was validated using an experimental system consisting of sialyl-Lewis X expressing colon carcinoma (Colo-205) cells adherent to a plastic surface coated with a construct of E-selectin. By comparing the model prediction with the experimentally measured percentage of adherent cells for both a range of coating densities and various levels of imposed relative centrifugal force, we can estimate the two-dimensional, no load affinity (K_a) for binding reaction between surface bound receptors and ligands as well as the ligand density on the carcinoma cells. We have also estimated the maximum bond stretch (γ) of the E-selectin - sLe^x bond. This sub-angstrom value is in agreement with a previous estimation (Alon et al., Nature, vol. 374, p.539-542, 1995). We are also able to predict the behavior of such a simplified binding system in response to changes in receptor-ligand binding characteristics such as K_a and γ. (Supported by a grant from the Whitaker Foundation and NIH training grant No. GM08433)

Tu-Pos222

A MECHANICAL ANALYSIS OF A MICROPIPET ASPIRATED RED BLOOD CELL LOADED BY A POINT FORCE. ((C. ZHU and S. CHESLA)) School of Mechanical Engineering, Georgia Institute of Technology, Atlanta, GA 30332

The micropipet technique is one of several experimental methods recently employed to measure single bond detachment forces in cellular adhesion. This method utilizes a micropipet aspirated red blood cell (RBC) as a force transducer. Using a finite difference computational method, Evans et. al. (Biophys. J., vol. 59, p838-848, April 1991) analyzed this problem and clearly showed that the technique was sensitive enough to make it attractive for measuring molecular detachment strengths. However, the issue of accuracy was not addressed. The determination of the transducer accuracy and how it depends on experimental parameters is a non-trivial problem and requires rigorous mechanical analysis concerning cell deformation under a point load. We describe an analytical approach based on a boundary layer analysis in which the singularity at the pole (where the point load is applied) is handled by rescaling the thin shell equilibrium equations to obtain an inner solution near the pole. This is then matched to an outer solution valid for the remaining cell membrane. A perturbation technique was used to decouple the governing equations of the stress field from those of the strain field, allowing the stress field to be statically determined and the deformed shape of the cell resolved. With this approach, a sensitivity evaluation of the experimental parameters important to an accurate force measurement is simplified, as well as the solution for the RBC force-deformation relationship itself. The presented solution is also compared and evaluated versus our own finite difference derived solution and shows good agreement. (Supported by NSF grant No. BCS-935037, NIH grant No. R29A138282 and NIH training grant No. GM 08433)

FOLDING AND SELF-ASSEMBLY II

Tu-Pos223

PROTEIN FOLDING AND ENZYMATIC ACTIVATION OF *PSEUDOMONAS AERUGINOSA* EXOTOXIN A. ((B.K. Beattie & A.R. Merrill)), Guelph-Waterloo Centre for Graduate Work in Chemistry, Dept. of Chem. and Biochem., Univ. of Guelph, Guelph, ON, Canada, N1G 2W1. (Spon. by Joan Boggs).

Pseudomonas aeruginosa Exotoxin A (ETA) and its C-terminal peptide that includes the catalytic domain responsible for its ADP-ribosyl-transferase (ADPRT) activity were studied by high performance size-exclusion liquid chromatography (HPLC), fluorescence spectroscopy, and circular dichroism (CD) spectroscopy. The enzymatic function of ETA can be activated *in vitro* by incubation with reducing agent (10 mM DTT) and denaturant (4 M urea) and the effect of various activation conditions (pH, urea, and DTT) on enzymatic activity was studied. Upon enzymatic activation, structural changes induced within both proteins' structures were monitored by HPLC and CD spectroscopy. These changes were correlated with concomitant alterations in the enzymatic activity of the proteins. The pH optimum of ADPRT activity for both ETA and PE40 was between 7.0 - 8.0 decreasing to nearly zero at acidic (pH 5.0) and basic (pH 11-12) values. Analysis of the pH titration data revealed the presence of two clearly separate pK, values which implicate a His residue (likely His 440 and 426) and a Tyr or Lys residue (possibly Tyr 481). The identity and possible role of an active site Lys residue is not known. Additionally, a significant increase in the Stokes' radii of both proteins was detected when the pH was lowered from 8.0 to 6.0. The enzymatic activity of PE40 was not affected by urea or DTT and its Stokes' radius decreased monotonically with increasing urea concentration. Also, the ΔG_N values for the folding of ETA (-18 kJ/mol) and PE40 (-33 kJ/mol) were determined by fluorescence methods using urea as the chemical denaturant [supported by the Medical Research Council of Canada, ARM].

Tu-Pos224

Low-Temperature Time-Resolved and Steady-State Fluorescence Spectroscopy Studies of Five Single-Tryptophan Mutants of *E. coli* Adenylate Kinase. ((T. Fulmer*[1], P. T. C. So*, M.Glaser[1], W. W. Mantulin*[1])) *Laboratory of Fluorescence Dynamics, Department of Physics, University of Illinois at Urbana-Champaign, [1]Department of Biochemistry, University of Illinois at Urbana-Champaign, Urbana, IL 61801.

The enzyme adenylate kinase (AK) from *E. coli* catalyzes the reaction ATP + AMP <==> 2ADP in the presence of magnesium. Based on the comparison of several high-resolution x-ray crystal structures, it is thought that the enzyme undergoes large domain movements upon substrate binding. Because the wild type AK is devoid of tryptophans, it is reasonable to construct a library of single-tryptophan mutants, with the tryptophans placed in various functionally and structurally important locations. These single-tryptophan mutants can then be used as probes of the protein dynamics of the wild-type enzyme and extensively characterized using a variety of fluorescence spectroscopic techniques. The present study attempts to address the dynamics of the native state of the enzyme (see accompanying poster for unfolding studies). In order to slow the rate of interconversion between the native AK's conformational states, it was necessary to do studies of the native-state dynamics at reduced temperatures. AK was placed in a solution of 80% glycerol, and changes in time-resolved fluorescence parameters were monitored over the temperature range from 25C to -70C. The lifetimes were analyzed as distributions, where the width of the distribution was assumed to be a sensitive indicator of local heterogeneity and interconversion between conformations. By this analysis, the five single-tryptophan mutants divided up into two groups, presumably depending on whether the tryptophan environment was buried and nonpolar or fully solvent-exposed. The differences could be attributed to protein substates or to substates of the glycerol. The ability of the five mutants to bind substrates was also studied in 80% glycerol using the bisubstrate analog Ap5A. It was found that the glycerol effectively closed shut the ATP binding flap, in this way preventing the Ap5A from occupying the ATP site. Control studies using steady-state methods confirmed this conclusion. [*Supported by NIH grant RR03155.]

Tu-Pos225

THERMODYNAMIC COMPARISON OF A HYDROGEN BOND AND A HYDROPHOBIC INTERACTION AT A COMMON SITE.
((P.D.Ross & M.V. Rekharsky)) NIH, Bethesda MD 20892 and NIST, Gaithersburg, MD 20899

For simple small molecule complexes we show that the values of the thermodynamic parameters depend only upon the portions of the molecule undergoing a change in its environment and are insensitive to the same ligand substitution being located external to the binding site. The 1:1 complexes of phenethlamine and hydrocinnamic acid with beta-cyclodextrin have $\Delta G^0 \cong$ -2 and -3 kcal mol^{-1}, respectively, and from 15-45°C both have ΔC_p = - 60 cal $K^{-1}mol^{-1}$ (eu). Complexes with an added hydrogen bond, indicated by red-shifted absorption and emission spectra, have ΔC_p = - 40 eu. The H-bond contribution is positive, $\Delta\Delta C_p$= 20 eu, while the contribution of an added CH_2 group is negative, $\Delta\Delta C_p$ = - 8 eu. The contribution of the hydrophobic CH_2 interaction to complex stability is about the same at all temperatures while the contribution to stability from the H-bond decreases with increasing temperature. These results would suggest that the thermal denaturation of proteins and nucleic acids occurs when the melting of hydrogen bonds sufficiently reduce the stability of the structure until the disruptive solvolytic forces overcome the constant stability non-bonded hydrophobic interactions

Tu-Pos226

LOSS OF TRYPTOPHAN FLUORESCENCE IN α-CRYSTALLIN CORRELATES WITH THE LOSS OF ITS CHAPERONIN FUNCTION((J.A. Schauerte, A. Gafni))
Inst of Gerontology, Dept of Biological Chemistry, Univ of Michigan, Ann Arbor, MI 48109

The rapid aggregation of rabbit muscle phosphoglycerate kinase during incubation at 52°C was completely inhibited in presence of 1/3 moles α-crystallin monomer per mole enzyme. When α-crystallin was irradiated with 290nm UV light, the tryptophan fluorescence intensity declined reflecting the destruction of these residues. A correlation is shown between the reduction in α-crystallin fluorescence during UV-irradiation, and the loss of its ability to protect phosphoglycerate kinase against heat induced aggregation. The biexponential kinetics of tryptophan fluorescence loss suggests the non-equivalent susceptibility of the two tryptophans of α-crystallin (Trp-9 and Trp-60) to photooxidation. Previous reports indicate that the less solvent-exposed residue, Trp-9, is more susceptible to photooxidation. The loss of chaperonin function correlates more closely with the destruction of the more photolabile tryptophan residue, suggesting that Trp-9 may play a significant role in the chaperonin activity of α-crystallin. Since a loss of tryptophan fluorescence in intact eye lenses in vivo has been demonstrated to occur upon exposure to UV light, as well as during aging, it is proposed that the enhanced rate of lens opacification and cataract formation, as well as the increased levels of damaged lens proteins, which accumulate under these conditions, are the result of the gradual loss of the chaperone-protein efficacy of α-crystallin.[NIA grant #AG09761]

Tu-Pos227

TEMPERATURE DEPENDENCE OF IONIZATION REACTIONS OF PROTEINS.
((R. Wang, J. Dwyer, F. Huang* and B. García-Moreno E.)) Dept. of Biophysics, Johns Hopkins Univ., Baltimore, MD 21218 and *Dept. of Biochemistry, Univ. of Maryland, School of Medicine, Baltimore, MD 21201

Temperature effects on electrostatic interactions in proteins have never been investigated systematically by either experimental or computational approaches. At present our efforts to characterize the temperature dependence of ionization reactions of proteins are focused on: 1) measurement of proton titration curves of sperm whale myoglobin and staphyloccocal nuclease as a function of temperature by the means of potentiometric titration, and 2) development of computational algorithms for structure-based prediction of temperature effects on titration behavior of proteins.

To compute the effects of temperature on the ionization behavior of proteins it was necessary to consider explicitly the effects of temperature on the intrinsic (i.e. model system) pKa values of ionizable side chains, on the dielectrics of the system, and on the Debye-Hückel parameter. Excellent agreement was found between predicted and experimental proton titration behavior over the temperature range of 5 to 45°C. The temperature dependence of ionization was found to be determined primarily by the intrinsic enthalpy of ionization of the charged side chains and the dielectric of the solvent. The stabilizing free energy of interaction between oppositely charged side chains increases with increasing temperature. The implications for the mechanism of stabilization of thermophilic proteins will be discussed.

Tu-Pos228

VERIFICATION AND REFINEMENT OF HOMOLOGY BASED MODEL OF THE C-TERMINAL DOMAIN OF COLICIN E1 BY SITE-DIRECTED SPIN LABELING.
Łukasz Salwiński and Wayne L. Hubbell, Jules Stein Eye Institute and Department of Chemistry and Biochemistry, UCLA, Los Angeles, CA (Spon. C. Altenbach)

In order to test the accuracy of a homology-based model of the C-terminal domain of colicin E1 a series of double cysteine mutants was prepared and reacted with a sulfhydryl selective nitroxide spin label. Dipolar broadening of the EPR spectra of the 354/489, 491/411, 493/521, 494/521 and 410/456 double labeled proteins indicate that the nitroxides in each of the pairs are localized within 5 to 15 Å. This shows that the loop between helices 8 and 9 is surrounded, as expected from the model, by the helices 1, 5 and C-terminal end of helix 10.

Figure 1

On the other hand the 505/382, 505/383, 505/384 and 509/382 double mutants show no significant interaction between the spin labels, contrary to predictions based on the model.

The results, together with previously presented data on the secondary structure and exposure of the 492-510 region (*Bioph. J.* **68**:A369,1995), have been used to refine the structural model.

Tu-Pos229

CHARACTERIZATION OF A DIMERIC EQUILIBRIUM UNFOLDING INTERMEDIATE AND KINETIC ANALYSIS OF COLICIN E1 DENATURATION.
((B. A. Steer, A.A. Di Nardo & A.R. Merrill)), Guelph-Waterloo Centre for Graduate Work in Chemistry, Dept. of Chem. and Biochem., Univ. of Guelph, Guelph, ON, Canada, N1G 2W1.

The colicin E1 channel peptide is monomeric and has a compact and predominantly α-helical solution structure. The partially unfolded intermediate, first described by Steer and Merrill (1995) *Biochemistry, 34*, 7225-7233, which exists in approximately 4 M guanidine hydrochloride was shown to comprise the hydrophobic C-terminal core of the peptide. This intermediate has been further characterized by size-exclusion high performance liquid chromatography and sodium dodecyl sulfate polyacrylamide gel electrophoresis. Characterisation of the intermediate using these techniques revealed that the partially unfolded structure is a dimer which results from strong hydrophobic peptide-peptide interactions involving the C-terminal hydrophobic cores of two partially denatured monomeric peptides. The kinetics of colicin E1 channel peptide denaturation were investigated using stopped-flow fluorescence spectroscopy. Denaturation of the native peptide and formation of the partially unfolded intermediate dimer structure obeyed a single exponential time-course and was relatively fast ($t_{1/2}$ = 0.22 s). Denaturation of the intermediate dimer to monomeric unfolded peptides was much slower and followed double exponential kinetics ($t_{1/2}(1)$ = 5.8 s and $t_{1/2}(2)$ = 50 s). These equilibrium and kinetic unfolding data describe an unique unfolding mechanism and are consistent with the idea that the colicin E1 hydrophobic α-helical hairpin domain inserts into the membrane bilayer as two tightly associated hydrophobic antiparallel helices [supported by the Natural Sciences and Engineering Research Council of Canada (A.R.M.)].

Tu-Pos230

Fluorescence and Circular Dichroism Studies of the Native States and Equilibrium Unfolding Properties of Five Single-Tryptophan Mutants of *E. coli* Adenylate Kinase.
((T. Fulmer*†, M. Glaser†, W. W. Mantulin*†)) †Department of Biochemistry, University of Illinois, Urbana, IL; *†Laboratory of Fluorescence Dynamics, Department of Physics, University of Illinois at Urbana-Champaign, Urbana, IL. 61801

The enzyme adenylate kinase (AK) from *E. coli* (MW 23.5 kD) is a monomeric protein that has been cloned, overexpressed, and purified to homogeneity. It is thought to be a highly flexible protein with significant domain movements upon substrate binding. The wild type AK is devoid of tryptophan, providing the opportunity to construct single-tryptophan mutants of the enzyme which can then be characterized using fluorescence spectroscopy. In the present study, the native states, as well as the equilibrium unfolding properties, of five single-tryptophan mutants of *E. coli* adenylate kinase were studied using steady-state and time-resolved fluorescence and circular dichroism spectroscopies. Since the single-tryptophan mutations were found to leave the wild-type enzyme's function and global structure largely unperturbed, it was reasoned that the single tryptophan residues could be used as reporter groups of the various local microenvironments of the wild-type enzyme. In this way, using circular dichroism to follow changes in the protein's global secondary structure as well as fluorescence spectroscopies to monitor both local and global changes in the protein's tertiary structure, the five mutants were chemically denatured using guanadine hydrochloride. The process of thermal denaturation was also studied. A set of equilibrium unfolding curves was thus generated for each mutant. A comparison of the unfolding curves found for each mutant showed interesting differences depending on which fluorescence variable was monitored as a function of the equilibrium unfolding axis. The curves for each mutant could be rationalized based on the known location of the single-tryptophan residue, as deduced from the available high-resolution x-ray crystal structures. Furthermore, comparison of equilibrium unfolding curve sets between mutants showed interesting differences. For example, the buried tryptophan reporter (Phe86Trp) contrasted with the the surface tryptophan reporter (Ser41Trp). We are currently examining the kinetics of these folding reactions. [*Supported by NIH grant RR03155.]

Tu-Pos231

ON THE NATURE OF THE PARTIALLY UNFOLDED STATE OF YEAST ISO-2-CYTOCHROME *C* PROTEINS. ((Alice R. Ritter*, Ying Shi+, Alice Fisher+, James A. Ferretti* and Hiroshi Taniuchi+)) *Laboratory of Biophysical Chemistry, NHLBI, and +Laboratory of Chemical Biology, NIDDK, NIH, Bethesda, MD 20892.

We have examined the structural behavior and the nature of the reversible order-disorder transition of wild-type and mutant yeast iso-2-cytochrome *c* proteins as a function of temperature using Nuclear Magnetic Resonance (NMR), circular dichroism (CD) and ultraviolet/visible (UV/Vis) spectroscopy over the temperature range 275-353K. To accomplish these studies we have cloned and expressed the wild-type protein and the mutants M64L, M98L and M64L/M98L in order to study the effects of selective replacement of amino acids. CD spectra of the four proteins reveal a highly cooperative transition resulting in a loss of secondary structure with increasing temperature. The midpoint of the transition is at approximately 328K for all four proteins. However, examination of the ^{1}H NMR spectra shows a linear change in chemical shift over this temperature range for many resonances, implying a non-cooperative unfolding of the tertiary structure. UV/Vis data at 695 nm imply a gradual lengthening of the M80 S-Fe bond.

Tu-Pos232

SPECTRIN DOMAIN STABILITY AS MEASURED SOLVENT DENATURATION: IMPLICATIONS FOR MINIMUM DOMAIN LIMITS((T. Mitchell, N. Menhart, M. Meerson, N. Topouzian, and L. W.-M. Fung)) Department of Chemistry, Loyola University of Chicago, Chicago, IL, 60626

As a major component of the highly elastic and deformable erythrocyte membrane skeleton, spectrin is thought to be responsible for the typical biconcave shape of the red blood cell. Spectrin is composed of two polypeptides that associate to form an ab dimer, which may then associate to form an $(ab)_2$ tetramer, and higher oligomers. Sequence homology has identified a number of approximately 106 amino acid repeats in both the a and b polypetides. These individual sequence repeats have been proposed to form stable, independent structural domains, consisting of a triple helical structure. We have expressed several spectrin fragments including those representative of the first repeat, first two repeats, and the first three repeats. Each of these repeats contain two highly conserved tryptophan residues, which may be used in fluorescence measurements to probe the structures of these fragment peptides. Using this intrinsic fluorescence, changes produced by chemical denaturants (urea or guanidine hydrochloride) can be monitored, and the relative stability of these peptides against these denaturants may be determined. Since spectrin is known to change its conformation in an ionic strength dependent manner, we measured the fluorescence changes under both low and high ionic strength conditions. From these studies, we found that the peptide consisting of a single repeat is not as stable as the multiple repeat peptides. The multiple repeat peptides were nearly as stable as spectrin itself. Thus, the repetitive sequence motifs may not be independent structural domains, but rather interactive stabilizing subunits.

In our kinetic studies, we found that unusually long equilibration times were needed for the multiple repeat peptides, in contrast to the single repeat peptide, which equilibrated in less than 1 min. Rate constants for the urea mediated denaturation were on the order of 200 min^{-1}, and these rate constants were ionic strength dependent. These data suggest that there are cooperative interactions between the repeats. (Supported by Loyola University of Chicago and NSF.)

Tu-Pos233

DOMAIN STRUCTURE OF SPECTRIN FRAGMENTS AS PROBED BY PROTEOLYSIS AND SECONDARY STRUCTURE ANALYSIS ((Denise Lusitani, Nick Menhart, and L.W.-M. Fung)) Department of Chemistry, Loyola University of Chicago, Chicago, IL, 60626.

The human erythrocyte skeletal protein spectrin is composed of a number of approximately 106 amino acid repeats. These repeats have been proposed to fold into independent triple a-helical structural domains. We have cloned fragments of a-spectrin containing the individual repeats (α1, α2, and α3) as well as larger fragments containing two such repeats (α12, α23) and three repeats (α123). In order to assess how well these fragments can fold into structural domains, we examined them for resistance to proteolysis and secondary structure, and compared these results to intact spectrin. Proteolytic studies showed that certain fragments were more resistant to proteolysis than other fragments of the same size. This indicates that fragments with specific sequences fold into a compact structure. The larger peptides (α12, α23, α123) could be proteolysed into smaller fragments of a molecular weight corresponding to single repeats, which were resistant to further proteolysis. The secondary structure analysis was determined by circular dichroism (CD) and fourier transform infrared (FTIR) spectroscopy. Secondary structural element contents of these peptides were obtained and compared with intact spectrin to obtain folding information on these peptides. (Supported by Loyola University of Chicago and NSF.)

Tu-Pos234

DISTANCES ON CLONED, REPEATING UNITS OF SPECTRIN MEASURED BY FLUORESCENCE ENERGY TRANSFER. ((A. H. Khan and R. I. MacDonald)) Dept. BMBCB, Northwestern University, Evanston, IL 60208.

Peptides consisting of one or two repeating units of chicken brain α-spectrin were labeled with pairs of fluorophores suitable for measuring distances between them by energy transfer. 1,5-IAEDANS inserted on a naturally occuring, single cysteine served as the donor and carboxyfluorescein was inserted as the acceptor under conditions favoring labeling of the N-terminal amino acid. Site specific labeling was indicated by the significantly longer R of the 2-unit peptide than of a single-unit peptide identical to one of the single units of the 2-unit peptide. R values calculated from steady state energy transfer for the 2-unit peptide in 10mM $NaPO_4$, pH 7, indicated end-to-end, not side-to-side, alignment of the two units. R values of the 2-unit peptide increased in the presence of 5M urea but exhibited little change when the salt concentration and temperature were raised to the physiological range. Scans of the tryptophan fluorescence of labeled peptides and urea denaturation curves obtained for labeled peptides indicated that these peptides remained folded in a manner similar to unlabeled peptides. Supported by NIH 1PO1 HL45168.

Tu-Pos235

DETERMINISTIC PRESSURE DISSOCIATION AND UNFOLDING OF TRIOSE PHOSPHATE ISOMERASE: PERSISTENT HETEROGENEITY OF A PROTEIN DIMER. ((A.W.M. Rietveld and S.T. Ferreira)) Dept. of Biochemistry, ICB/CCS, Federal University of Rio de Janeiro, Rio de Janeiro, RJ 21944-590, Brazil

Subunit dissociation and unfolding of rabbit muscle triose phosphate isomerase (TIM) induced by hydrostatic pressure (1 bar to 3.5 kbar) were investigated by fluorescence spectroscopy. Unfolding produced a 27 nm red-shift of the intrinsic fluorescence emission, a decrease in fluorescence anisotropy from 0.14 to about 0.03, and a 1.5-fold increase in quantum yield. Fluorescence resonance energy transfer measurements with TIM that was separately labeled with 5-((((2-iodoacetyl)amino) ethyl)amino)naphthalene-1-sulfonic acid or fluorescein-5-isothiocyanate indicated that subunit dissociation and unfolding took place concomitantly. Contrary to the expected for a process involving subunit dissociation, pressure effects on TIM were not dependent on protein concentration. Experiments involving a series of pressure jumps demonstrated the existence of persistent heterogeneity in pressure sensitivity in the population of TIM dimers. This kind of deterministic behavior is similar to that exhibited by higher order protein aggregates, and suggests that not all individual dimers are energetically identical in solution. The heterogeneity of native TIM revealed by sensitivity to pressure could not be detected by traditional means of protein separation, such as polyacrylamide gel electrophoresis and size exclusion gel chromatography, suggesting that the energetic heterogeneity originates from conformational heterogeneity of the protein.
Supported by: FINEP, FAPERJ, CNPq and CAPES (Brazil) and The Pew Charitable Trusts (USA)

Tu-Pos236

DETECTION OF A STABLE INTERMEDIATE IN THE UREA-INDUCED UNFOLDING OF OVINE PLACENTAL LACTOGEN. ((G.D. Cymes, C. Grosman*, J.M. Delfino and C. Wolfenstein-Todel)) Instituto de Química y Fisicoquímica Biológicas (UBA-CONICET), and *Depto de Química Analítica y Fisicoquímica. Facultad de Farmacia y Bioquímica, UBA. Junín 956, (1113) Buenos Aires, Argentina. (Spon. by B.A. Kotsias)

The urea-induced equilibrium unfolding of ovine placental lactogen, purified from ovine placenta, was followed by ultraviolet absorption spectroscopy, intrinsic tryptophan fluorescence, far-ultraviolet circular dichroism, and size-exclusion chromatography. The normalized denaturation transition curves obtained from the above methods were not coincident, thus suggesting the existence of, at least, one partially-folded form. Denaturation resulted in an initial disruption of the tertiary structure, whereas the degree of compactness diminished and the secondary structure was disrupted at higher concentrations of the denaturant. Furthermore, satisfactory fits of the curves obtained from far-UV circular dichroism and size-exclusion chromatography required a model which involves a stable intermediate in addition to the native and unfolded forms. This intermediate state was characterized as compact, largely α-helical, and lacking the native-like tertiary packing around its tryptophan residues, and was the predominant species in solution near 4M urea. These results suggest that this stable intermediate resembles a molten globule, and is similar to those observed to occur during the denaturation of other related proteins also belonging to the growth hormone family.

Tu-Pos237

THERMAL UNFOLDING OF *E. COLI* DODECAMERIC GLUTAMINE SYNTHETASE IN 3M UREA. ((N.J. Nosworthy and A. Ginsburg)) NHLBI, NIH, Bethesda, MD 20892. (Spon. by A. Shrake)

The thermal unfolding of glutamine synthetase (GS; 622,000 Mr) at pH 7 in 3M urea has been investigated. The presence of 3M urea inhibits aggregation reactions during unfolding of GS. Thermally induced reactions have been monitored by differential scanning calorimetry, spectral measurements for Trp exposure, circular dichroism at 222nm for loss in secondary structure, and light scattering for dissociation and/or aggregation. Addition of GS to 3M urea, 20mM Hepes, 0.1mM $MnCl_2$ pH 7 results in the formation of an unstable dodecamer which slowly dissociates to unfolded monomer. Gel filtration profiles of the reaction at 0 to 48hrs at ~25°C show two detectable species: folded GS dodecamer and unfolded monomer. The time course of the CD change is sigmoidal which indicates that kinetic intermediates exist. Heating the unstable dodecamer increases the rate of monomer formation. Thermal progress curves are coincident which confirm the existence of only two detectable species. For complete dissociation and unfolding of GS in the absence and presence of 3M urea, ΔH=14±4 cal/g and $\Delta H \cong 3.5$ cal/g respectively. The lower ΔH value in the presence of urea can be attributed to exothermic binding of urea to unfolded monomer (~10 cal/g). A 10-fold dilution of the unfolded monomer formed at 65°C gave ~ 50% recovery of enzymatic activity at 20°C.

Tu-Pos238

REVERSIBLE THERMAL UNFOLDING OF RIBONUCLEASE T1 ENTRAPPED IN AOT REVERSE MICELLES. ((M. C. R. Shastry and Maurice R. Eftink)) Department of Chemistry, University of Mississippi, University, MS 38677

Ribonuclease T1 has been entrapped in the water pools of AOT (a negatively charged detergent) reverse micelles. CD (far and aromatic) and fluorescence studies strongly suggest that the entrapped protein retains a similar tertiary structure to that in solution. Proteins that are entrapped in reverse micelles usually undergo irreversible thermal unfolding. However, we have found conditions under which entrapped ribonuclease T1 shows reversible thermal unfolding. Using a pH of 7 (where the protein is also negatively charged) and using reverse micelles having a Wo (ratio of water molecules to AOT) of 5-12, we find a reversible transition for this protein with a T_m of ≈50 °C and an apparent ΔH°_{vH} of ≈ 90 kcal/mole (transitions monitored by changes in the protein's fluorescence). Furthermore, we find these T_m and ΔH°_{vH} values to be dependent on the thermal scan rate (both values being larger for faster scan rates), with the greatest dependence at Wo ≈ 9. These results suggest that the confinement of the protein reduces its unfolding relaxation time. This research was sponsored by NSF grant MCB 9407167.

Tu-Pos239

EFFECT OF TRYPTOPHAN ANALOGS ON THE STABILITY OF *STAPHYLOCOCCAL* NUCLEASE, ITS V66W MUTANT AND ITS Δ^{136} FRAGMENT. ((C. Y. Wong)) Department of Biology, Johns Hopkins University, Baltimore, MD 21218 and ((Maurice R. Eftink)) Department of Chemistry, University of Mississippi, University, MS 38677

5-Hydroxytryptophan (5HW) and 7-azatryptophan (7AW) have recently been used by several groups for biosynthetic incorporation into proteins as spectrally enhanced fluorescence probes. We have tested whether these tryptophan analogs perturb the stability of a protein by studies with WT nuclease A, its V66W mutant (having two tryptophan sites at positions 140 and 66), and the Δ^{136} fragment (still having the 66 site). We will present steady-state and time-resolved fluorescence and CD data for these proteins. Also we will present thermodynamic data (thermal and guanidine-HCl equilibrium unfolding) showing that 5HW has minimal effect on the stability of the three protein forms (including the retention of a non-two-state behavior for V66W), whereas 7AW has a destabilizing effect, particularly on the fragment. Spectroscopic and stability data will also be presented for these proteins containing 4-, 5-, and 6-fluorotryptophan. This research was supported by NSF grant MCB 9407167.

Tu-Pos240

GLOBAL ANALYSIS OF DATA FOR THE UREA AND pH INDUCED UNFOLDING OF *STAPHYLOCOCCAL* NUCLEASE A, ITS V66W MUTANT, AND ITS Δ^{136} FRAGMENT. ((R. Ionescu and Maurice R. Eftink)) Department of Chemistry, University of Mississippi, University, MS 38677.

We have performed a multi-dimensional study of the unfolding of nuclease, as induced by urea and acidic pH. We have tested whether a global analysis of the multiple data sets enables a more accurate recovery of thermodynamic fitting parameters. The basic model used to describe the transitions is that of Barrick and Balwin (*Biochemistry* **32**, 3790), which includes the pK_a for n groups that become protonated in the unfolded state, the ΔG°_{un} for unfolding at the reference condition, and a denaturant index, m. For WT nuclease a two-state process seems to describe either the pH or urea data sets. Linked analysis of both types of data sets provides a less adequate fit, however, which leads us to reconsider the assumptions of the model (i.e., is m actually independent of pH, do the pK_as vary with urea concentration, is the process two-state?). For both V66W and the fragment, the unfolding is more complex, with evidence for an unfolding intermediate. This research was supported by NSF grant MCB 9407167.

Tu-Pos241

ENERGETICS OF PROTON BINDING TO HISTIDINES IN THE FOLDED AND UNFOLDED STATES OF STAPHYLOCOCCAL NUCLEASE. ((J. Dwyer, C. Fitch and B. García-Moreno E.)) Institute for Biophysical Research on Macromolecular Assemblies and Department of Biophysics, Johns Hopkins University, Baltimore, MD, 21218.

We have measured the individual contribution of histidine residues to the stability of staphylococcal nuclease by comparing the energetics of proton binding to the four histidines (H8, H46, H121, H124) in the folded and unfolded states of the protein. pKa values were measured in the native state by ^{1}H-NMR, and in the denatured state from the difference between potentiometric proton titration curves of wild type and His → Ala mutants measured in the presence of 6M GuHCl. The pKa values of the four histidines in 6M GuHCl were nearly identical suggesting that the unfolded state is similar for all of these mutants. The pKa values measured in denaturing conditions are higher than the values in the folded state. This may be partly attributable to the 6M Cl^- in solutions containing denaturants. The titration curves of the His → Ala mutants were also measured in the native state to explore the linkage between the histidine and the conformation of the protein. Apparent pKa values were obtained from difference titration curves of native wild type and native mutant proteins. These pKa values were compared with those obtained by NMR and for some residues significant differences were observed. This suggests important conformational linkage between these residues and the protein.

Tu-Pos242

COLD DENATURATION OF LIVER ALCOHOL DEHYDROGENASE UNDER HIGH HYDROSTATIC PRESSURE. ((D. Foguel, F.M. Pereira and Silva, J.L.)).Depart. of Biochemistry, Federal University of Rio de Janeiro, 21941-590, Rio de Janeiro, Brazil. (Spon. by CNPq, FAPERJ, CAPES, FINEP and EEC)

Liver Alcohol Dehydrogenase (LADH) is a dimeric protein involved in the metabolism of alcohol in mammals. The position of one of its two tryptophan residues makes this protein suitable for fluorescence spectroscopy studies since it lies in the interface of the dimer. Upon dissociation, this residue becomes exposed to the solvent resulting in a red shift of its fluorescence emission. Hydrostatic pressure has been used as a tool to dissociate dimers, trimers, tetramers as well as large oligomers such as virus particles. Another advantage of this tool is that pressure decreases the water freezing point of water to subzero temperatures allowing experiments to be performed in a temperature range where the cold denaturation phenomenon of proteins takes place. Here we investigated the cold denaturation of LADH under pressure. The application of high pressure at room temperature is not effective in promoting dissociation of the enzyme. On the other hand, the decrease in temperature down to -10 $^\circ$ C was able to produce reversible spectroscopic alterations in the tryptophan emission spectra that ressemble those promoted by urea. However, the protein that is submitted to high pressure and low temperature is completely inactive when assayed by the reduction of NAD in the presence of ethanol. The complete inactivation of LADH by pressure and low temperature treatments probably due to the loss of its catalitic zinc atom that could take place upon protein denaturation. The thermodynamic parameters pointed out that the folded dimeric state of LADH is stabilized by entropy.

Tu-Pos243

Secondary Structure and Thermal Stability of Recombinant Human Factor XIII in Aqueous Solution. [(A. Dong, L. Kreilguård, B. Kendrick, J. Matsuura, M.C. Manning, and J.F. Carpenter)] Department of Chemistry and Biochemistry, University of Northern Colorado, Greeley, CO 80639 and Department of Pharmaceutical Sciences, School of Pharmacy, University of Colorado Health Sciences Center, Denver, CO 80262

The secondary structure and thermal stability of the recombinant human factor XIII in aqueous solutions have been investigated by Fourier transform infrared and circular dichroism spectroscopy and differential scanning calorimetry. The infrared amide I spectrum of the protein in H_2O solution recorded at 25 °C exhibited an absorbance maximum near 1642 cm^{-1}, indicating the presence of a predominantly β-sheet structure. Quantitative analysis of the amide I spectrum revealed that the native factor XIII contains 54-58% β-sheet, 13-16% α-helix, 10% 3_{10}-helix, and 19% turn structures. The concomitant appearances of a strong low-wavenumber β-sheet band at 1641 cm^{-1} and a weak high-wavenumber β-sheet band at 1689 cm^{-1} indicate that the β-sheet structure is predominantly antiparallel. These results are consistent with those reported by X-ray crystallographic analysis [Yee et al. (1994) *Proc. Natl. Acad. Sci. USA* 91, 7296-7300]. The thermal denaturation of factor XIII started at 5 °C higher temperature in H_2O than in D_2O. However, the middle point of denaturation as determined by IR is about 3 °C lower in H_2O than in D_2O. The denatured state of the protein in H_2O contains less random coil than its counterpart in D_2O.

Tu-Pos244

THERMAL UNFOLDING AND DISSOCIATION OF THE *ACANTHAMOEBA* MYOSIN II COILED-COIL ROD. ((M. Zolkiewski, M.J. Redowicz, E.D. Korn, J.A. Hammer III and A. Ginsburg)) NHLBI, NIH, Bethesda, MD 20892-0340.

The thermal stability of the myosin II rod has been studied by circular dichroism (CD) and differential scanning calorimetry (DSC). The complete rod domain of myosin II (residues 849-1509, M_r ~ 150,000) has been expressed in *E. coli*. At a high ionic strength (0.6 M KCl, pH 7.5), purified myosin II rod is a coiled-coil dimer of mainly α-helical polypeptide chains. CD and DSC experiments show that the thermal unfolding of the myosin II rod is highly cooperative (T_m ~ 40°C, ΔH~400 kcal/mol) and is coupled to a decay of secondary structure. This behavior is similar to that previously found for the intact myosin II but the rod unfolding reaction is completely reversible. DSC data are scan-rate dependent, which suggests that the approach to equilibrium during unfolding of the myosin II rod is slow. The unfolding of the rod is coupled to a dissociation of the two chains, as shown by the lower apparent molecular weight of the protein at high temperatures in HPLC gel filtration and by the concentration dependence of the transition temperature observed in CD. The CD and DSC data for the thermal transition are consistent with a two-state mechanism: $N_2 \rightleftharpoons 2U$, where the native dimeric rod (N_2) unfolds as two unfolded monomers (U) form. This mechanism is significantly different from those for skeletal muscle myosin rod and tropomyosin, for which others have found several partially folded intermediates. However, the two-state unfolding of the myosin II rod is similar to that of small dimeric proteins containing the coiled-coil, leucine zipper motif.

Tu-Pos245

INVESTIGATION OF ELECTROSTATIC INTERACTIONS IN TWO-STRANDED COILED-COILS THROUGH RESIDUE SHUFFLING. ((Y. Yu*, O.D. Monera#, R.S. Hodges# and P.L. Privalov*)) *Dept. of Biophysics, The Johns Hopkins Univversity, Baltimore, MD 21218, USA; # Dept. of Biochemistry, Univ of Alberta, Edmonton, Alberta T6G 2H7, Canada. (Spon. by P.L. Privalov)

The effects of electrostatic interactions on the stability of coiled-coils were investigated using the strategy of shuffling the sequence, under certain symmetry constraints, to generate a series of six peptides without changing the overall content of amino acid residues. Shuffling the sequence provides peptides with thermodynamically similar unfolded states. Employing scanning microcalorimetry and CD spectroscopy to monitor the stability and structure, it was found that in solutions with low electrolyte concentration, ion pairs contribute significantly to the stability of the coiled-coil conformation and the coiled-coils are more stable at neutral pH than at acidic pH. However, NaCl dramatically stabilizes the coiled-coil conformation at acidic pH while has little effect at neutral pH, causing the coiled-coil conformation becoming more stable at acidic pH than at neutral pH at 0.1M NaCl. Most surprisingly, the increase in Gibbs energy of stabilization of the coiled-coil state with increasing pH at low ionic strength proceeds with a decrease of the enthalpy and entropy of unfolding. This observation can be best explained by hydration of ionized groups upon unfolding of coiled-coils which is associated with significant negative enthalpy and entropy effects.

Tu-Pos246

THERMAL STABILITY OF FOUR-HELIX BUNDLE PROTEINS WITH VARIOUS SUBSTITUTIONS IN HYDROPHOBIC CORE REGION. ((H. Morii, M. Ishimura, S. Honda and H. Uedaira)) National Institute of Bioscience and Human-Technology, Tsukuba, Ibaraki 305, Japan. (Spon. by Y. Okamoto)

Helix bundle structure is a characteristic motif of proteins. Many efforts by means of de novo design have been done for it during these years. Generally, water-soluble helix bundles are constructed with amphiphilic α-helices so that they fold into compact form with hydrophobic residues as interior. it is noted that some designed proteins have molten-globule characteristics and/or multi-stable conformation different from native proteins. Here, we focused on this problem, using de novo designed proteins of 94 residues, which contain the same two 46-residue peptide chains linked by branching and have pseudo-C_2 symmetry. Several mutants involving the substitutions in hydrophobic core region were chemically synthesized and were analyzed thermodynamically. Among them folded and unfolded mutants were observed, depending on the positions of mutation. The circular dichroism spectra of folded ones gave typical α-helix pattern commonly and they exhibited a change to denatured form by heating. The substitutions of core residues in N-terminus helix, even that from leucine to glutamine, have little influence on the thermal stability of the protein. While, the similar substitutions in C-terminus helix lowered the denaturation temperature of the protein significantly. From the dye-binding experiments the protein may be molten-globule, however, it does not seem to have quite nonspecific folded structure, because C-terminus helix would have special contribution on the folding.

Tu-Pos247

COMPARISON OF PARALLEL AND ANTI-PARALLEL HELICAL COILED-COILS USING QUATERNION CONTACT RIBBONS ((A. Shaw[§], K. Albrecht[†], J. Hart[†] and A.K. Dunker[§])) [§]Dept. of Biochemistry & Biophysics and [†]Dept. of Electrical Engineering & Computer Science, Washington State University, Pullman, WA 99164

The α-helical coiled-coil (Crick, *Acta Cryst.* 6: 689-697, 1953) is receiving increasing attention in part because the proposal that numerous DNA binding proteins dimerize via the "leucine-zipper" motif (Landschulz et al., *Science* 240: 1759-1764, 1988) has been substantially confirmed by the discovery that the b-zip peptide forms a parallel coiled-coil with knobs-into-holes packing (O'Shea *et al., Science* 254: 539-544, 1991). We used our earlier studies on knobs-into-holes packing (Dunker and Zaleske, *Biochem. J.* 163: 45-57, 1977) as the basis for the development of a tool, called the quaternion contact ribbon, for the simplification of the visualization of the coiled-coil interface (Albrecht et al., *Proc. Pacific Symp. Biocomp.*, In Press). This tool greatly simplifies visualization of the twisted coiled-coil interface by transforming the contact space into a straightened projection. This simplified projection can reveal interesting features, which can then be subjected to further analysis in the original structure. Note that the set of α-carbons of an α-helix occupy the same set of coordinates following a 2-fold rotation about an axis perpendicular to and passing through the helix axis and also passing through one of the α–carbons. Because of this symmetry that is independent of helix direction, the set of α-carbons of the two helices in a parallel coiled-coil could occupy the same set of coordinates as the set of α-carbons in an anti-parallel coiled-coil. Comparison of the packing interfaces of parallel with anti-parallel coiled-coils using the quaternion contact ribbon reveals, however, substantial differences in the α-carbon positions in the parallel as compared to anti-parallel coiled-coil. Further studies are underway to quantify the relative backbone shifts between the two types of coiled-coils and to identify the causes for these structural differences.

Tu-Pos248

HOST GUEST SET OF TRIPLE-HELICAL PEPTIDES.((Naina Shah[1], John A.M.Ramshaw[2], Alan Kirkpatrick[2], Chirag Shah[1] and Barbara Brodsky[1]))
[1]UMDNJ-Robert Wood Johnson Medical School, Piscataway NJ 08854,
[2]CSIRO, Parkville 3052, Australia

The ability of the collagen triple-helix to associate or bind to other molecules depends on its specific amino acid sequence, $(Gly\text{-}X\text{-}Y)_n$, and a peptide approach was taken to evaluate the interactions of individual Gly-X-Y triplets. A set of host-guest peptides of the form $Ac(Gly\text{-}Pro\text{-}Hyp)_3\text{-}\underline{Gly\text{-}X\text{-}Y}\text{-}(Gly\text{-}Pro\text{-}Hyp)_4\text{-}Gly\text{-}Gly\text{-}CONH_2$ was synthesized to include triplets found commonly in collagen. The X and Y positions of the guest triplet included: the three most common residues, Pro, Hyp and Ala; the most frequent hydrophobic residue, Leu; and the only commonly occurring aromatic residue, Phe. All peptides formed stable triple-helical structures and showed a wide range of thermal stabilities (T_m = 21°C - 44°C), depending on the identity of the guest triplet. Thermodynamic parameters calculated for these peptides showed imino acids to be important stabilizing elements of the triple-helix, by virtue of its favorable entropic contribution. The continuum seen in both thermodynamic parameters and melting temperatures emphasized the importance of residues other than Pro and Hyp. There was no hydrophobic stabilization of the triple-helix in these peptides, since replacement of Ala by Leu or Phe conferred no stability. Both Leu and Phe were more destabilizing in the Y position than in the X position, due to an unfavorable entropy change. Thermodynamic information obtained from these studies can be utilized in establishing a scale of triple-helix propensities and clarifying the interactions stabilizing this conformation.

Tu-Pos249

COOPERATIVE FOLDING AND COMPLEX KINETICS IN A SERIES OF AMINO FRAGMENTS OF THE α SUBUNIT OF TRYPTOPHAN SYNTHASE. ((J.A. Zitzewitz, I.A. Perkons and C.R. Matthews)) Department of Chemistry and Center for Biomolecular Structure and Function, The Pennsylvania State University, University Park, PA 16802. (Spon. by K. Merz)

The α subunit of tryptophan synthase from *Escherichia coli* is a 268-residue eight-stranded α/β barrel protein. In the denaturant-induced equilibrium unfolding of the α subunit, a stable intermediate is significantly populated at 3.3 M urea. This intermediate has been proposed to contain cooperatively folded structure in the amino-terminal region. In the current study, we have characterized a series of amino-terminal fragments in an effort to identify the structural elements present in this stable equilibrium intermediate. Stop-codon mutagenesis was used to produce this series of fragments, ranging in size from 92 to 214 residues and containing incremental elements of secondary structure. Equilibrium unfolding studies by circular dichroism and fluorescence show that fragments at least as small as 147 residues are capable of folding cooperatively. The progressive addition of secondary structural elements leads to enhanced cooperativity and stability in the longer fragments. Multiphasic folding kinetics in some of the fragments demonstrate that the folding mechanisms are more complex than simple two-state reactions. This work was supported by NIH grants GM 23303 (CRM) and GM 14954 (JAZ).

Tu-Pos250

EQUILIBRIUM DISSOCIATION OF TRYPTOPHAN SYNTHASE SUBUNITS STUDIED BY SEDIMENTATION EQUILIBRIUM ((D.B. Millar, S. Darawshe and A.P. Minton)) NIDDK, NIH, Bethesda, MD 20892

Tryptophan synthase is composed of two α subunits (MW 29500) and a dimeric β_2 subunit (MW 86000) arranged in a quasilinear array of the form αββα. Indirect measurements suggest that upon dilution, the enzyme undergoes sequential dissociation of α subunits according to the scheme $\alpha_2\beta_2 \rightleftharpoons \alpha + \alpha\beta_2$ ($K_{d1} = 2k_d$); $\alpha\beta_2 \rightleftharpoons \alpha + \beta_2$ ($K_{d2} = \gamma k_d^2/2$), where k_d is an intrinsic equilibrium constant for dissociation of α subunit from either site in the holoenzyme, and γ is a cooperativity parameter, such that if $\gamma > 1$, dissociation of the first α facilitates dissociation of the second, and if $\gamma < 1$, dissociation of the first α inhibits dissociation of the second. Sedimentation equilibrium experiments carried out on purified β_2 established that the β_2 dimer is stable under all of the conditions used in the present study. The enzyme was centrifuged to sedimentation equilibrium in a Beckman XL-A analytical ultracentrifuge at 5°C at loading concentrations between 0.2 and 2 mg/ml, in buffers containing excess pyridoxal phosphate. Replicate experiments were also conducted in buffer containing sub-denaturing concentrations (≤ 150 mM) of the chaotropic agent guanidine isothiocyanate (GuSCN). Measured gradients were analyzed via conventional sedimentation equilibrium theory together with conservation of signal constraints. The value of log k_d was readily determinable at each GuSCN concentration, and ranged between -6.0 in the absence of GuSCN to -4.6 at 125 mM GuSCN. Due to the limits of sensitivity of the XL-A absorbance optics, only an upper limit for γ could be established at GuSCN concentrations < 125mM, but this upper limit is significantly less than unity. At 125 mM GuSCN, the best-fit value of log γ with 95% confidence limits was found to be -1.0 (-0.5,+0.25). We conclude that the sequential dissociation of α subunits is negatively cooperative, as suggested by previous investigators on the basis of indirect evidence.

Tu-Pos251

DECAY ASSOCIATED SPECTRA OF TRYPTOPHAN SYNTHASE AS A FUNCTION OF APPLIED HYDROSTATIC PRESSURE. ((*Lesley Davenport, #Jay R. Knutson, +S. Ashraf Ahmed and +Edith W. Miles)) *Dept. Chem., Brooklyn College of CUNY, Brooklyn, NY 11210, #LCB/NHLBI and +LPB/NIDDK, NIH, Bethesda, MD 20892.

The dimer-monomer (D-M) transition for apo β_2-tryptophan synthase from *S.typhimurium* (a single Trp protein) has been obtained from variation of the center of spectral mass of Trp emission *vs.* hydrostatic pressure (0-2 kbar). We noted, however, unusual increases in fluorescence intensity with a peak around 1 kbar, the mid-point of D-M profiles. Decay-associated spectra (DAS) were measured as a function of increasing pressure by mounting an SLM high pressure spectroscopy cell in the modified sample compartment of our TCSPC system. Excitation (at 297nm) was achieved using a cavity dumped dye laser system (5ps, 4MHz, 200μW). Impulse response 'lamp' functions were obtained (before and after the pressure run) with Ludox. Global analyses yielded two distinct sets of DAS; the set below 1 kbar was comprised of 0.8, 2.3 and 7 ns lifetimes, with $\%I_{345nm}$ of 28, 47 and 25, respectively. The set from 1.25-2 kbar was comprised of 0.6, 2.5 and 6.4 ns lifetimes with corresponding $\%I_{345nm}$ of 12, 44 and 44. The intensity and mean lifetime increases near 1 kbar are in accord with the increase in weight of the long component. Experiments are now in progress to dissect the time and pressure dependence of the interchange between these protein conformers.

Tu-Pos252

ENERGETICS OF SUBDOMIAN ORGANIZATION OF α-LACTALBUMIN ((Hendrix, T.M., Griko, Y.V., and Privalov, P.L.)) The Johns Hopkins University, Department of Biophysics, Baltimore, MD 21218.

Molecular organization of bovine α-lactalbumin in context of its two subdomain structure has been investigated by studying its derivatives differing in the number of disulfide bond. It was shown that reduction of the 6-120 and 28-111 disulfide crosslinks leads to disruption of the α-helical domain but does not lead to unfolding of the entire cooperative structure of LA but only to its destabilization. The β-domain remains stable in aqueous solution and has the native-like properties of cooperative structure and the calcium binding ability. The stabilization of the β-domain by calcium appears to be largely entropic. Removal of calcium leads to unfolding of the β-domain. It was concluded that in spite of fact that α-domain stability is greater than β-domain, its structure is not crucial for the formation of tertiary structure and the calcium binding site in LA. The structural and thermodynamic aspects of stability of the α- and β-domains are discussed.

K CHANNELS II

Tu-Pos253

Structural Modeling and Molecular Dynamics Studies of the K^+ Channel ((Pamidighantam V. Sudhakar, Shankar Subramaniam, and Eric Jakobsson)) Department of Molecular and Integrative Physiology, Center for Biophysics and Computational Biology, Beckman Institute, National Center for Supercomputing Applications, University of Illinois, Urbana, IL 61801.

Using a model built by Guy and Durell for the ion selective pore region of the Shaker K^+ channels as the starting point, we have added to the pore region a structural model for the S5 and S6 transmembrane segments, based on published mutagenesis and functional studies. A noteworthy feature of the model is that it was constructed without regard to the placement of the aromatic residues, but emerged with the aromatic residues preponderantly placed to be in the phospholipid head group region. Since the S5 and S6 regions appear to form part of the hydrophilic pore lining, and since the presumed physical basis for the aromatic placement is favorable interactions with phospholipid head groups, this result suggests that in the membrane assembly there may be phospholipid molecules among the transmembrane protein segments. This would be in contrast to the picture that the protein transmembrane segments pack closely together with the phospholipid only on the outside. We have begun molecular dynamics on a hydrated channel, using boundary conditions similar to those previously developed in our laboratory for studying the gramicidin channel, and also used in studying a sodium channel pore model. We will report on mobility of water and ions in and near the channel and relative flexibility of diffferent parts of the channel. Supported by NSF, NCSA, and Pfizer Inc.

Tu-Pos254

STRUCTURAL MODEL OF K^+ CHANNEL BLOCK BY SCORPION TOXINS. ((G. Lipkind and H.A. Fozzard)) University of Chicago, Chicago, IL 60637.

Mutational studies have identified part of the S5-S6 loop of voltage-dependent K^+ channels (P region) responsible for TEA block and permeation properties. We have proposed a structural motif for the K^+ channel pore on the basis of external and internal TEA binding sites (Lipkind, Hanck & Fozzard, 1995, PNAS, in press). In the model, P regions form nonregular extended hairpins and C-ends face the inner walls of the pore, while N-ends are located outside. Several scorpion venom peptide toxins - charybdotoxin (ChTX), kaliotoxin (KITX), and agitoxin (AgTX) - block the channel. Docking of scorpion toxins with the model of Kv1.3 (Asp-386 and His-404 on the N- and C-ends of P loops) started by location of the extended conformation of Lys-27 side chain into the central axis of the pore, followed by energy minimization. In the optimal arrangement, Arg-24 of KITX or AgTX forms a hydrogen bond with Asp-386 carboxyl of one subunit, and Asn-30 is in immediate contact with Asp-386 of the opposing subunit in the tetramer. Residues of toxins in proximity to the side chain of Lys-27 (Phe-25, Thr-36, Met-29, and Ser-11 in KITX) interact with the C-end His-404's of four neighboring subunits. For ChTX the absence of the strong interaction with Asp-386 is compensated by additional non-bonded interactions, formed by Tyr-36 and Arg-34. Steric contacts of residues in position 380 of the S5-P linker with residues on the upper part of toxins permit reconstruction of the K^+ channel outer vestibule walls, which are about 30 Å apart and about 9 Å high. Molecular modelling shows complimentarity of our pore model to the scorpion toxin spacial structures, and supports our proposal that the N-terminal borders of the P loops surround residues of their C-terminal halves, which face the narrow conductance path.

Tu-Pos255

MOLECULAR MODELLING OF THE PORE OF POTASSIUM CHANNELS BY RESTRAINTS-DIRECTED DISTANCE GEOMETRY.
((I.D. Kerr and M.S.P. Sansom)) Laboratory of Molecular Biophysics, University of Oxford, The Rex Richards Building, South Parks Road, Oxford, OX1 3QU.

Voltage-gated potassium (Kv) channels maintain the resting membrane potential of cells. There is a large body of site-directed mutagenesis data for Kv channels which may contain structural information. We have interpreted these data as a set of topological restraints, allowing us to thread the H5 sequence onto different secondary structural templates. The templates are scored for their agreement with the mutagenesis data, enabling us to compile 30 possible configurations for β-barrels which may be explored further as models of the pore region of Kv channels. These configurations differ in the lengths of β-strands, the β-turn length, the pattern of pore-lining and outward facing residues, and the shear number of the β-barrel. Large ensembles of 8-stranded β-barrel structures (with a poly-alanine sequence) satisfying the restraints defining each configuration have been rapidly generated by distance geometry. Sidechain atoms corresponding to the residues in the H5 sequence of Shaker-A Kv channel are added to selected structures from each ensemble by simulated annealing. Analysis and comparison of these models allows identification of the most plausible configurations, which may then be refined to generate possible models of the Kv channel pore domain. As none of the initial templates exactly agrees with all mutagenesis data we are investigating distortions from idealised β-barrel geometries.

This work was supported by the Wellcome Trust.

Tu-Pos256

A COMPUTATIONAL EVALUATION OF THE YW-GATED MODEL USING A MODEL PORE STRUCTURE OF INWARD-RECTIFIER POTASSIUM CHANNEL. ((M.-J. Hwang, P.K. Yang, W.S. Tzou, C.Y. Lee)) Institute of Biomedical Sciences, Academia Sinica, Taipei, 11529 Taiwan, R.O.C. (Spon. by C.W. Wu)

According to the YW-gated model (Lee, 1992, FEBS *Lett* 299:119-123), the four tyrosine residues in the pore region (e.g., Y445s of the *Shaker* protein) form hydrogen bonds with each other to prohibit ions from passing through in the closed state, while in the open state the same tyrosine residues become free radicals via an electron exchange process with nearby aromatic residues and sensored by charged group to repel each other to allow ion passage. In order to evaluate this model of ion transport mechanism we have built a β barrel of the pore region, similar to that of Bogusz and Busath (1992, *Protein Engin.* 5:285-293) but somewhat shorter and with the IRK1 sequence, through restrained molecular dynamics and energy minimization. Potential energy profiles for transporting a potassium ion through the pore region in both closed and open states are calculated and compared. For the open state, new molecular mechanics parameters for modeling tyrosine radical are derived from fitting to energy surface data computed with *ab initio* methods. Results from this study will be presented at the meeting.

Tu-Pos257

HOMOLOGY MODELING OF THE β SUBUNIT OF A VOLTAGE-GATED K^+ CHANNEL ((K.V. Soman)) Department of Molecular Physiology & Biophysics, Baylor College of Medicine, One Baylor Plaza, Houston, TX 77030-3498; *ksoman@bcm.tmc.edu*

K^+ channel β subunits (Kvβ) are auxiliary cytoplasmic proteins that modulate channel inactivation by association with the pore-forming α subunits. The highly conserved, 329-residue long, C-terminal core sequence of Kvβ proteins has been found to belong to an oxidoreductase superfamily [*T. McCormack & K. McCormack, Cell, 79, 1133-1135, 1994*]. We exploit this sequence similarity using *homology modeling* techniques to build 3-D models for a Kvβ3 subunit. The X-ray structures of *aldose reductase* and *3-α-hydroxysteroid dehydrogenase* are used as reference proteins. When aligned optimally, 78 residues of the Kvβ3 core are identical to at least one of the reference proteins and about 40 other positions have *conservative* substitutions. The *Asp-Tyr-Lys* catalytic triad of the reference proteins is found conserved in Kvβ3 (and in other known Kvβ sequences), strengthening the possibility of an enzymatic function for the Kvβ's. Initial crude models indicate that the method indeed folds the Kvβ3 chain into the expected *$(\alpha/\beta)_8$ or TIM barrel* structure of the reference proteins. Refined model(s) will be presented and structure-function correlations will be explored. (partially supported by a Grant-in-Aid from the *American Heart Association, Texas Affiliate, Inc.)*

Tu-Pos258

SECONDARY STRUCTURE PREDICTION OF *SHAKER* TYPE POTASSIUM CHANNEL β SUBUNITS ((K. Majumder[1] and K.V. Soman[2])) Departments of [1]Cell Biology and [2]Molecular Physiology & Biophysics, Baylor College of Medicine, One Baylor Plaza, Houston, TX 77096

Based on sequence, the β3, β1, and β2, subfamilies of voltage-activated K^+ channel (Kv) auxiliary subunits have two distinct domains: a C-terminal core that accounts for most of the protein, and a short N-terminus. The known β3 and β1 members have a common 329-residue core sequence; the β2 core is 85% identical to these. The N-termini, believed to be responsible for the functional effects of the Kvβ proteins, are of highly variable sequence and length: 79, 72, and 38 residues in β3, β1, and β2, respectively. Rat Kvβ1 accelerates the inactivation of *Shaker* channels by means of a "ball peptide" analogue in its N-terminus [Rettig et al., Nature **369**, 289-294,1994]. In the case of β2 and β3 proteins, no mechanism of action has been established. We report here the predicted secondary structures for the N-termini of all three subfamilies, by two methods. The predictions indicate that the β3 N-terminus is likely to have a predominantly α-helical structure with insignificant amounts of β-strand, the β1 is likely to have considerably more strand and less helix than β3, and the β2 N-terminal may not have any helix at all. Thus, the differences in inactivation properties among the Kvβ subfamilies could be structure- as well as sequence- related. (supported by a Grant-in-Aid from the American Heart Association, Texas Affiliate, Inc.)

Tu-Pos259

IN SITU HYBRIDIZATION REVEALS EXTENSIVE DIVERSITY OF K^+ CHANNEL mRNA IN ISOLATED FERRET CARDIAC MYOCYTES ((V. Brahmajothi, M.J. Morales, S. Liu, R.L. Rasmusson, D.L. Campbell and H.C. Strauss)) Duke University Med. Ctr., Durham, NC 27710 (Spon. James D. Crapo)

The molecular basis of K^+ channels that generate repolarization in heart is uncertain. In part, this reflects the similar functional properties different K^+ channel clones display when heterologously expressed, in addition to the molecular diversity of the voltage-gated K^+ channel family. To determine the identity, regional distribution, and cellular distribution of voltage-sensitive K^+ channel mRNA subunits expressed in ferret heart, we used fluorescent labelled oligonucleotide probes to perform *in situ* hybridization studies on enzymatically isolated myocytes from the SA node, right and left atrium, right and left ventricle and interatrial and interventricular septum. The most widely distributed K^+ channel transcripts in the ferret heart were Kv1.5 (present in 69.3-85.6% of myocytes tested depending on anatomical region from which myocytes were isolated) and Kv1.4 (46.1-93.7%), followed by Kv1.2, Kv2.1, and Kv4.2. Surprisingly, many myocytes contain transcripts for Kv1.3, 2.2, 4.1, and members of the Kv3 family. Kv1.1 and 1.6, which were rarely expressed in working myocytes, were commonly expressed in SA nodal cells. IRK was expressed in atrial (52.4-64.0%) and ventricular cells (84.3-92.8%), but was nearly absent (6.6%) in SA nodal cells. MinK was most frequently expressed in SA nodal cells (33.7%) as opposed to working cells (10.3-29.3%). Kvβ3 was infrequently expressed in 17.2-29.2% of all cell types. These results show that the diversity of K^+ channel mRNA in heart is greater than previously suspected, and that the molecular basis of K^+ channels may vary from cell to cell within distinct regions of the heart and also between major anatomical regions.

Tu-Pos260

THE ROLE OF THE Kv4.3 POTASSIUM CHANNEL IN CARDIAC MYOCYTE FUNCTION ((Jane E. Dixon, Wenmei Shi and David McKinnon)) Dept. of Neurobiology, SUNY, Stony Brook, NY 11794

We have previously suggested that the Kv4.2 gene encodes the transient outward current (I_{to}) in rat cardiac myocytes (Dixon and McKinnon, 1994, Circ. Res., 75:252). To determine whether this was also the case in species which have a more traditional 'spike and dome' cardiac action potential we conducted a systematic analysis of potassium channel gene expression in canine ventricular muscle. There are several significant differences in the pattern of potassium channel gene expression in canine compared with rat ventricular myocytes. Surprisingly, neither the Kv4.2 or Kv4.1 genes are expressed in canine ventricle, even though these cells express an I_{to} that has very similar biophysical properties to the rat I_{to}. Using degenerate oligonucleotides and PCR we identified a new potassium channel gene expressed in canine heart, Kv4.3, which encodes the most abundant K channel mRNA expressed in canine ventricle. The results suggest that the Kv4.3 channel encodes part or all of the I_{to} found in canine heart. Similar results have been obtained from human heart.

The Kv4.3 channel mRNA is also expressed in rat heart and the differential pattern of expression of Kv4.2 and Kv4.3 can explain the differences in the biophysical properties of I_{to} found in different regions of rat myocardium. Changes in I_{to} function induced by changes in thyroid hormone status can also be explained by differential regulation of the transcription of the Kv4.2 and Kv4.3 genes.

Tu-Pos261

FUNCTIONAL AND PHARMACOLOGICAL CORRESPONDENCE BETWEEN Kv4.2 AND CARDIAC TRANSIENT OUTWARD CURRENTS. ((S.W. Yeola and D.J. Snyders)) Vanderbilt University, Nashville, TN 37232. (Spon. by E. Delpón)

The transient outward current (I_{TO}) plays an important role in early repolarization and overall time course of the cardiac action potential. Two K^+ channel α-subunits cloned from cardiac tissue (Kv1.4 and Kv4.2) form rapidly inactivating channels. The Kv1.4 subunit has been suggested as a major component of I_{TO}, but recovery from inactivation is about 100-fold slower compared to native I_{TO}, a discrepancy that is not corrected by coexpression with available Kvβ-subunits. To test whether Kv4.2 could form the molecular basis for I_{TO}, we compared functional and pharmacological properties of Kv4.2 and Kv1.4 with those of I_{TO}. Kv4.2 currents expressed in a stable mammalian cell lines displayed fast inactivation (τ_{inac}=31 ms at +50 mV) with a half-inactivation potential of -41 mV. Recovery from inactivation was rapid (τ_{recov}=160 ms at -90 mV) and strongly voltage-dependent. Flecainide (10 µmol/L) had minimal effects on Kv1.4 currents, but reduced Kv4.2 peak current by 53% and increased the apparent rate of inactivation (τ_{inac}=15 ms) consistent with open channel block. Quinidine (10-20 µmol/L) induced a reduction of peak current and an acceleration of apparent inactivation in both isoforms. The Kv4.2 current displayed use-dependent unblock in the presence of 4-AP. The functional properties of Kv4.2 and especially the flecainide sensitivity resemble those of I_{TO} in rat (and human) myocytes better than Kv1.4. These results provide functional support for the hypothesis that Kv4.2 is a major isoform contributing to cardiac I_{TO}, consistent with independent biochemical evidence that indicates that Kv4.2 mRNA and protein is readily detected in rat myocytes. Supported by HL47599.

Tu-Pos262

THE MECHANISM OF INACTIVATION OF A SUBTHRESHOLD A-TYPE POTASSIUM CHANNEL. ((H. Jerng and M. Covarrubias)). Department of Pathology, Anatomy and Cell Biology, Jefferson Medical College, Thomas Jefferson University, Philadelphia, PA 19107.

We have investigated the molecular mechanism underlying inactivation of a subthreshold A-type K^+ channel encoded by mKv4.1 (a member of the *Shal* family). Channels were expressed in *Xenopus* oocytes (XO) or mouse fibroblasts (NIH-3T3) and studied using the two-electrode voltage clamp technique or tight-seal whole-cell recording. Inactivation kinetics in XO was well described as the sum of three exponential terms. Time constants at +40 mV were (in ms): 284±22, 74±3 and 15±2. While the slow component contributes to ~50% of the multiexponential decay, the other two represent ~25% each. Time constants and fractional amplitudes were independent of current size (between 2 and 25 µA peak current) and were weakly voltage-dependent. In NIH-3T3 cells currents decayed more rapidly and were well described as the sum of two exponential terms. Time constants at +40 mV were (in ms): 73±10 and 11±1. These values closely match the fast and intermediate components observed in XO. Deletion analysis revealed that putative cytoplasmic domains at the N and C termini determine the fast component of inactivation. At the C-terminus, regions between residues 422 and 456 and between 494 and 554 seemed particularly important. These domains have a relatively high content of arginine and lysine. We are currently testing the importance of these basic residues by site-directed mutagenesis. We propose that rapid inactivation of mKv4.1 may be mediated by the concerted action of cytoplasmic domains at both N and C termini. Supported by NIH grant NS32337 (M.C.).

Tu-Pos263

RESTORATION OF I_{to} BY NOREPINEPHRINE EXPOSURE IN CHAGASIC CANINE EPICARDIAL MYOCYTES. ((W-P. Han[1], S.C. Barr[2], R.F. Gilmour, Jr.[1])) Departments of Physiology[1] and Clinical Sciences[2], Cornell University, Ithaca, NY 14853. (Spon. by L.M. Nowak)

Chagas' disease, resulting from infection by the parasite *Trypanosoma cruzi (T. cruzi)*, is associated with a reduction of the transient outward K^+ current (I_{to}) in canine epicardial myocytes during the acute stage of the disease. With abatement of the parasitemia, I_{to} returns to normal. The acute stage of infection also is associated with destruction of sympathetic nerve terminals, which return after the parasitemia has subsided. To determine whether the lack of innervation might be responsible for the reduction of I_{to}, secondary to the absence of norepinephrine (NE) - mediated trophic effects, we recorded I_{to} using the whole cell voltage clamp technique in isolated epicardial myocytes obtained from dogs after 20-25 days of infection with *T. cruzi* (n = 5). The myocytes were incubated for 2-24 hrs in wash solution alone or wash solution plus: NE (1.0 µM); NE and prazosin (0.1 µM); isoproterenol (0.1 µM); phorbol 12-myristate 13-acetate (PMA, 0.1 µM). I_{to} measurements were made in drug-free solution. I_{to} densities at +40 mV after 0, 2, 4, 6 and 24 hrs of NE exposure were 1.6 ± 0.2, 2.3 ± 0.4, 1.6 ± 0.2, 3.2 ± 0.5 and 8.9 ± 1.2* pA/pF (n = 11, 4, 5, 7 and 13 cells, respectively; *P<0.05 vs 0 hrs). I_{to} was increased by PMA (to 5.1 ± 0.6* pA/pF, n = 7), but was not increased by NE + prazosin or by isoproterenol. Cell capacitance was not significantly affected by NE (90.4 ± 8.6 vs 96.7 ±10.8 pF for 0 vs 24 hrs). These data suggest that the reduction of I_{to} in chagasic myocytes may reflect the lack of the trophic effects of sympathetic innervation and that induction of I_{to} by chronic NE exposure may be mediated by protein kinase C.

Tu-Pos264

NOREPINEPHRINE EXPOSURE RESTORES I_{to} IN EPICARDIAL MYOCYTES FROM DOGS WITH INHERITED VENTRICULAR ARRHYTHMIAS AND SUDDEN CARDIAC DEATH ((L.M. Pacioretty[1], N.S. Moïse[2], R.F. Gilmour Jr.[1])). Departments of Physiology[1] and Clinical Sciences[2], Cornell University, Ithaca, NY 14853-6401

We have shown previously that the density of the transient outward K^+ current, I_{to}, is reduced in left ventricular (LV) epicardial myocytes obtained from German shepherd dogs with inherited sudden death. I_{to} density in right ventricular (RV) myocytes is greater than in LV myocytes. As assessed by MIBG imaging, the density of sympathetic innervation is greater in the right ventricles of these dogs than in the left ventricles. To determine whether the lack of innervation might be responsible for the reduction of I_{to}, secondary to the absence of norepinephrine (NE) - mediated trophic effects, we recorded I_{to} using the whole cell voltage clamp technique in LV myocytes obtained from affected dogs (n = 3). The myocytes were incubated for 20-24 hours in wash solution alone or wash solution plus: NE (1.0 µM); NE and prazosin (0.1 µM); isoproterenol (0.1 µM). I_{to} measurements were made in drug-free solution. I_{to} density at +40 mV was 6.2 ± 1.4 pA/pF after no exposure to NE and 12.7 ± 1.8* pA/pF after exposure to NE (n = 11 and 5, respectively; *P<0.05). I_{to} was not increased by isoproterenol or by NE + prazosin. The τ for I_{to} decay was unchanged by NE exposure (28.4 ± 1.9 vs 29.9 ± 2.2 msec for -NE vs +NE). Boltzmann analysis of steady-state inactivation showed no differences in the slope factor, but a shift in $V_{1/2}$ from -33.6 mV in -NE to -36.6 mV in +NE. These data suggest that the reduction of I_{to} in LV epicardial myocytes may reflect the lack of the trophic effects of sympathetic innervation. Further studies are needed to identify the mechanism by which chronic NE exposure induces I_{to}.

Tu-Pos265

COASSOCIATION OF KIR 3.1 AND KIR 3.4 WHEN EXPRESSED IN *XENOPUS* OOCYTES. ((Matthew E. Kennedy and David E. Clapham)). Department of Pharmacology, Mayo Clinic, Rochester, MN 55905.

The inwardly-rectifying K^+ channel family regulates cell resting membrane potential and, therefore, cell excitability. The Kir 3.x subfamily of inward rectifiers contains potassium-selective channels activated by G-protein $\beta\gamma$ subunits. The atrial $I_{(KACh)}$ potassium channel slows heart rate in response to vagal nerve excitation. $I_{(KACh)}$ recently has been shown to exist as a heteromultimer of two inwardly-rectifying potassium channels, Kir 3.1(GIRK1) and Kir 3.4(CIR). We have developed a heterologous expression system for studying Kir 3.1 and Kir 3.4 interactions in *Xenopus* oocytes. Introduction of a six amino acid epitope tag into the NH_2- or C-terminus of Kir 3.4(AU1) or Kir 3.1(AU5) does not alter channel function as assessed by muscarinic-M_2 receptor-mediated activation of inwardly-rectifying K^+ current in *Xenopus* oocytes. Wild type Kir 3.1 was coimmunoprecipitated with epitope-tagged Kir 3.4(AU1) when coexpressed in *Xenopus* oocytes. Interestingly, introduction of three amino acids in the putative extracellular region of Kir 3.1 to produce the AU5 epitope eliminated detectable channel activity in oocytes but produced a dominant negative form of Kir 3.1 that is capable of inhibiting coexpressed wild type Kir 3.1/Kir 3.4 currents.(Supported by NS09776-01.)

Tu-Pos266

Identification of specific regions within heteromeric inwardly rectifying K^+ channel subunits responsible for current potentiation. ((Kim W. Chan, Jinliang Sui and Diomedes E. Logothetis)) Department of Physiology and Biophysics, Mount Sinai School of Medicine, CUNY, New York, NY 10029.

Co-expression of inwardly rectifying K^+ channel subunits hbGIRK1 (a human brain Kir3.1 channel) and KGP (a human pancreatic Kir3.4 channel) produced several fold greater currents than either subunit alone (current potentiation). Specific antibodies recognizing either the KGP or the hbGIRK1 subunit co-precipitated both proteins when co-expressed in oocytes, providing evidence for their heteromeric assembly in the oocyte system. We proceeded to test whether specific regions of the two subunits were responsible for the resultant current potentiation. Amino acid sequence alignment of hbGIRK1 and KGP revealed the least identity in both amino (N-) and carboxy (C-) termini. Incremental deletions of the C-terminus of hbGIRK1 resulted in corresponding decreases in the size of the current resulting from co-expression with the wild-type KGP subunits. We constructed six chimeras between the two channels by swapping the N-, the C-terminus or both termini. Functional expression of each chimera indicated that single transcripts which contained the C-terminus of hbGIRK1 and the central portion of KGP yielded potentiated currents when compared to the rest of the constructs or the wild-type subunits. Identical deletions of the C-terminus of hbGIRK1, but now as part of the chimeric construct with the KGP subunit, gave similar results as before. The small currents obtained with certain chimeras or deletion constructs were not due to a functional impairment since co-expression with the appropriate wild-type or chimeric subunit caused significant changes in the levels of the expressed currents. We are currently characterizing the single-channel properties of the chimeric channel constructs.

Tu-Pos267

Endogenous K_{ATP} channel activity in three mammalian cell lines. ((Jinliang Sui, Peter Rose, and Diomedes E. Logothetis)) Department of Physiology and Biophysics, Mount Sinai School of Medicine, CUNY, New York, NY 10029.

Heterologously expressed recombinant channels (members of the Kir family) in mammalian cell lines have been claimed to represent ATP-sensitive potassium (K_{ATP}) channels (Ashford et al, Nature 370:456, 1994; Inagaki et al., J. Biol. Chem. 270:5691, 1995; Chan et al., Biophys. J. 68:A353, 1995). Yet, other studies have shown that similar or identical recombinant channels failed to produce K_{ATP} channel activity (Krapivinsky et al., Nature 374:135, 1995; Duprat et al, Bioch. Biophys. Res. Comm. 212:657, 1995; Chan et al., submitted for publication). Here, we have studied three untransfected mammalian cell lines (Chinese Hamster Ovary, CHO, Hamster, BHK21, and human, HEK293, epithelial kidney) which have been used in the above heterologous expression studies. We find that all three cell lines contain channels which display biophysical characteristics typical of K_{ATP} channels. Channel activity showed bursting kinetics, open-time constants ranging between 1-3 ms, two intraburst closed-time constants with the fast component ranging between 0.3-0.6 ms, single-channel conductances ranging between 50-65 pS, and weak inward rectification. Such channel activity was obtained in 10-20% of the patches (CHO: 80/401; BHK21: 33/176; HEK293: 9/87). Intracellular application of ATP could inhibit channel activity. Moreover, Glibenclamide (1-20 μM), a specific K_{ATP} channel blocker inhibited endogenous channel activity in CHO cells. These results indicate that putative recombinant K_{ATP} channels heterologously expressed in CHO, BHK21 or HEK293 cells would have to be convincingly distinguished from similar endogenous channels.

Tu-Pos268

CLONING OF AN INWARDLY RECTIFYING K CHANNEL FROM GUINEA PIG ATRIUM. ((Ruth L. Martin, Bin Xu, Dorothy A. Hanck and John W. Kyle)) University of Chicago, Chicago, IL 60637.

Temperature and internal Mg^{2+} concentration ($[Mg^{2+}]_i$) have different effects on the rectification property of I_{K1} in ventricular myocytes, isolated from different species. At reduced temperature (15° C), reducing $[Mg^{2+}]_i$ (<10^{-9} M) produced linearization of the I_{K1} current-voltage relationship of guinea pig myocytes, while at 37° C, guinea pig I_{K1} remained inwardly rectifying. In contrast, reducing $[Mg^{2+}]_i$ did not alter inward rectification of I_{K1} recorded from cat or rabbit myocytes independent of temperature. To investigate the roles of $[Mg^{2+}]_i$ and temperature on I_{K1} inward rectification at the molecular level, we have screened a guinea pig atrial cDNA library using mouse IRK1 as a probe. We have isolated a 2.2 kb clone (GPHIRK1) which has a deduced amino acid sequence that is highly homologous to the mouse IRK1 isoform. Expression of cRNA in *Xenopus* oocytes and transient transfection of GPHIRK1 into a mammalian cell line (tsA201), results in a strongly inwardly rectifying K^+ current. This current has N-shaped conductance and is completely blocked with 500 μM Ba^{2+}_o.

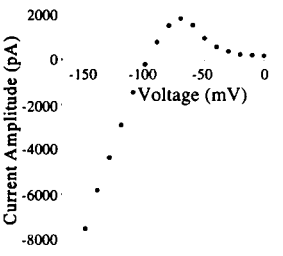

Tu-Pos269

PHYSICAL MECHANISM OF THE INTRINSIC VOLTAGE-DEPENDENT GATING IN INWARD-RECTIFIER POTASSIUM CHANNELS. ((C.Y. Lee, P.K. Yang, T.H. Huang and M.J. Hwang)) Institute of Biomedical Sciences, Academia Sinica, Taipei, 11529 Taiwan, R.O.C. (Spon. by M.F. Tam)

In the absence of internal Mg^{2+} ions, inward rectifier K^+ (K_{ir}) channels still exhibits voltage dependent gating. We propose that a glutamate in the P-region could be responsible for the intrinsic gating. The role of this glutamate may be similar to D447 in the *Shaker* K^+ channel. However, in the tertiary structure, D447 is located above Y445, while the glutamate could be located below a conserved tyrosine residue corresponding to *Shaker*'s Y445. This difference makes the intrinsic opening probability of K_{ir} channels increase with increasing hyperpolarization. Mutation of D172 in IRK1 to a neutral residue may alter the potential energy at an electron acceptor site in the M1 segment, shifting the voltage dependence toward depolarized potentials, and consequently changing the instantaneous gating. The effects of polyamines can also be explained. According to this model, the IRK1 channel could be converted into an outwardly rectifying channel (intrinsic opening probability increases with increasing depolarization) if the glutamate is mutated into valine and simultaneously replacing GYGF in the P-region by the *Shaker*'s GYGD.

Tu-Pos270

N-GLYCOSYLATION STUDIES OF ROMK1 REVEAL UNEXPECTED EXTRACELLULAR REGIONS IN THE PORE-FORMING SEGMENT ((Ruth A. Schwalbe, Zhiguo Wang, and Arthur M. Brown)) Rammelkamp Center for Education and Research, MetroHealth Campus, Case Western Reserve University, Cleveland, Ohio

Inwardly rectifying K^+ channels (IRKs) maintain the resting membrane potential, excitability and potassium exchange.The proposed topological model of IRKs consists of two transmembrane segments (M1 and M2) linked by a pore-forming segment (H5), and intracellular amino- and carboxyl-termini. Recent studies have identified critical pore determinants in the M2 and carboxyl-terminal, not H5, as is the case for voltage-dependent K^+ channnels (Kvs). We investigated the membrane topology of ROMK1, a weak IRK, by introducing novel N-glycosylation sites. This tripeptide consensus sequence acts as a probe for extracellular sites. Glycosylation was measured by gel shift assays and electrophysiological changes measured before and after tunicamycin correlated perfectly. The results of these two different methods found that H5 is mainly extracellular rather than mainly within the membrane. In fact very little if any of H5 may penetrate the membrane. Engineered N-glycosylation sites at the amino- and carboxyl-termini, along with the M1 segment gave results consistent with the proposed model. However, the M2 domain appears to be shifted towards the carboxyl-terminal by at least 10 amino acids. (Supported by NIH grant HL36930 to Arthur M. Brown and NIH training grant HL07676 to Ruth A. Schwalbe.)

Tu-Pos271

CLASS III ANTIARRHYTHMIC DRUGS BLOCK A CLONED HUMAN INWARD RECTIFIER POTASSIUM CHANNEL BY INTERACTING WITH THE PUTATIVE TRANSMEMBRANE SEGMENT M2. ((J. Kiehn, B.Wible, E. Ficker, M. Taglialatela, A. M. Brown,)) Rammelkamp Center for Research, Case Western Reserve University, Cleveland, OH

Dofetilide and D-sotalol are widely used Class III antiarrhythmic drugs and are Methansulfonanilide-derivatives. We have identified a cloned human inward rectifier K^+ channel (hIRK) as one molecular target for these compounds.

After removal of polyamines and Mg^{2+} from the intracellular side of the macropatches the outward-current of hIRK was blocked by Dofetilide and D-sotalol with IC_{50} = 533 nM and 717 nM respectively at 40 mV and 20°C. The block is strongly time-, voltage- and use-dependent and shows characteristics of an open channel block. Recovery from Dofetilide block is very slow with Tau of 1200 ms at - 80 mV membrane potential.

By using a chimeric approach and site-directed mutagenesis we mapped the residues responsible for slow unblocking of Dofetilide. We identified a single point mutation I177C which accelerated the unblocking 10 fold at - 80 mV. Thus this locus may be part of or tightly linked to the binding site for Dofetilide in hIRK. (supported by the "Deutsche Forschungsgemeinschaft" and NIH-grants HL-37044 and HL-36930).

Tu-Pos272

FUNCTIONAL MODULATION OF ROMK1 CHANNELS BY AN ATP-BINDING CASSETTE PROTEIN, CFTR, IN *XENOPUS* OOCYTES. ((A.Ruknudin, D.H Schulze, S.K. Sullivan*, W.J.Lederer, and P.A. Welling)) Departments of Microbiology/Immunology, Medicine and Physiology, Columbia Univ*, NYNY, and Univ. of Maryland, Baltimore, MD

Although the exact molecular nature of K_{ATP} channels remains unknown, an attractive hypothesis has emerged with the recent cloning of the pancreatic islet cell sulfonylurea receptor (SUR), a candidate β-islet cell K_{ATP} subunit. Specific members of the ATP-binding cassette protein family which bind glibenclamide, like SUR and the cytic fibrosis transmembrane regulator (CFTR), may functionally interact with a member of the inward-rectifier K channel family (Kir) to form K_{ATP}. We examined this hypothesis as applied to CFTR and ROMK1, a Kir channel and possible component of a renal epithelial K_{ATP} channel. When expressed alone in *Xenopus* oocytes, ROMK1 was insensitive to glibenclamide (up to 100μM), exhibited a high open-probability and a single channel conductance of 36 pS. CFTR was glibenclamide-sensitive and exhibited a single channel slope conductance of 10 pS. Whole cell currents in oocytes co-injected with ROMK1 and CFTR cRNA (molar ratios from 1:1 to 1:10 ROMK : CFTR), were K selective and inwardly-rectifying like ROMK1. Single channel analysis revealed, however, functional modulation of ROMK1 by CFTR. Newly expressed channels were K-selective, displayed a high open-probability, like ROMK1, but had an intermediate single channel slope conductance (≈17pS). Furthermore, P_{open} of the intermediate conductance K+ channel was rapidly reduced by half when 20 μM glibenclamide was applied to the cytoplasmic side of the patch, suggesting that ROMK1 acquired sensitivity to glibenclamide. In conclusion, we have demonstrated functional interaction of CFTR with ROMK1, a result which may provide some insight into the molecular makeup of K_{ATP}.

Tu-Pos273

CONDUCTANCE AND Ba^{2+} SENSITIVITY OF INWARD RECTIFIER HIR ARE pH SENSITIVE, WITH THE pH SENSOR LOCATED BETWEEN M1 AND H5 ((François Périer, Kathryn L. Coulter, Carolyn M. Radeke and Carol A. Vandenberg)) Neuroscience Research Institute and Dept. of Molecular, Cellular and Developmental Biology, University of California at Santa Barbara, Santa Barbara, CA 93106.

We have found that the inward rectifier potassium channel HIR (K_{IR} 2.3) is modulated by extracellular pH in the physiological range. In contrast, IRK1 (K_{IR} 2.1) is pH insensitive. These results suggest that HIR may be involved in modulation of cellular excitablility during periods of neuronal activity and during ischemic acidosis in cardiac and neuronal tissues when extracellular pH is altered. We present evidence that a proton-induced decrease in HIR single-channel conductance underlies the pH sensitivity of HIR observed at the macroscopic level, and accounts for the low single-channel conductance observed for HIR at physiological pH. Protons also influence the block of HIR by extracellular Ba^{2+}. The apparent rate and extent of Ba^{2+} block are reduced by protons, suggesting that occupation of the channel by protons prevents access of Ba^{2+} into the pore. We used HIR/IRK1 chimeric and mutant channels to localize the molecular determinant of HIR pH sensitivity to a single histidine residue, H117, in the H5-proximal section of the M1-to-H5 linker region. HIR pH sensitivity could be eliminated by substitution of H117 by E, the corresponding residue in the pH-insensitive IRK1 channel. We propose that H117 determines a specific molecular conformation that permits a group to be titrated by a proton, but does not provide the titratable group modulating HIR current, because substitution of H117 with non-titratable residues did not eliminate H^+ modulation of current. We present evidence that this titratable group is one of two conserved cysteines located in the M1-to-H5 and H5-to-M2 linkers.

Tu-Pos274

INHIBITORY INTERACTIONS BETWEEN TWO INWARD RECTIFIER K^+ CHANNEL SUBUNITS MEDIATED BY THE TRANSMEMBRANE DOMAINS. ((S.J. Tucker, C.T. Bond, P. Herson, M. Pessia & J.P. Adelman)), Vollum Institute for Advanced Biomedical Research, Oregon Health Sciences University, Portland, Oregon, 97201.

Expression of K_{ir} 4.1 (BIR10) in *Xenopus* oocytes results in inwardly rectifying K^+ currents whereas expression of K_{ir} 3.4 (CIR/rcKATP-1) results in little or no channel activity. We have demonstrated that coexpression of K_{ir} 4.1 with K_{ir} 3.4 causes a specific inhibition of the K_{ir} 4.1 current which is dependent upon the ratio of the coinjected mRNAs; a tenfold excess of K_{ir} 3.4 completely inhibits K_{ir} 4.1 currents (<5% control current). Using a panel of chimeras between K_{ir} 4.1 and K_{ir} 3.4 we have investigated this inhibitory effect and show that 1) it is mediated by interactions between the predicted transmembrane domains (TMs) of the two subunit classes and 2) that both TMs of K_{ir} 3.4 are necessary and sufficient for this inhibitory effect. Other subunits within the K_{ir} 3.0 family also exhibit this inhibitory effect on both K_{ir} 4.1 and the closely related K_{ir} 1.1 (ROMK-1). We have also demonstrated that the mechanism of inhibition is likely due to the cotranslational assembly of the two subunits into an 'inviable complex' which becomes degraded, rather than by formation of stable non-conductive heteromeric channels. These results provide insight into the assembly and regulation of inwardly rectifying K^+ channels and the domains which define their interactions.

Tu-Pos275

SUBUNIT POSITIONAL EFFECTS REVEALED BY NOVEL HETEROMERIC INWARDLY RECTIFYING K^+ CHANNELS. ((M. Pessia, S.J. Tucker, K. Lee, C.T. Bond & J.P. Adelman)), Vollum Institute, Oregon Health Sciences University, Portland, OR 97201.

Expression of K_{ir} 4.1 (BIR10) in *Xenopus* oocytes results in inwardly-rectifying potassium currents which exhibit a time-dependent decay at more negative potentials. In cell-attached patch recordings K_{ir} 4.1 channels rectify strongly and have a unit conductance of 12.3 ± 0.3 pS in the inward direction. K_{ir} 5.1 (BIR9) expression did not produce functional channels. However, coexpression of K_{ir} 5.1 and K_{ir} 4.1 resulted in whole cell currents markedly different from K_{ir} 4.1; the currents exhibited stronger rectification and a slow time-dependent component of activation (tau = 2.43 ± 0.11sec.) Cell-attached patches contained a principal conductance level of 43.2 ± 1.7pS. Chimeras between K_{ir} 5.1 and K_{ir} 4.1 showed that the differences in macroscopic kinetics were due, at least in part, to the C-terminal domain, and coexpression of K_{ir} 5.1 with six other cloned inward rectifier subunits was without effect. Expression of tetramers each containing two K_{ir} 4.1 and two K_{ir} 5.1 subunits, but with different relative positions (4-4-5-5 and 4-5-4-5), demonstrates that the relative positions of the different subunits profoundly affects channel activity. These results illustrate that K_{ir} 5.1 specifically associates with K_{ir} 4.1 to produce channels with distinct conductance and kinetic properties, and that the positions of the contributing subunits affect inward rectifier function.

Tu-Pos276

EFFECTS OF LOW INTRACELLULAR pH ON THE INWARD RECTIFIER K CHANNEL IRK1. ((S.A. John, R-C. Shieh, and J.N. Weiss)) UCLA School of Medicine, Los Angeles, CA 90095.

The effects of lowering intracellular pH (pH_i) on inward and outward currents through IRK1 channels were investigated in giant inside-out patches excised from oocytes expressing wild-type IRK1. In symmetrical 100 mM KCl and a Mg- and polyamine-free bath solution, currents were elicited by voltage clamp pulses from -80 to +70 mV from a holding potential of -30 mV, and subtracted from currents obtained in the presence of 30 mM internal TEA, which completely blocked IRK1 currents. Decreasing pH_i from 7.2 to 6.8, 6.4, 6.0 and 5.0 progressively decreased the amplitude of outward and inward currents. The block of IRK1 current by low pH_i had a pK_i of 6.25 and an Hill coefficient of 1.6, and was voltage-independent except at pH 6.4, where a shallow voltage-dependence was noted. Outward currents showed a persistent voltage-dependent inactivation even after prolonged (>5 min) washing in Mg- and polyamine-free bath solution, and the inactivation kinetics were not significantly altered at low pH_i. The block of IRK1 by low pH_i is similar to that described previously for inward rectifier K currents in starfish oocytes and skeletal muscle. Since decreases in pH_i of >1 unit are common in the setting of ischemia, our findings suggest that inhibition of IRK1 may contribute to cellular depolarization and its pathophysiological consequences during ischemia in tissues expressing these channels, such as heart and brain.

Tu-Pos277

CLONING OF A *XENOPUS* INWARDLY RECTIFYING K CHANNEL SUBUNIT THAT PERMITS GIRK1 EXPRESSION IN OOCYTES. ((K.E. Hedin, N.F. Lim, D.E. Clapham)) Department of Pharmacology, Mayo Foundation, Rochester, MN 55905.

Expression of GIRK1 in *Xenopus* oocytes yields an inwardly rectifying K current resembling I_{KACh}, the atrial G protein-gated inward rectifier. Yet, I_{KACh} was recently shown to be a heteromultimer of GIRK1 and CIR (Krapivinsky, et al., Nature, 374:135-141). Reasoning that an endogenous protein might be substituting for CIR in the oocyte expression system, we screened a *Xenopus* ovarian library with CIR probes and isolated a clone that encodes a protein 78% identical to CIR and that we called XIR. Coinjecting XIR and GIRK1 mRNAs into oocytes produced ACh-activated inwardly rectifying K currents much larger than the current observed in oocytes expressing either clone alone. Thus XIR, like CIR, can form heteromultimers with GIRK1. Also like CIR, coexpression of G protein $\beta1\gamma2$ subunits with the XIR yielded large agonist-independent currents indicative of constitutively activated channels. The ACh-stimulated current of oocytes expressing GIRK1 alone was decreased 80% by coinjecting antisense oligonucleotides specific for XIR, while the current in GIRK1/CIR expressing oocytes was unaffected. Furthermore, the single channel characteristics of XIR/GIRK1 were indistinguishable from those previously reported for GIRK1 channels expressed alone in oocytes. Thus, we conclude that GIRK1, without XIR or another CIR homologue, cannot efficiently form I_{KACh} channels in oocytes, and that the existence of native homomultimeric GIRK1 channels is unlikely. It is essential that future studies of G protein-regulated K channels take into account the tendency of GIRK1 to form I_{KACH}-like channels by combining with endogenous proteins. (Supported by NIH grant DK 49184-01P3 and NHLBI training grant HL07111-20P)

Tu-Pos278

SINGLE CHANNEL ANALYSIS OF BLOCK OF THE G-PROTEIN ACTIVATED POTASSIUM CHANNEL FROM RAT ATRIUM (KGA/GIRK1) BY THE C-TERMINAL PEPTIDE. ((T. Luchian[1], N. Dascal[2], N. Davidson[3], H.A. Lester[3] and W. Schreibmayer[1])) [1]: Institute for Medical Physics and Biophysics, University of Graz, Harrachgasse 21/4, A-8010 Graz, Austria. [2]: Department of Physiology and Pharmacology, Tel Aviv University, Ramat Aviv 61390, Israel. [3]: Biology Division, California Institute of Technology, Pasadena, CA 91125, U.S.A.

The DS6 peptide, comprising 17 amino acids from the carboxy-terminal end of the KGA/GIRK1 channel (aa 485-501), blocks the G-protein activated channel, heterologous expressed in oocytes of *Xenopus laevis* (Schreibmayer et al., 1995). In order to get insight into the interaction of the DS6 peptide with the activated channel, we recorded single channel currents from excised (inside out) membrane patches of oocytes and expressing only one functional channel. DS6 produced prolonged silent interburst intervals and also reduced burst duration were observed under the influence of DS6. Open times and closed times within a burst, were hardly affected by the peptide. Our data show that the high affinity block of the homooligomeric KGA/GIRK1 channel by DS6 is exerted by the peptide acting as blocker with slow on and off rates (time scale of seconds). Since the G-protein gated potassium channel from rat atrium is believed now to exist as a heterooligomer, containing the CIR/GIRK4 subunit in addition to KGA/GIRK1 (Krapivinsky et al., (1995)), we extended our analysis to heterooligomeric KGA/GIRK1//CIR/GIRK4 channels. Qualitatively the results were similar, the DS6 peptide exerting even higher affinity for the heterooligimeric channel (which contains less intrinsic DS6 elements).

Schreibmayer W., Dascal N., Davidson N. and H.A. Lester. Biophys. J. 68/2, A35 (1995).
Krapivinsky, G., Gordon, E.A., Wickman, K., Velimirovic, B., Krapivinsky, L. & Clapham, D.E. Nature 374, 135-141 (1995)

Supported by HFSP (RG-379/94), US-Israel BNSF, NIH, NIMH, Austrian National Bank (OENB 4992) and Austrian Research Foundation (SFB007).

Tu-Pos279

GENERATION OF I_{KATP} BY COUPLING OF BIR, A MEMBER OF THE INWARD RECTIFIER FAMILY, WITH THE SULFONYLUREA RECEPTOR. ((T. Gonoi, N, Inagaki, N, Namba, L. Aguilar-Bryan*, J. Bryan* and S. Seino)) Chiba University, Chiba 260, Japan, *Baylor Collage of Medicine, Houston, TX 77030, USA

K_{ATP} channels play a key role in insulin secretion of pancreatic β-cells by coupling metabolic activity to membrane potential. We have cloned a new member (BIR) of the inward rectifier K channel family from an insulin secreting mouse β-cell line, MIN6. Coexpression of BIR with the sulfonylurea receptor (SUR) generates ATP-sensitive K currents (I_{KATP}) in COS1 cells in excised inside-out patch-clamp configuration. The single channel conductance is 76 pS at -60 mV. ATP inhibits channel activity in a dose-dependent manner with IC50 of 10 μM. Channel activity is suppressed by the non-hydrolyzable ATP analog, AMP-PNP and glibenclamide, and is enhanced by diazoxide. Transfection of BIR or SUR alone does not generates I_{KATP}. Northern blot analysis reveals that BIR mRNA is expressed at high levels in pancreatic islets and insulin-secreting clonal cells MIN6 and HIT-T15, where SUR mRNA also is expressed at high levels. The present study shows that pancreatic β-cell K_{ATP} channels are a complex composed of at least two subunits, BIR and SUR.

Tu-Pos280

REGULATION OF THE MITOCHONDRIAL K_{ATP} CHANNEL BY PALMITOYL COA, ADENINE AND GUANINE NUCLEOTIDES, AND K^+ CHANNEL OPENERS ((Keith D. Garlid, Petr Paucek, and Vladimir Yarov-Yarovoy)) Dept. of Chemistry, Biochemistry, and Molecular Biology, Oregon Graduate Institute, Portland, OR 97291-1000

K_{ATP} channels are metabolic signalling devices, and disorders in their regulation may be involved in diabetes, obesity and cardiac ischemia. New evidence indicates that the mitochondrial K_{ATP} channel (mitoK_{ATP}) may be an integral component of this signalling pathway. MitoK_{ATP} is an intracellular receptor for diazoxide ($K_{1/2} \approx 0.4$ μM) and cromakalim ($K_{1/2} \approx 1$ μM). MitoK_{ATP} is blocked by ATP ($K_{1/2} \approx 25$ μM) and palmitoyl CoA ($K_{1/2} \approx 260$ nM), and activated by GTP ($K_{1/2} \approx 7$ μM) and GDP ($K_{1/2} \approx 140$ μM). We have demonstrated—using reconstituted mitoK_{ATP}, BLM, and intact mitochondria—that regulation by nucleotides and palmitoyl CoA is unipolar and mediated from the *cytosolic* side of the inner membrane. Preliminary evidence suggests that mitoK_{ATP} is a heteromultimer including a sulfonylurea receptor. Our results raise the possibility that ATP is *not* an important regulator of mitoK_{ATP} *in vivo*. We propose that the regulatory sites on each mitoK_{ATP} are always occupied by 2 or more ligands that have high affinity and reflect the metabolic state of the cell. The proposed ligands are long-chain acyl CoA esters and GTP. (Supported by NIH grant GM 31086.)

Tu-Pos281

REGULATION OF PARTIALLY PURIFIED K_{ATP} CHANNEL FROM CARDIAC SARCOLEMMA BY NUCLEOTIDES AND K^+ CHANNEL OPENERS ((Petr Paucek, Peter A. Schindler, Vladimir Yarov-Yarovoy and Keith D. Garlid)) Department of Chemistry, Biochemistry, and Molecular Biology, Oregon Graduate Institute, Portland, OR 97291-1000

We purified the cardiac sarcolemmal K_{ATP} channel (cellK_{ATP}) using methods developed for the mitochondrial K_{ATP} channel (mitoK_{ATP}) [Garlid et al. (1995) Methods Enzymol. 260, 331-349]. CellK_{ATP} was reconstituted into liposomes, and K^+ flux was assayed using the fluorescent probe PBFI. K^+ flux through cellK_{ATP} was inhibited by Mg-free ATP ($K_{1/2} = 639$ μM, $n_H = 1$) and glyburide ($K_{1/2} = 58$ nM, $n_H = 1$). ATP inhibition was reversed by the K^+ channel openers (KCOs) EMD57970 ($K_{1/2} = 3.8$ nM, $n_H = 3$), EMD60480 ($K_{1/2} = 22$ nM, $n_H = 3$), cromakalim ($K_{1/2} = 17$ μM, $n_H = 2$) and diazoxide ($K_{1/2} = 855$ μM, $n_H = 1$). The $K_{1/2}$ values for the benzpyranyl derivatives are remarkably similar to those observed with mitoK_{ATP}. In contrast, the $K_{1/2}$ value for diazoxide is 1000-fold higher for cellK_{ATP} than for mitoK_{ATP}. Purified cardiac cellK_{ATP} was incorporated into planar lipid bilayers and found to have a conductance of 27 pS under gradient conditions (800 mM KCl *cis*: 80 mM KCl *trans*). Conductance was blocked asymmetrically by ATP. *Trans* ATP (1 mM) inactivated this channel, whereas *cis* ATP had no effect. (Supported by NIH grant GM 31086.)

Tu-Pos282

DO INWARD AND OUTWARD RECTIFIER K^+ CHANNELS CO-ASSEMBLE ? A COMPARISON WITH THE TOK1 CHANNEL. ((J. Tytgat[1,2], S. H. Heinemann[3] and P. Daenens[2])) Lab. of Physiology[1] & Toxicology[2], University of Leuven, 3000 Leuven, Belgium. Max-Planck-Gesellschaft[3], z.F.d.W.e.V., AG Mol.& zell. Biophysik, 07747 Jena, Germany.

It is known that some K^+ channels can form heteromultimers through assembly of different types of subunits. Recently, an outwardly rectifying K^+ channel was described (TOK1; Ketchum *et al.*, *Nature* **376**:690 (1995)), with a hydropathy profile reminiscent of a *Shaker*-type channel attached to an inward rectifier-like channel. We have investigated whether inward and (delayed) outward rectifier K^+ channel subunits can assemble to produce functional channels. First, we constructed a tandem channel by covalently linking residue D249 in the C-terminus of the IRK1 channel to residue I43 in the N-terminus of the RCK1 (Kv1.1) channel. Secondly, we performed co-injection experiments in *Xenopus* oocytes with mRNA coding for IRK1 and RCK1. Two different protocols were applied in the presence of 2 and 100 mM $[K^+]_o$: V_{hold} 0 mV with V_{test} +60 to -160 mV, V_{hold} -90 mV with V_{test} -80 to +30 mV. The concatenated construct did not reveal functional expression in oocytes. In contrast, the co-injection experiments revealed K^+-selective currents, with characteristics that could be approximated by the algebraic sum of the 2 K^+ current types alone. These results suggest evidence neither for heteromultimer formation, nor for resemblance to the TOK1 channel.

Tu-Pos283

IDENTIFICATION AND ANALYSIS OF KAT1 POTASSIUM CHANNEL PORE MUTANTS USING A YEAST EXPRESSION SYSTEM ((Robert L. Nakamura, Julie A. Anderson, Richard F. Gaber)) Department of Biochemistry, Molecular Biology, and Cell Biology, Northwestern University, 2153 Sheridan Road, Evanston, IL 60208.

The pore is the most highly conserved region of voltage-gated K+ channels. This region between the fifth and sixth transmembrane domains is responsible for the cation selectivity of these channels. We have targeted the pore for mutagenesis using a yeast genetics system. A mutant strain of *S. cerevisiae* deficient in potassium uptake (*trk1Δ trk2Δ*) cannot grow on media containing low concentrations of K+. Potassium uptake via Kat1 in this strain confers growth on low K+. *KAT1* dependent growth is unaffected by the presence of potentially toxic concentrations of competing cations (Na+, Li+, Cs+, Ca++) in the media, consistent with the high selectivity of the channel. Saturation mutagenesis of the Tyr263-Gly264 "signature" sequence of the pore has revealed that an aromatic residue at position 263 is essential for wild-type selectivity. Many mutant channels confer sodium sensitivity on the cells suggesting increased sodium permeability. Examination of mutant channels in Xenopus oocytes by two electrode voltage-clamp has confirmed these findings. Through large scale mutagenesis we have screened thousands of mutants for altered ion selectivity in order to map the residues which contribute to the structure of the pore. In addition, selectivity of mutant Kat1 channels is being examined directly in yeast by electrophysiological methods in whole cell and single channel configurations.

Tu-Pos284

EFFECT OF CYTOPLASMIC pH ON THE GATING BEHAVIOR OF THE K^+ CHANNEL KAT1. ((T. Hoshi and I. Marten)) Dept. of Physiology and Biophysics, The University of Iowa, Iowa City, IA 52242.

The gating of the inward-rectifying potassium channel KAT1 can be modulated by the intracellular proton concentration. Lowering the cytoplasmic pH shifted the voltage dependence of the KAT1 gating properties to more positive potentials.

To study the internal pH effect on KAT1, we mutated the putative targets for protonation facing the cytosolic side. We examined the electrical features of wildtype and mutated channels expressed in *Xenopus* oocytes by using the macro-patch method.

We found that mutations of the histidine residue at position 118 in the S2-S3 linker region affected the gating characteristics of KAT1. A negatively charged residue at this position induced a shift of the half-activation potential to more negative potentials. H118D and H118E were sensitive towards cytoplasmic pH in a similar manner as the wildtype channel. The substitution to a positively charged residue (H118R) did not remove the internal pH effect on the voltage dependence of KAT1. In addition, the activation time course was faster in the presence of a positively charged amino acid than in the presence of a neutral or negatively charged residue at position 118.

These results may indicate that the effect of cytoplasmic protons on the voltage dependence of KAT1 is based on electrostatic interactions with H118 in the S2-S3 linker of this potassium channel.

(Supported by HFSP, NIH.)

Tu-Pos285

FUNCTIONAL COMPARISON OF PLANT ION CHANNELS EXPRESSED IN YEAST. ((Adam Bertl and Clifford L. Slayman)) Botanisches Institut I, Universität Karlsruhe (TH), Germany; and Department of Cellular and Molecular Physiology, Yale School of Medicine, New Haven CT, USA

The yeast *Saccharomyces cerevisiae* is a powerful tool both in screening of libraries for genes of membrane proteins and in examining the detailed functions of membrane proteins and their mutants: i.e., in structure-function studies. We have used yeast mutants lacking one or both of their two major K^+ uptake systems to characterize two isoforms of K^+ channel from the common thale cress (*Arabidopsis thaliana*) by patch-clamp techniques. Genes for these two channels, *KAT1* and *AKT1*, were originally identified in yeast-expression libraries by their ability to rescue K^+-defective yeast for growth on submillimolar K^+ (Anderson et al., *P.N.A.S.* **89**: 3736, 1992; Sentenac et al., *Science* **256**:663, 1992); and that rescue depended upon channel-type ionic currents (Bertl et al., *P.N.A.S.* **92**: 2701, 1995; Bertl, Sentenac, & Reid, in prep.).

Both genes express easily in yeast at high densities (~1000 channels per cell) compared with the native yeast K^+ channels (~100), and both types of channel (Kat1p, Akt1p) are small: 5-10 pS for Kat1p and ~25 pS for Akt1p, in 150 mM external KCl. Both are inward rectifiers, activating at *large* membrane voltages (neg. to -100 mV), and are K^+-selective, with P_K/P_{Na} = 10-20. The two differ, however, in their sensitivity to inhibitors, their detailed selectivity, and their rate of relaxation following critical changes. Thus, as judged from residual channel currents in the presence of mM Ba^{++} or TEA^+, barium ions block Akt1p more effectively than Kat1p, and vice versa for TEA^+. Cs^+ has proven the most potent inhibitor of Akt1p, blocking ~25% of channel current at 10 *μM*. More surprisingly, Akt1p--but *not* Kat1p--requires ~10 min to recover K^+ permeability following brief replacement of K^+ by NH_4^+; but Akt1p actually becomes hypersensitive to K^+ after brief replacement by Na^+. The relationships between such physiological differences and the obvious structural differences in the two channel proteins are being investigated.

Tu-Pos286

A MINIMAL POTASSIUM CHANNEL UNDERLIES THE SLOW K^+ CURRENT IN PIG OVARIAN GRANULOSA CELLS. ((Diane E. Mason, Marilyn G. Tomich, and Lisa C. Freeman)) Department of Anatomy and Physiology, Kansas State University, Manhattan, KS 66506-5602.

A slow K^+ current has been described in pig ovarian granulosa cells, and attributed to a Shaker-type K^+ channel (Mattioli et. al., *J Membrane Biol* 1993;134:75-83). However, the biophysical and pharmacological characteristics of this non-inactivating, time- and voltage-dependent K^+ current are more consistent with the hypothesis that the current is associated with a minimal K^+ channel (min-K) protein. The granulosa cell slow K^+ current is significantly inhibited by clofilium (100 μM) and azimilide (10 μM) but not 4-aminopyridine (1 mM). When reverse transcribed RNA from pig ovary or isolated granulosa cells is used in PCR with oligonucleotides based on conserved sequences in the coding regions of cloned min-K proteins, min-K reaction products of the expected sizes are consistently detected. These preliminary results support the hypothesis that a min-K protein underlies the slow K^+ current in pig granulosa cells. Elucidating the primary structure of this min-K protein will be important, because, in contrast to other min-K currents, the granulosa cell slow K^+ current is inhibited by agents that increase cAMP.

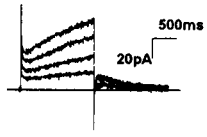

Tu-Pos287

EFFECTS OF THIMEROSAL ON THE SLOW DELAYED RECTIFIER CURRENT INDEPENDENT OF A COVALENT MODIFICATION OF SULFHYDRYL GROUPS. ((J-A Yao, B Zhu, G-N Tseng)) Dept. of Pharm., Columbia U., New York, NY

Thimerosal (TMS) has been used as a sulfhydryl-specific reagent to probe the functional roles of free -SH groups on ion channels. We studied the effects of TMS (50 μM) on a slow delayed rectifier current (hI_{sK}) in oocytes induced by a human IsK clone and the slow delayed rectifier current (I_{Ks}) in canine ventricular myocytes (CVM). Extracellular application of TMS increased hI_{sK} (by 85±24 % ±20 mV, n=6). This was mainly due to a negative shift in the voltage-dependence of channel activation. The threshold of hI_{sK} activation became more negative, and the apparent $V_{0.5}$ of activation was shifted from 22.2±4.2 to 13.3±2.0 mV. The hI_{sK} deactivation was slowed. TMS did not alter the reversal potential of hI_{sK}. The effects of TMS were reversible after washout and reproducible in the same oocytes, indicating that they were not due to a covalent modification of -SH groups. Another sulfhydryl reagent, DTDP (50 μM), did not have significant effects on hI_{sK}. In CVM, TMS also enhanced I_{Ks} (by 43+24% at +60 mV, n=4), along with a negative shift in the activation curve. The $T_{1/2}$ of deactivation at -20 mV was prolonged from 145±34 to 285±84 ms. We conclude that TMS has an "agonist" effect on hI_{sK} in oocytes and I_{Ks} in CVM by stabilizing the activated state of the channels. This was independent of -SH group modification, suggesting that caution should be exercised when using TMS as a "specific" sulfhydryl reagent.

Tu-Pos288

DIFFERENTIAL TERFENADINE SENSITIVITIES OF HERG AND Kv1.5 SUGGEST A POSSIBLE MECHANISM FOR CARDIOTOXIC EFFECTS. ((M.-L. Roy, R. Dumaine, M. Sanguinetti*, M. Keating*, and A.M. Brown.)) Rammelkamp Center for Research, MetroHealth Med. Center, Case Western Reserve University Sch. of Med., Cleveland, OH 44109, and *Cardiology Division, Univ. of Utah Health Sci. Center, Salt Lake City, UT 84112.

Terfenadine, a widely used antihistamine, has often been associated with QT prolongation and *torsades de pointes* when simultaneously administered with the fungicide ketoconazole, a drug known to alter first-pass hepatic metabolism. In heart, terfenadine blocks I_{kr} and I_{ksr} currents in the nM and submicromolar concentration ranges, respectively. Recent work has provided strong evidence linking I_{ksr} (a component of the classical I_K) to Kv1.5, a member of the *Shaker* K^+ channel family, and I_{kr} to HERG. We heterologously expressed Kv1.5 and HERG in Xenopus oocytes to compare their sensitivities to terfenadine. Currents were recorded using the two-electrode voltage clamp technique.

The block of HERG steady-state and tail currents showed an apparent K_d of 354 nM, similar to that reported for atrial I_{kr}. In contrast, we found a K_d of 5 μM for Kv1.5. The block reached a steady-state faster on HERG (<7 min) than Kv1.5 (>20 min). We did not observe use- or voltage-dependent block for either channel. Our results provide new evidence linking HERG to I_{kr} and suggest that HERG may play a primary role in terfenadine cardiotoxicity.

Supported by A.H.A. (Northeastern Ohio Affiliate) to M.L.R. and NS 23877 to A.M.B..

Tu-Pos289

INSTANTANEOUS AND TIME-DEPENDENT COMPONENTS OF RECTIFICATION OF H-*ERG* EXPRESSED IN *XENOPUS* OOCYTES. ((Shimin Wang, Michael J. Morales, Shuguang Liu, Harold C. Strauss and Randall L. Rasmusson)) Duke Univ. Med. Ctr., Durham, NC

h-*erg* has been demonstrated to display inward rectification in response to a depolarizing pulse. A recent study has suggested that rectification involves a time- and voltage-dependent rapid inactivation process due to the presence of a rising phase or "hook" at the onset of deactivation tail currents. However, there have been no direct measurements of the time- and voltage-dependent properties of rectification at depolarized potentials. We measured the instantaneous current to voltage relationship for h-*erg* channels using the saponin permeablized variation of the cut-open oocyte clamp technique. We devised a three pulse protocol to activate the current and remove inactivation that allowed us to analyze both instantaneous current and the time course of decay. h-*erg* channels were activated with a 600 ms P1 pulse to +50 mV. The potential was then stepped to a P2 potential of -80 mV for 60 ms (i.e. until the peak of the tail current) to remove most of the inactivation without allowing much deactivation. A final 100 ms P3 pulse was applied in 10 mV steps to potentials between -100 and +50 mV. Analysis of instantaneous current amplitude during the P3 pulse showed substantial inward rectification in the region positive to -20 mV. Instantaneous rectification was present in symmetric or asymmetric $[K^+]_o$ (98 or 2 mM). The time dependent or inactivation mediated component of rectification during a single pulse was dominant in producing the negative slope region of conductance. This time dependent component was strongly voltage sensitive with time constants of 14 ms at -20 mV and 3 ms at +50 mV (n=3). This time dependent component was slowed by 98 mM $[K^+]_o$ (28 and 12 ms at -20 and +50 mV, respectively). The increased rate of inactivation at depolarized potentials and previously reported increased rate of removal of inactivation at hyperpolarized potentials is difficult to reconcile with a Woodhull type blocking particle model and therefore suggests that channel conformational changes modulate inactivation.

Tu-Pos290

MAMMALIAN EXPRESSION OF *HERG* REVEALS HIGH AFFINITY TO DOFETILIDE. ((A. Chaudary and D.J. Snyders)) Vanderbilt University, Nashville, TN 37232. (Spon. by J.A. Johns)

The biophysical properties of *HERG* currents expressed in oocytes resembled those of the I_{Kr} component in cardiac myocytes but the current lacked methanesulfonanilide sensitivity. Another report suggested that *HERG* behaves more as a traditional inward rectifier. Because these discrepancies could be caused by the *Xenopus* oocyte expression system, we examined *HERG* currents expressed in HEK293 cells using the lipofectamine approach. Transfected cells identified by the coexpressed green fluorescent protein displayed outward potassium currents with a reversal potential of -85±0.6 mV (n=9, K_o=4 mM). Activation kinetics were strongly voltage-dependent: τ=2.0±0.2 s at -20 mV and 188±21 ms at +20 mV. Midpoint and slope factor for channel activation were -15.5±1.7 mV and 7.2±0.3 mV, respectively. Marked inward rectification was observed beyond +10 mV, and the tail currents at -40 mV displayed an initial rising phase with τ=10 ms, followed by a multiexponential decline. The rising phase is consistent with rectification due to fast inactivation. The EC_{50} for block by dofetilide (DOF) was 12±2 nM. Induction of block depended on depolarization beyond the threshold for channel opening and developed with τ=3-4 min with 30 nM DOF. This suggested open channel block, but no tail current cross-over or other significant changes in voltage-dependent channel properties were observed. The affinity and kinetics for *HERG* block by DOF closely resemble those for I_{Kr} block in cardiac myocytes. These results indicate that the *HERG* gene product encodes an α-subunit that, when expressed in mammalian cells, displays both the major functional and pharmacological properties of native I_{Kr}. Supported by HL47599 and HL46681.

Tu-Pos291

THE N-TERMINUS OF A K^+ CHANNEL β SUBUNIT (KVβ3) INCREASES THE RATE OF C-TYPE INACTIVATION IN AN N-TERMINAL DELETION MUTANT OF A KV1.4 α SUBUNIT (FK1). ((Randall L. Rasmusson, Jonny O. Wee, Robert C. Castellino, Harold C. Strauss and Michael J. Morales)) Duke University Medical Center, Durham, NC

Kvβ1 has been demonstrated to increase inactivation rate of Kv1 K^+ channels through a "ball and chain", or N-type, mechanism. Kvβ3 increases the rate of inactivation of some but not all Kv1 α subunits. Deletion of the N-terminal of a Kv1.4 channel (FK1Δ2-146) uncovers an inactivation process consistent with C-type inactivation. Co-expression of FK1Δ2-146 with Kvβ3 in *Xenopus* oocytes decreased the time constant of inactivation from 1795±81 ms to 409±27 ms at +50 mV (n=11,10) as measured using the two-electrode voltage clamp technique. Inactivation of FK1Δ2-146+Kvβ3 was slower than would be predicted for most N-type inactivation rates. Inactivation of FK1Δ2-146+Kvβ3 showed several characteristics that were consistent with C-type inactivation of FK1Δ2-146: 1) Inactivation of FK1Δ2-146+Kvβ3 was incomplete at depolarized potentials (61%±1.9%, n=6, 5 sec pulses); 2) The inactivation rates of both FK1Δ2-146 and FK1Δ2-146+Kvβ3 were greatly slowed by increasing external [K^+] from 2 to 98 mM; 3) Mutation of a *lys* to a *tyr* at position 532 (K532Y) near the C-terminal side of the external mouth of the channel pore largely removed C-type inactivation from FK1Δ2-146 and rendered the inactivation rate insensitive to co-expression with Kvβ3 (n=4); and 4) Kvβ3 did not alter the recovery rate of FK1Δ2-146 (n=4,5). To examine the role of the Kvβ3 N-terminus on C-type inactivation, we formed a chimeric construct of the first 79 N-terminal amino acids of Kvβ3 and FK1Δ2-146. This chimeric construct showed a faster inactivation rate that was also sensitive to extracellular K^+. The inactivation rate of this chimeric construct was reduced by the K532Y mutation. Our results suggest that one consequence of Kvβ3 association with Kv1.4 α-subunits is to increase the rate of C-type inactivation and that the N-terminal of Kvβ3 acts intracellularly to effect this increase.

Tu-Pos292

CLONING AND FUNCTIONAL CHARACTERIZATION OF THE Kvß1.3 SUBUNIT ((S.K.England, V.N. Uebele, J.V. Kodali, P.B. Bennett, and M.M. Tamkun)) Dept. Molecular Physiology and Biophysics and Pharmacology, Vanderbilt University, School of Medicine, Nashville, Tennessee 37232.

Voltage-gated K^+ channels can form multimeric complexes with accessory ß-subunits. We report a new K^+ channel ß-subunit cloned from human heart, hKvß1.3, that has 74-83% overall identity with previously cloned ß-subunits. Comparison of hKvß1.3 with the previously cloned hKvß3 and rKvß1 proteins indicates the C-terminal 328 amino acids are identical, while unique variable length N-termini exist. Analysis of human ß-subunit cDNA and genomic nucleotide sequences confirm that these three ß-subunits are alternatively spliced from a common ß-subunit gene. Co-expression of hKvß1.3 in *Xenopus* oocytes with the delayed rectifers rKv1.1 and hKv1.5 indicate that this ß-subunit has distinct effects on members of this subfamily. Kvß1.3 conferred a partial inactivation on both rKv1.1 and hKv1.5 during voltage steps to positive membrane potentials and slowed deactivation by 2-fold at -40 mV in both channels. In addition, hKvß1.3 modified the hKv1.5 current by: 1) converting the outwardly rectifying current-voltage relationship to one showing strong inward rectification and, 2) inducing a 13 mV hyperpolarizing shift in the hKv1.5 activation curve. These two effects were not seen with rKv1.1. Mutants lacking the variable N-terminal region of hKvß1.3 had no functional effects on hKv1.5. Further mutational analysis of N-termini of Kvß1.3 will determine the domains responsible for the inactivation and rectification properties.

Tu-Pos293

FUNCTIONAL DIFFERENCES IN hKv1.5 CURRENTS EXPRESSED IN MAMMALIAN CELL LINES ARE DUE TO THE PRESENCE OF ENDOGENOUS Kvß2.1 SUBUNITS. ((V.N. Uebele, S.K. England, A. Chaudhary, D.J. Snyders and M.M. Tamkun)) Dept. Pharmacology, Vanderbilt University, School of Medicine, Nashville, Tennessee 37232.

The voltage-gated K^+ currents observed following hKv1.5 α subunit expression in HEK 293 and mouse L-cells differ in the voltage dependence of activation and degree of slow inactivation. Molecular cloning, immunopurification and Western blot analysis demonstrated that an endogenous L-cell Kvß2.1 subunit assembled with transfected hKv1.5 protein. In contrast, both mRNA and protein analysis failed to detect a ß subunit in the HEK 293 cells, suggesting that functional differences observed between these two systems are due to endogenous L-cell Kvß2.1 expression. In the absence of Kvß2.1, midpoints for activation and inactivation of hKv1.5 in HEK 293 cells were -0.2±2.0 mV (n=8) and -9.6±1.8 mV (n=6), respectively. When hKv1.5 was coexpressed with Kvß2.1 these values were -14.1±1.8 mV (n=9) and -22.1±3.7 mV (n=5), respectively. The activation kinetics were also shifted leftward on the voltage axis. The ß subunit also caused a 1.5-fold increase in the degree of slow inactivation at +50 mV, thus reconstituting the L-cell current phenotype in the HEK 293 cells. These results indicate that 1) ß subunits are not required for α subunit expression, 2) the Kvß2.1 subunit alters Kv1.5 α subunit function, and 3) endogenous ß subunits are expressed in heterologous expression systems used to study K^+ channel function. These expression systems provide useful tools to study alpha-beta subunit assembly in a mammalian cellular environment.

CALCIUM CHANNELS II

Tu-Pos294

1,25-DIHYDROXYCHOLECALCIFEROL (1,25-$(OH)_2D_3$) REDUCES INTRACELLULAR CALCIUM STORES AND ENHANCES STORE DEPENDENT CALCIUM INFLUX (SDCI) IN HL-60 CELLS. ((J.P. Gardner, M. Balasubramanyam and G.P. Studzinski)) UMDNJ-New Jersey Medical School, Newark, NJ 07103.

1,25-$(OH)_2D_3$ induces promyelocytic HL-60 cells to differentiate towards monocyte-like cells. During differentiation, increased cytosolic Ca (Ca_i) and expression of surface receptors for chemotactic factors "prime" the cell for activation and triggering of the respiratory burst pathway. We examined whether the Ca store/SDCI pathway contributed to altered Ca_i following exposure of HL-60 cells to 10^{-7} M 1,25-$(OH)_2D_3$. In cells suspended in Ca-free medium, peak $\Delta[Ca]_i$ values elicited by ATP-induced Ca mobilization occurred with similar EC_{50} values ([ATP]≅275 nM) in 72hr 1,25-$(OH)_2D_3$- and vehicle (EtOH)-treated cells, however, peak $\Delta[Ca]_i$ was reduced ~55% in differentiated cells. Decreased Ca mobilization was associated with a 25-35% reduction in intracellular Ca store size, determined in cells in Ca-free solution challenged with thapsigargin (Tg, 100 nM) or ionomycin/Tg. 1,25-$(OH)_2D_3$-treated cells exposed to 100 μM ATP or Tg in Ca-free medium for 3 minutes with subsequent addition of 1 mM Ca exhibited a respective 0.8-1.2-fold stimulation in ΔCa_i response compared to nondifferentiated cells. Enhanced SDCI was also seen in 1,25-$(OH)_2D_3$-treated cells as an increase in the rate of Mn entry after exposure to ATP or Tg. Finally, the increase in SDCI appeared within 8 hrs of 1,25-$(OH)_2D_3$-treatment and before the elevation of Ca_i or decrease in intracellular Ca stores. These alterations in Ca homeostasis are significantly different from DMSO- (neutrophil) differentiated HL-60 cells. Upregulation of the Ca store/SDCI pathway during 1,25-$(OH)_2D_3$-induced differentiation may contribute to monocyte maturation or cell activation processes.

Tu-Pos295

VOLTAGE-DEPENDENT AND SPONTANEOUS ELEVATIONS OF FREE CYTOPLASMIC CALCIUM CONCENTRATION MEDIATED BY T-TYPE CALCIUM CHANNELS IN NON-OBESE DIABETIC MOUSE TUMOR ß-CELLS. ((L. Wang, A. Bhattacharjee and M. Li)) Dept. of Pharmacology, U. of South Alabama College of Medicine, Mobile, AL 36688. (Spon. by A.E. Taylor)

Previous studies have shown that non-obese diabetes (NOD) mouse pancreatic ß cells and the cell line derived from the NOD ß cells (NIT-1) express high levels of T-type calcium currents. Here we document profound increases in intracellular free calcium concentration mediated by T-type calcium channels. By using fluorescence imaging and current-clamp techniques, we have demonstrated the roles of T-type currents in both voltage-dependent and spontaneous elevations of cytoplasmic free calcium. Nickel (200 μM) blocked 75% of the calcium influx induced by 30 mM KCl, whereas nickel had little effect on the calcium influx in βTC-3 cells. The blockade effect of nickel remained in a more depolarizing condition (50 mM KCl), suggesting that T-type calcium currents play a crucial role in calcium influx at a wide range of membrane potentials. Current-clamp studies revealed that the mechanism of T-type calcium channels involved a decrease of the latency of action potential onset and an increase in the frequency of the action potentials. Nickel (100 μM) also blocked spontaneous calcium activity of the cells measured with fluorescence imaging method and decreased the spontaneous electrical activity of the cells. These results suggest that T-type calcium channels increases calcium influx in both a voltage-dependent and a spontaneous manner in NIT-1 cells. Abnormal expression of T-type calcium channels may be factorial in altered calcium homeostasis, thereby leading to ß cell destruction.

Tu-Pos296

DOES SODIUM-HYDROGEN EXCHANGE INFLUENCE CALCIUM CHANNEL CURRENTS IN DORSAL ROOT GANGLION NEURONS?
((L. Polo-Parada, M.J Callahan and S.J. Korn)) Physiol. and Neurobiol., University of Connecticut, Storrs, CT 06269

Elevation of intracellular calcium (Ca) in many neurons, including chick dorsal root ganglion neurons (DRGs), causes intracellular acidification. Under some conditions, Ca channel currents can be inhibited by reduction of intracellular pH (pH_i) by as little as 0.1 unit (see companion poster). We are investigating whether cellular mechanisms that regulate pH_i influence Ca channel function. In the absence of bicarbonate transport, DRGs maintained a resting pH_i of 7.39 ± 0.03 (n=49 @ 30°C). Reduction of external Na^+ or addition of EIPA (100 μM; an inhibitor of Na^+/H^+ transport), caused a slow reduction of resting pH_i and prevented recovery from NH_4^+-induced acid load. Addition of intracellular BAPTA had little or no effect on resting pH_i but prevented acidification produced by reduction of Na^+ or addition of EIPA. In perforated patch recordings, Ca current stimulation (100 ms, 0.1 Hz) produced a slow intracellular acidification of about 0.15 pH units with little associated change in Ca current magnitude. This acidification was prevented by inclusion of intracellular BAPTA, and reduced when the Ca current duration was reduced. With smaller Ca currents (50 ms duration), application of EIPA enhanced Ca current-induced acidification. These results suggest that Na^+-H^+ transport may reduce acidification associated with Ca channel activity. We are currently investigating whether this transporter protects Ca channels from any Ca-induced acidification that does occur. *Supported by the Whitaker Foundation, NSF and the UCONN Research Foundation.*

Tu-Pos297

SENSITIVITY OF N-TYPE CALCIUM CHANNELS TO INTRACELLULAR pH DEPENDS ON THE ACTIVITY OF ANOTHER CALCIUM CHANNEL MODULATOR.
((M.J. Callahan, L. Polo-Parada and S.J. Korn)) Physiol. and Neurobiol., Univ. Connecticut, Storrs, CT 06269

Previous reports from our lab and others demonstrated that calcium (Ca) currents in chick dorsal root ganglion neurons (DRGs) are sensitive to intracellular pH (pH_i) ; acidification inhibits currents and alkalinization potentiates currents. We are investigating the physiological conditions under which this modulation may be relevant. We used both standard whole cell and perforated patch recordings on chick DRGs loaded with BCECF to study modulation of N-type Ca channel currents. In standard whole cell recordings, Ca current magnitude increased in a graded fashion between pH_i 7.0 and 7.5. This pH-sensitivity was highly sensitive to control Ca current density; cells with lower current density were more sensitive to changes in pH_i and cells with high current density were insensitive to pH_i. Intracellular inclusion of 5 mM BAPTA increased control current density but did not qualitatively affect these results. When currents were recorded with the perforated patch technique in the absence of exogenous Ca chelators, currents were never affected by pH_i changes in this same range, regardless of control current density. However, inclusion of BAPTA in perforated patch recordings resulted in a decreased control Ca current density and marked pH_i-sensitivity. The rate of change in Ca current magnitude was slow relative to the rate of change of pH_i. Taken together, these data suggest that the pH_i-sensitivity of N-type Ca channels depends on the activity of a Ca-dependent Ca channel modulator. *Supported by the Whitaker Foundation, NSF and the UCONN Research Foundation.*

Tu-Pos298

REDOX MODULATION OF L-TYPE CALCIUM CHANNELS IN FERRET VENTRICULAR MYOCYTES: DUAL INDIRECT AND DIRECT MODULATION BY CYCLIC GMP AND S-NITROSYLATION.
((D.L. Campbell, J.S. Stamler, and H.C. Strauss)) Duke University Medical Center, Durham, NC, USA 27710.

Naturally occuring N-oxides (NO_x) and S-nitrosothiols (RSNO) could potentially modulate cardiac L-type calcium current, ICa,L, by two mechanisms: (i) an indirect effect via activation of guanylate cyclase, and (ii) a direct effect upon the L-channel or an associated subunit(s). Cellular redox state could also be an important determinant of underlying mechanism. We tested for indirect versus direct effects of extracellularly applied NO_x and RSNO on basal whole cell ICa,L in ferret right ventricular myocytes (gΩ seal patch clamp). The effects of 0.1-1 mM SIN-1 (which generates both NO and O_2^-, which combine to form $OONO^-$) were complicated, in that it could either increase (6/12 myocytes) or decrease (6/12) peak ICa,L (0 mV). However, 1 mM SIN-1 plus superoxide dismutase (1000-3000 u/ml) produced a consistent moderate inhibition of ICa,L (n = 3). 10-100 μM 8-Br-cGMP consistently decreased ICa,L, consistent with the hypothesis that NO indirectly inhibits ICa,L. In contrast, both 1 mM S-nitrosoglutathione (GSNO) and 1 mM S-nitrosocysteine (CySNO) consistently increased ICa,L, suggesting the presence of an extracellular regulatory "redox switch" site that is not responsive to NO but is capable of reacting with S-nitrosothiols. To test this hypothesis we altered extracellular sulfhydryl redox state. 1-5 mM dithiothreitol (DTT), a sulfhydryl reducing agent, caused a consistent inhibition of ICa,L which could be reversed by 200 μM 5,5'-dithio-bis[2-nitrobenzoic acid]) (DTNB), a thiol oxidizing agent. The stimulatory effects of both GSNO and DTNB could be reversed by 1-5 mM DTT. Our results indicate that: 1) both indirect (cGMP-dependent) and direct (S-nitrosylation-dependent) channel subunit systems are involved in modulation of ICa,L; 2) NO and S-nitrosothiols exhibit discrete and opposite activities on ICa,L; and 3) Ca^{2+} homeostasis in ventricular myocytes is redox regulated.

Tu-Pos299

PREACTIVATED PTX-SENSITIVE G-PROTEINS INDUCE VOLTAGE-DEPENDENT INHIBITION OF N-TYPE CALCIUM CURRENT IN RAT SYMPATHETIC NEURONS
((Ingrid Ehrlich & Keith S. Elmslie)) Dept. of Physiology, Tulane University Medical Center, New Orleans, LA 70112

N-type calcium current can be inhibited by neurotransmitters in a voltage-dependent manner. It is hypothesized that this inhibition occurs through direct G-protein-channel coupling. The voltage dependence is thought to result from disruption of G-protein-channel coupling. However, the G-protein subunit mediating this inhibition is unknown. Before testing individual subunits, we wanted to demonstrate that heterotrimeric G-proteins preactivated with GTPγS could inhibit calcium current.

PTX-sensitive G-proteins (α plus βγ) were applied intracellularly via the patch pipette while monitoring calcium current using the whole-cell patch clamp technique. Dialysis with 5 or 10 nM G-protein resulted in voltage-dependent inhibition of calcium current. Control experiments showed that the G-protein buffer alone (which included β-mercaptoethanol, ethylene glycol, and the detergent Thesit) did not induce current inhibition. Proteolysis of the G-proteins with trypsin abolished their effect on calcium current. Unlike our G-protein buffer, another buffer containing the detergent CHAPS and the reducing agent dithiothreitol (DTT) induced calcium current inhibition even in the absence of preactivated G-proteins. This effect was not blocked by GDPβS. These results demonstrate that whole-cell dialysis can be used to intracellularly apply active G-protein subunits to induce voltage-dependent inhibition of N-type calcium channels.

Supported by PhRMA and AHA-LA affiliate.

Tu-Pos300

REGULATION OF L-TYPE CALCIUM CURRENT BY cGMP IN RABBIT VENTRICULAR CELLS.
((Rajiv Kumar and Ronald W. Joyner)) Department of Pediatrics, Emory University, Atlanta, GA, 30322

We studied cGMP-mediated regulation of L-type Ca^{2+} current (I_{Ca}, pA/pF) in isolated adult (AD) and newborn (NB, 1-4 day old) cells using whole cell patch clamp. I_{Ca} was elicited by a depolarizing pulse to +15 mV from a holding potential of -40 mV. In NB cells perfusion of 30 μM 8BrcGMP or 10 μM 8-Chlorophenylthio-cGMP (8CPT-cGMP), which are more potent activators of cGMP dependent protein kinase than cGMP, increased basal I_{Ca} in NB cells from 2.4±0.2 pA/pF to 4.3±0.3 pA/pF, ($p<0.004$, n=6). However, in AD cells even 100 μM 8BrcGMP had no effect on basal I_{Ca}. Methylene blue (MB, 0.1-100 μM), an inhibitor of G-cyclase, was used to decrease intracellular cGMP levels. In NB cells, concentrations of MB ≥ 1 μM produced significant irreversible inhibition of basal I_{Ca} from 2.4±0.2 to 0.85±0.2 pA/pF ($p<0.005$, n=5) and 0.55±0.08 pA/pF ($p<0.003$, n=3) by 10 and 100 μM MB, respectively). MB even at 100 μM had no significant effect in AD cells. In NB cells, the inhibitory effect of MB on I_{Ca} was completely blocked by the presence of 8BrcGMP in the pipette. 8BrcGMP also increased I_{Ca} even after inhibition by MB. Protein kinase inhibitor peptide (PKI, 1 μM), inhibited basal I_{Ca} by 40-60 % and blocked the stimulatory effect of 30 μM cAMP in NB cells, but internal perfusion of 8CPT-cGMP was still able to increase I_{Ca}. In NB cells, 0.1 μM Isoproterenol produced only a 50-70 % increase in basal I_{Ca} , but this effect was enhanced in the presence of 30 μM cGMP or 8BrcGMP. These studies clearly show that cGMP plays a crucial role in regulation of basal and β-adrenergic stimulated I_{Ca} in NB cells. This suggests that the effects of cGMP are not antagonistic of cAMP on I_{Ca} in NB cells and the role of cGMP in the regulation of I_{Ca} in NB cells is fundamentally different than in the AD cells.

Tu-Pos301

MODULATION OF SINGLE SMOOTH MUSCLE L-TYPE Ca^{2+} CHANNELS BY PURIFIED PROTEIN PHOSPHATASES TYPE 1 AND 2A.
((K. Schuhmann and K. Groschner)) Dept. of Pharmacology and Toxicology, University of Graz, Universitätsplatz 2, A-8010 Graz, Austria.

Gating behavior of L-type Ca^{2+} channels is thought to be determined in large part by phosphorylation/dephosphorylation of proteins of the channel complex. We studied the effects of protein dephosphorylation on the function of single L-type Ca^{2+} channels in excised inside-out patches obtained from human umbilical vein smooth muscle. Dephosphorylation was induced by cytoplasmic application of purified serine/threonine protein phosphatases type 1 (PP1) or 2A (PP2A). Single-channel currents were recorded with 10 mM Ba^{2+} as charge carrier. Calpastatin (1 U/ml) was used to stabilize channel activity in inside-out patches. Exposure of inside-out patches to PP2A (2 U/ml) substantially suppressed channel activity, while exposure to PP1 (2 U/ml) slightly increased channel activity. Both protein phosphatases were found equally effective in terms of dephosphorylation of p-nitro-phenyl-phosphate under the conditions employed in patch-clamp experiments, and okadaic acid (1 μM) completely prevented PP2A-induced inhibition.

Our results support the idea that PP2A and PP1 dephosphorylate distinctly different regulatory sites at smooth muscle L-type Ca^{2+} channels, and suggest that specific patterns of phosphorylation correspond to specific functional states of the channel.

Supported by the Austrian Research Funds (S6605)

Tu-Pos302

Modulation of the Cloned Skeletal Muscle L-type Ca^{2+} Channel by Anchored cAMP-Dependent Protein Kinase. ((B.D. Johnson, J.P. Brousal, T. Scheuer and W.A. Catterall)) Dept. of Pharmacology, University of Washington School of Medicine, Seattle, WA 98195-7280. (Spon. by T. Hinds)

Ca^{2+} influx through the skeletal muscle Ca^{2+} channel regulates the force of contraction in response to adrenergic stimulation and high frequency stimulation. Modulation of the skeletal muscle Ca^{2+} channel by cAMP-dependent phosphorylation and by depolarizing prepulses was reconstituted and analyzed for cloned Ca^{2+} channel transiently expressed in the tsA-201 cells. Cloned Ca^{2+} channel gave currents which were similar in time course, current density, and dihydropyridine sensitivity to native Ca^{2+} channel in the CB3 skeletal muscle cell line. Tail currents following depolarizations decayed with a time course which was slowed 2-3 fold as depolarizations increased from 0 mV and +60 mV and was slowed 4-7 fold following longer depolarizations to +80 mV for times between 5 and 75 ms. PKA stimulation by Sp-5,6-DCL-cBIMPS (cBIMPS) increased currents through both native and expressed channels 2-4 fold. The rapid time- and voltage-dependent slowing of tail currents required the activity of PKA, as it was enhanced by cBIMPS and reduced by a peptide PKA inhibitor and also required anchoring of PKA by A Kinase Anchoring Proteins (AKAPs), as it was blocked by the AKAP peptide HT-31. Comparison of channel activation and deactivation time courses before and after application of cBIMPS suggests that the expressed channel may be more heavily phosphorylated at rest than the native channel. (Supported by the MDA).

Tu-Pos303

MIBEFRADIL (Ro 40-5967) IS A SELECTIVE BLOCKER OF MYOCARDIAL T-TYPE *vs.* L-TYPE Ca CHANNELS.
((Eric A. Ertel)) F. Hoffmann - La Roche, CH-4002 Basel, Switzerland.

Mibefradil (Ro 40-5967) is a recently developed Ca antagonist from a new chemical class (tetralene) which, unlike diltiazem or verapamil, is able to relax vascular muscle and slow heart rate without reducing cardiac contractility. Mibefradil blocks vascular T-type Ca channels more potently than L-type (Mishra & Hermsmeyer, 1994). Because its cardiac properties might also stem from selectivity towards T-type Ca channels, I used whole-cell patch-clamp on freshly dissociated guinea pig atrial myocytes to examine cardiac Ca currents. I find that mibefradil blocks T-type Ca channels (IC_{50} ≈ 3 μM from a holding of -90 mV) with >10-fold higher potency than L-type (<20% block at 10 μM). When L- and T-type Ca channels are separated based on their different deactivation rates, the higher potency of mibefradil on T-type is apparent from the complete block of the slowly-decaying tail current and slight block of the rapidly-decaying component (Fig). Furthermore, block is voltage-dependent. With 10 μM, the availability (h_∞) curve for L-type Ca channels is shifted ≈10 mV more negative, indicating more potent block at depolarized voltages. At 3 μM, the curve for T-type Ca channels is also shifted ≈10 mV. In conclusion, the cardiac properties of mibefradil may result from selectivity for T-type Ca channels, combined with voltage dependence of block. In the heart, mibefradil would block only T-type Ca channels, leading to bradycardia without negative inotropy.

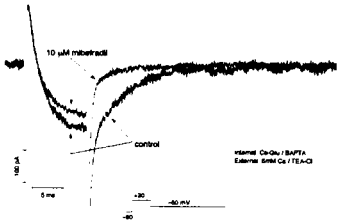

Tu-Pos304

Human Atrial Plateau Inward Currents Are Large, Stable, And Increased by Sub-nanomolar Ibutilide. Kai S. Lee & Esther W. Lee. Cardiovascular Pharmacology, Upjohn Laboratories, Kalamazoo, MI 49007

Human atrial plateau inward currents have not been well characterized, especially their pharmacology. We studied the plateau inward current in human atrium and compared it to that of guinea-pig under identical conditions. Human atrial cells were freshly isolated from atrial tissues of patients that had undergone heart surgery. Guinea-pig atrial cells were obtained using standard methods (Lee et al, *Nature* 278:269-271,1979,). Using the suction pipette method (Lee et al, *Nature* 265:751-753, 1977), cells were perfused internally and externally with Cs^+ at 37° C, and held at -40 mV. Step depolarization beginning at -20 mV elicited an inward current that peaked to -1861±49 pA at 20 mV, with sustained inward current of -264±9 pA at 50 ms. The human inward current was stable, with less than 10% "run-down" in 30 minute's recording time. In contrast, the corresponding values for guinea-pig atrial cells having similar capacitance were -412±15.4 pA, -142±7 pA, and 10 minutes. Ibutilide fumarate, a highly potent class III antiarrhythmic compound in clinical trials, activated the human atrial inward current concentration-dependently beginning at 10^{-10}M, reached maximal at 10^{-8}M where the peak and sustained inward currents at 20 mV became -2264±56 and -394±39 pA respectively. The ibutilide induced inward current was sensitive to external Na^+ and Ca^{2+}. We conclude that the freshly isolated human atrial cell provides a robust, stable and clinically relevant preparation for the characterization of native human inward ion channels and for the study of important therapeutic drugs.

Tu-Pos305

VOLTAGE DEPENDENCE AND KINETICS OF THE ACTION OF VERAPAMIL ON CALCIUM CURRENT IN RAT VENTRICULAR MYOCYTES.
((H. Nawrath and J.W. Wegener)) Department of Pharmacology, University of Mainz, D-55101 Mainz, Federal Republic of Germany.

The voltage- and time-dependent effects of verapamil (1 μM) on L-type calcium current (I_{Ca}) were investigated in rat ventricular myocytes using the whole cell voltage clamp method. Verapamil reduced the magnitude of I_{Ca} without changing the time course of the current. The application of twin pulses (interval 100 ms) showed that the duration of the first pulse significantly determined the magnitude of I_{Ca} during the second pulse. Variation of the first pulse between 12 and 3000 ms revealed the time-dependent onset of block, described by τ_{on}=370 ms at 0mV and by τ_{on}=240 ms at +20mV. When the interval duration between the two test pulses was varied between 1 ms and 60 s, a time-dependent offset of block was observed, described by τ_{off}=8100 ms at -80 mV. Recovery of I_{Ca} under control conditions was described by τ=13 ms. A computer simulation of drug association and dissociation, taking into account the described time constants of verapamil of binding at 0 mV and unbinding at -80 mV, predicted well the development of block at 0.2 Hz (τ=7s) and 1.0 Hz (τ=1.7 s), using 180 ms depolarizing pulses to 0 mV. When the inactivation of I_{Ca} was partially removed by Ba^{2+}, the effect of verapamil was abolished. It is proposed that verapamil binds to calcium channels in their inactivated state at more positive potentials and dissociates from the channels in the resting state at more negative potentials.

Tu-Pos306

EFFECTS OF SEVOFLURANE ON THE CARDIAC L-TYPE Ca^{2+} CURRENT. ((G.C. Rehmert, Z.J. Bosnjak, W.M. Kwok)) Department of Anesthesiology, Medical College of Wisconsin, Milwaukee, WI 53226. (Spon. by X. Xu)

We examined the effects of a volatile anesthetic, sevoflurane (Sevo), on the cardiac L-type calcium current ($I_{L\text{-}Ca}$) in guinea pig ventricular myocytes. Under whole-cell patch clamp conditions Sevo inhibited peak $I_{L\text{-}Ca}$ by 24± 4%, 36±8%, 76±6% at 0.5 mM (n = 12), 0.9 mM (n = 6), and 1.9 mM (n = 6), respectively. After stimulation of $I_{L\text{-}Ca}$ with 0.5 μM forskolin, the inhibitory action of Sevo (9 mM) was less effective, blocking peak $I_{L\text{-}Ca}$ by 19.0±5.6% (n=3). In contrast, the ability of Sevo to depress $I_{L\text{-}Ca}$ was not affected by 0.1 μM isoproterenol. In the presence of 0.9 mM Sevo alone, the steady-state inactivation curve shifted to more hyperpolarizing potentials by 8.7±1.8 mV. In the continued presence of Sevo, $V_{1/2}$ was further shifted by -15.6± 1.6 and -13.3±2.4 mV in the presence of forskolin (n=3) and isoproterenol (n=3), respectively. In the absence of Sevo, forskolin (n=3) and isoproterenol (n=3) shifted the inactivation $V_{1/2}$ by -10.3±0.8 and -7.7±2.2, respectively. The rate of recovery from inactivation was also determined in the presence of 0.5 mM Sevo. Compared to control, Sevo slowed the rate of recovery from inactivation by 32±8 msec (n=6). The time constant of current inactivation was also slowed by 10.0±2.1 msec in the presence of 0.5 mM Sevo (n=6). Our results suggest that Sevo may preferentially bind to the inactivated state of the L-type Ca^{2+} channel. Furthermore, the result that the inhibition of $I_{L\text{-}Ca}$ by Sevo is less effective in the presence of forskolin, but not isoproterenol, may indicate an interaction between the two molecules in the lipid membrane due to their lipophilic properties.

Tu-Pos307

PHARMACOLOGICAL CHARACTERIZATION OF CAFFEINE-SENSITIVE RYANODINE RECEPTORS IN SEA URCHIN EGGS ((Andrew J. Lokuta[1], Carmen Beltran[2], Alberto Darszon[2] and Hector H. Valdivia[1])) [1]University of Wisconsin-Madison and [2]Instituto de Biotecnología, UNAM, Cuernavaca, México. (Sponsored by Matthew Wolff).

The presence of an intracellular calcium release channel in sea urchin eggs with properties similar to sarcoplasmic reticulum calcium release channels of striated muscle (i.e. ryanodine receptors, RyR) has been documented by several groups, but direct single channel recordings and a definite pharmacological profile of RyR in sea urchin eggs has not yet been provided. We carried out [^{3}H]ryanodine binding assays in sea urchin eggs (*L. pictus* and *S. purpuratus*) and studied the effects of classical modulators of striated muscle RyRs. A single class of high-affinity, Ca^{2+}-sensitive, [^{3}H]ryanodine binding site was detected in purified cortical microsomes under conditions of high ionic strength (0.5 M KCl). The binding affinity (K_D) was 13 ± 2.6 nM and the maximal density of receptor sites (B_{max}) was 2.4 ± 0.3 pmoles/mg. The activating effect of Ca^{2+} was sigmoidal and monophasic, having a threshold for detection at pCa 9 and saturating at pCa 5. Caffeine (10 mM) stimulated [^{3}H]ryanodine binding at low nanomolar [Ca^{2+}] but had little effect at 10 μM [Ca^{2+}]. Thus, similar to the effect with striated muscle RyR, caffeine stimulates [^{3}H]ryanodine binding in a Ca^{2+}-dependent manner. However, unlike striated muscle RyRs, a direct effect of calmodulin, cyclic ADP-ribose and ATP could not be detected, suggesting that the capacity of these modulators to release Ca^{2+} in whole sea urchin egg homogenates is the result of the combined action of several cytosolic modulators. Additional experiments including single channel recordings in planar lipid bilayers and immunoblot analysis of this Ca^{2+} release channel are underway. Supported by AHA, NIH, CONACyT and the HHMI.

Tu-Pos308

ROLE OF FATTY ACIDS IN Ca^{2+} SEQUESTRATION WITHIN INTRACELLULAR Ca^{2+} POOLS. ((K.E. Rys-Sikora and D.L. Gill)) Department of Biological Chemistry, University of Maryland School of Medicine, Baltimore, MD 21201.

A specific and sensitive GTP-activated translocation process mediates transfer of Ca^{2+} between $InsP_3$-insensitive and $InsP_3$-releasable Ca^{2+} pools. In the presence of oxalate, GTP-activated Ca^{2+} transfer results in a substantial increase in Ca^{2+} accumulation through the entry of oxalate into the $InsP_3$-releasable pool and formation of an insoluble Ca^{2+}-oxalate complex. Using permeabilized DDT_1MF-2 smooth muscle cells, it has been shown that fatty-acyl CoA derivatives (specifically palmitoyl- and myristoyl-CoA) completely reversed this GTP-mediated translocation process resulting in the termination of Ca^{2+}accumulation. In conjunction with these studies, the corresponding fatty acids were examined. Surprisingly, 10-100 μM palmitate (C16:0) had a major effect on GTP-mediated Ca^{2+} accumulation. The biphasic nature and PEG-dependence of the palmitate effect was characteristically similar to the effect of oxalate; however, the EC_{50} for palmitate was ~20 μM — at least 100-fold lower than that of oxalate. This activation of Ca^{2+} accumulation was highly specific for chain length and degree of saturation. Only pentadecanoic acid (C15:0) duplicated this effect; myristate (C14:0) was slightly effective whereas unsaturated fatty acids including palmitoleate (C16:1) were completely ineffective. Palmitate had no effect on mitochondrial Ca^{2+} uptake or on the Ca^{2+} leak rate induced by the addition of 3μM thapsigargin. Although the mechanism of action of these fatty acids on GTP-mediated Ca^{2+} accumulation is not known, preliminary data showed that both palmitate- and oxalate- activated Ca^{2+} accumulation in the presence of GTP was inhibited by the anion transport inhibitor 4,4'-diisothiocyanatostilbene-2,2'-disulfonic acid (DIDS). This may indicate passage of palmitate into a anion-permeable Ca^{2+} subpool wherein a Ca^{2+}-palmitate complex is formed. This activation on Ca^{2+} accumulation may reflect a significant physiological role for fatty acids in stabilizing Ca^{2+} within the lumen of Ca^{2+} pools. (NIH grant NS19304; NSF grant MCB 9307746).

Tu-Pos309

MN^{2+}-PERMEABILITY AND REGULATION BY CYTOSOLIC MN^{2+} OF THE INOSITOL-1,4,5-TRISPHOSPHATE RECEPTOR (IP_3R). ((Frank Striggow and Barbara E. Ehrlich)) Department of Physiology, University of Connecticut Health Center, Farmington, CT 06030-1305

We studied the permeability of Mn^{2+} through the IP_3R and the ability of this ion to affect the channel properties, because Mn^{2+} has been often used to quench intracellular fura-2 fluorescence. After incorporation of the IP_3R (cerebellum) into planar lipid bilayers, 55 mM Mn^{2+} on the *trans* (luminal) side of the channel was used as current carrier. Channel openings with a mean amplitude of 0.8 pA and a mean open time of 4.1 ms were observed after addition of 0.5 mM ATP, 200 nM Ca^{2+} and 2 μM IP_3 to the *cis* (cytosolic) side. The single channel conductance for Mn^{2+} was 17 pS. Thus, Mn^{2+} can be added at the end of the permeation sequence of the IP_3R: Ba^{2+} (88 pS) > Sr^{2+} (77 pS) > Ca^{2+} (53 pS) > Mg^{2+} (42 pS). In order to test the ability of cytosolic Mn^{2+} to regulate the IP_3R we used Ba^{2+} as the current ion, activated the IP_3R with 0.5 mM ATP and 2 μM IP_3, and increased stepwise the concentration of Mn^{2+} (*cis*). Mn^{2+} influenced the IP_3R open probability in a bell-shaped manner. In contrast to the steep bell-shaped dependence observed with cytosolic Ca^{2+}, the curve showed a wide plateau with maximum activation between 1 and 10 μM free Mn^{2+}. We conclude that Mn^{2+} can bind to both activating and inhibitory Ca^{2+} binding sites of the IP_3R. These binding sites have different selectivity sequences suggesting they are structurally different. Furthermore, the concentration of Mn^{2+} used to quench fura-2 fluorescence in studies of the IP3R must be chosen carefully.

Tu-Pos310

CALCIUM DEPENDENCE OF THE CEREBELLAR IP3R USING BARIUM AS THE CURRENT CARRIER
((E. J. Kaftan and B. E. Ehrlich)) Univ. of CT, Farmington, CT

The bell-shaped calcium dependence of the inositol 1,4,5-trisphosphate receptor (IP3R) has been shown to be important for cell signaling and calcium waves. Previous studies have shown that the entire sequence of activation and inhibition occurs within the expected physiological range of cytosolic calcium when maximal concentrations of IP3 were used [Bezprozvanny, Nature 351:751, 1991]. In addition, it has been suggested that calcium flowing through the channel could regulate activity by influencing the calcium concentration at the cytoplasmic regulatory binding sites of the channel. To address these issues we compared the bell-shaped dependence of the IP3R using barium as the current carrier. Additionally, we determined the effect of decreasing the IP3 concentration. We found that channel open probability when measured with 2 μM cytoplasmic IP3 exhibited a steep dependence on free cytoplasmic calcium concentration (Hill coefficient =2.3) with maximal activity occurring at 255 nM regardless of the current carrier. When these experiments were conducted at lower concentrations of IP3, less calcium was required to fully inhibit the channels. These results have allowed us to further separate the regulatory effects of IP3 and calcium on IP3R function.
Supported by NIH (HL33026) and the Patrick and Catherine Weldon Donaghue Medical Research Foundation.

Tu-Pos311

A NOVEL CALCIUM INFLUX PATHWAY INDUCED BY POOL DEPLETION ((C.A. Ufret-Vincenty, A. Alfonso and D.L. Gill)) Department of Biological Chemistry, University of Maryland School of Medicine, Baltimore, MD 21201.

Ca^{2+} influx through store-operated channels (SOCs) activated rapidly after Ca^{2+} pool depletion represents an important component of Ca^{2+} signals generated in cells. Here, we examine a new and distinct Ca^{2+} influx component which can be activated in cells after Ca^{2+} pools are emptied for a longer period of time using the intracellular Ca^{2+} pump inhibitors, thapsigargin (TG) or 2,5-di-*tert*-butylhydroquinone (DBHQ). Both blockers cause depletion of intracellular Ca^{2+} pools and cell growth arrest; upon refilling of pools, normal cell-cycle progression is resumed (Short, A.D., et al. PNAS 90, 4986-4990, 1993). Ca^{2+} homeostasis in growth-arrested DDT_1MF-2 cells subjected to TG- or DBHQ-treatment was investigated using the Ca^{2+}-sensitive dye, fura-2. In DDT_1MF-2 smooth muscle cells the SOC-mediated Ca^{2+} influx component after emptying Ca^{2+} pools is short-lived and appears to be rapidly deactivated. After long-term treatment (30 min or more) of DDT_1MF-2 cells with either 3 μM TG or 10 μM DBHQ, 10 mM caffeine induces a large transient influx of Ca^{2+} distinct from SOC-mediated Ca^{2+} entry. Caffeine has no effect in untreated DDT_1MF-2 cells. The disappearance of caffeine-induced Ca^{2+} influx is different for TG- and DBHQ-treated cells. Upon removal of DBHQ from DBHQ-arrested cells, bradykinin-sensitive Ca^{2+} pools immediately refill and cells become insensitive to caffeine. Reversal of TG-induced growth arrest with either high (20%) serum or 1-10 μM arachidonic acid, in each case allows agonist-sensitive Ca^{2+} pools to refill concomitantly with disappearance of caffeine-induced Ca^{2+} influx. In summary, the results show that the Ca^{2+} influx pathway activated by caffeine is observed under conditions of growth arrest induced by either TG or DBHQ and appears to be directly correlated with depletion of intracellular Ca^{2+} pools. (NIH grants NS19304 and GM15407; NSF grant MCB 9307746).

Tu-Pos312

IDENTIFICATION OF A HUMAN TRP HOMOLOG EXPRESSED PREDOMINANTLY IN THYMUS ((Xi Zhu, Michael Peyton, Ning Qin and Lutz Birnbaumer)) UCLA, Los Angeles, CA 90095-1778

Mutation of a photoreceptor Ca^{2+} permeable channel in *Drosophila* results in a transient receptor potential (*trp*). When expressed in either insect *Sf*9 or mammalian cells, the trp gene encodes a protein that permeates Ca^{2+} in response to store depletion. Therefore, mammalian homologues of trp may form Ca^{2+} influx channels which replenish the internal Ca^{2+} stores following receptor-stimulated intracellular Ca^{2+} release. Previously, using an Expressed Sequence Tag (EST) as a probe, we cloned a cDNA encoding a human trp gene (htrp-1) and found that it is expressed in most human tissues. Further analysis of the dbEST database revealed the existance of several fragments that may encode human trp homologues. Using one of them, EST R34716, we have now isolated a full-length cDNA that has an open-reading frame encoding a polypeptide of 821 amino acids. Part of its nucleotide sequence is also identical to EST D61017. Protein sequence alignment and phylogenetic analysis suggest that this human Trp (Htrp-3) is as related to Htrp-1 as it is to the Trp proteins found in *Drosophila* and *C. elegans*. As Htrp-1 and the *C. elegans* Trp, Htrp-3 shows, by hydropathy analysis, 7 putative transmembrane segments and a relatively short C-terminal tail. Northern analysis revealed that the mRNA for htrp-3 is 4 Kb long and it is present mainly in thymus, with very low amounts being present also in kidney, liver, lung, skeletal muscle, placenta, testis, and prostate. Htrp-3 is thus an additional candidate for non-voltage gated Ca^{2+} channels involved in store-operated Ca^{2+} entry. Its predominant expression in thymus suggests that it may be responsible for Ca^{2+} influx following intracellular Ca^{2+} release seen in T-cell activation.

Tu-Pos313

SUBUNIT TURNOVER OF Ca CHANNELS IN CEREBELLAR GRANULE CELLS TRANSFECTED WITH ANTISENSE OLIGONUCLEOTIDES. ((R.C. Lambert, Y. Maulet, J.L. Dupont, S. Volsen* and A. Feltz)) Neurobiologie Cellulaire, CNRS, 5 rue B. Pascal, 67084 Strasbourg, France; * Lilly Res. Centre Ltd, Surrey GU 20 6PH, U.K..

Antisense oligonucleotides strategy was used to deplete cultured granule cells of the cerebellum from the constitutive subunits of their Ca channels. The cells were transfected after 4 days in vitro by fluorescent phosphorothioate oligonucleotides. The effect of a generic β-subunit antisense was estimated by patch-clamp recordings in whole cell configuration, using 5 mM Ba in the extracellular medium and adding 1 mM ATP in the pipette solution. Ca current density recorded in granule cells tranfected with anti-β oligonucleotides or scrambled oligonucleotides were compared. As illustrated, Ca current was maximally decreased by 54 %, 4 days after transfection and recovered to almost initial amplitude 3 days later. In addition to this decrease in current density, knock out of the Ca channel β-subunits shifted the activation curve of the current to depolarized potentials and slowed down both activation and inactivation kinetics of the channels. Finally, anti-β oligonucleotide transfection decreased the neurite development of the cells as assessed by capacitance measurement: anti-β transfected cells had a capacitance of 5.8 pF 4 days after transfection to be compared to 7.7 pF in scrambled oligonucleotides treated cells. Experiments are presently run to estimate α1 subunits turnover.

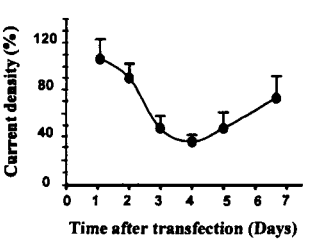

Tu-Pos314

REGULATION OF CLONED CARDIAC L-TYPE Ca CHANNELS EXPRESSED IN BABY HAMSTER KIDNEY (BHK) CELLS: A MODEL OF CELLULAR SIGNALING SYSTEM. ((Y.Hirano[1], T.Yoshinaga[2], S.Zhang[1], T.Niidome[2], K.Katayama[2] & M.Hiraoka[1])) [1]Dept.Cardiovasc.Dis., MRI, Tokyo Medical and Dental Univ. & [2]Eisai Tsukuba Research Lab. JAPAN

After introduction of cDNA of cardiac α_1 subunit, skeletal β and α_2/δ subunit, baby hamster kidney cells express functional Ca channels stably and in high density (BHKC12 cell line). Single channel recordings indicate that the properties of the cloned Ca channel in BHKC12 cells are almost identical to those of native cardiac L-type Ca channels, including voltage dependence of activation, unitary conductance, modulation by DHPs and up-regulation by 8Br-cAMP or pholbor esters. As in native cardiac Ca channels, changes in kinetic behavior during 8Br-cAMP application included increased number and duration of channel openings. PMA also increased the number of openings with long duration. These results indicate that BHK cells are equipped with endogenous kinases that regulate cloned Ca channels. We then examined whether these regulations could function or not when exogenous receptors that activate kinases are coexpressed. After coexpression of α_1 adrenergic receptors (using expression vector pBC containing the bovine α_{1C} receptor DNA, kindly supplied by Dr.Lefkowitz), application of phenylephrine successfully increased Ca channel activity. We conclude that BHK cells provide a useful expression system where the modulations, signal transduction systems and biophysical aspects of Ca channels can be studied at the single channel level.

Tu-Pos315

MOLECULAR CLONING OF A FUNCTIONAL *XENOPUS* OOCYTE CALCIUM CHANNEL β SUBUNIT. ((M.J. Roux, E. Tareilus, N. Qin, L. Birnbaumer, E. Stefani)) Department of Anesthesiology, UCLA School of Medicine, Los Angeles, CA 90095-1778.

Xenopus oocytes are widely used as an expression system to characterize cloned molecules, such as voltage-gated channels. Regarding calcium channels, cRNA injection of most of the cloned α_1 subunits (α_{1A} through α_{1E}, but not α_{1S}) is sufficient to induce Ca^{2+} currents, though the co-injection of an auxiliary β subunit usually enhances the current levels. It has thusfar been assumed that an α_1 subunit is sufficient to form a functional calcium channel. We report here the molecular cloning of a voltage-gated calcium channel β subunit from *Xenopus* oocytes. Its deduced amino acid sequence predicts a protein of 484 amino acids that most closely resembles the mammalian type 3 β subunit. This subunit (β3xo) appears to be expressed as an active protein in the oocyte on the basis of the following findings: 1. Injection of a *Xenopus* β subunit antisense oligonucleotide, but not a sense oligonucleotide, leads to significant reduction of endogenous oocyte voltage-activated Ca^{2+} channel currents. 2. The same maneuver prevented the normal expression of cardiac and neuronal Ca^{2+} channels (α_{1C} and α_{1E}). 3. Antisense oligonucleotides did not interfere with expression of a co-injected K^+ channel (*Shaker* B). 4. Injection of mammalian or *Xenopus* β subunit cRNA rescued α_{1E} Ca^{2+} channel currents in oocytes co-injected with *Xenopus* β subunit antisense oligonucleotides. 5. Co-injection of α_{1C} and α_{1E} subunits cRNA with the full length β3xo subunit cRNA resulted in facilitation of Ca^{2+} channel currents as happens with mammalian β subunits.
The total suppression of α1 expression caused by β subunit antisense oligonucleotides suggests an obligatory role for β subunit(s) in calcium channel assembly. The modulation of calcium channel currents by injected β3xo indicates a dual role for the β subunit(s): assembly at low concentrations and channel modulation at higher concentrations.
Supported by NIH grants to LB and ES (AR-43411 and AR-38970)

Tu-Pos316

MOLECULAR CHARACTERIZATION OF THE ENDOGENOUS CALCIUM CHANNELS OF *XENOPUS LAEVIS* OOCYTES. ((J.-H. Lee, L. Cribbs, and E. Perez-Reyes)) Loyola University Medical Center, Chicago, IL 60153.

Xenopus laevis oocytes provide an excellent system for the expression of exogenous proteins, including calcium channels. A major disadvantage to oocytes is that they express endogenous calcium channels. Surprisingly the functional expression of these channels is modified by the injection of mammalian calcium channel subunits. Specifically, the beta subunits of calcium channels can amplify the currents detected in oocytes 3- to 5-fold. In addition to increasing the amount of endogenous current detected, betas also modify the time course of inactivation. Our previous studies, performed in collaboration with Drs. Lacerda and Brown, indicated that betas altered the kinetics of both an N-type and a putative T-type channel (Biophys. J. 66:1833, 1994). We have used a PCR approach to identify which types of calcium channels are expressed at the mRNA level. Degenerate PCR primers were designed based on conserved regions found in all six of the known α_1 types. Partially purified poly(A+)RNA was reverse transcribed into cDNA, then used for PCR. The PCR product was subcloned and sequenced. Our results indicate that at least 5 α_1 genes are expressed in *Xenopus laevis* oocytes. Currents studies are evaluating the abundance of these messages and how this correlates with the pharmacological profile of the currents.

Tu-Pos317

Do chromaffin cells have capacitative Ca^{2+} influx ?

((Matthias Bödding & Reinhold Penner)), Max-Planck-Institute for Biophysical Chemistry, Department of Membranebiophysics, 37077 Göttingen, Germany

In non excitable cells, agonist-induced changes in $[Ca^{2+}]_i$ typically consist of a rapid transient increase mediated by release from intracellular stores, followed by a sustained plateau phase due to Ca^{2+} influx. A small and selective Ca^{2+} current (I_{CRAC}), which is closely linked to the filling state of IP_3 sensitive Ca^{2+} stores, is responsible for the secondary plateau phase. In excitable cells a similar influx pathway has not yet been identified, although similar biphasic changes in $[Ca^{2+}]_i$ are observed in bovine adrenal chromaffin cells following histamine stimulation. We probed for the possible presence of store-operated influx pathways in these excitable cells by combining the whole-cell patch-clamp recordings together with fura-2 fluorimetry.Procedures that are usually employed to activate I_{CRAC} in non excitable cells, i.e., active store depletion by ionomycin (10 μM), IP_3 (10 μM), caged IP_3 (400 μM) as well as passive depletion by perfusing high concentrations of EGTA (10-20 mM) or blocking Ca^{2+} ATPases by thapsigargin (1-10 μM) or 2,5-di-tert-butylhydrochinon (10 μM) all failed to generate CRAC-like currents in chromaffin cells. However, some of the treatments modified voltage-activated Ca^{2+} currents. Finally, the similarity of $[Ca^{2+}]_i$ patterns induced by the receptor agonist histamine (10-20 μM) in the presence and absence of extracellular Ca^{2+} suggest that a substantial part of the plateau phase is not only due to Ca^{2+} influx. In conclusion, our results do not support the view that depletion-activated Ca^{2+} currents play a major role in these neuroendocrine cells, although a modulation of voltage-dependent currents is a possibility.

SODIUM CHANNELS: STRUCTURE, FUNCTION AND REGULATION

Tu-Pos318

EFFECTS OF MUTATIONS AT GLYCINE AND PROLINE RESIDUES IN THE III-IV LINKER ON Na^+-CHANNEL INACTIVATION. ((S.-F. Chen[1], R. Dumaine[2] and G.E. Kirsch[2])) [1]Dept. of Molecular Physiology and Biophysics, Baylor College of Medicine, Houston, TX 77030; [2]Rammelkamp Center for Research, MetroHealth Medical Center, Cleveland, OH 44109.

Naturally occurring mutations involving glycine and proline residues in the cytoplasmic linker between domains III and IV of Na^+ channels have been found in human genetic diseases. We have conducted mutational analysis at three glycines and one proline in the III-IV linker of human heart (hH1a) Na^+ channel, to assess the role of the flexibility at these residues in fast inactivation. Substitution of alanine at G1480 resulted in ~1.7-fold slower inactivation and ~1.5-fold faster recovery but no change in the voltage dependence of activation, suggesting that the energy barrier for the conformational transition from noninactivated form to inactivated form of the III-IV linker is increased by G1480A. Valine substitution at P1505 exhibited a small but significant negative shift in the half inactivation potential but no change in the half activation potential. P1505V also showed ~2-fold faster inactivation but no remarkable change in the recovery rate, suggesting that the proline imposes a higher energy barrier for the inactivation transition of the III-IV linker. These results suggest that G1480 and P1505 of hH1a Na^+ channel are involved in a conformational transition during inactivation. A new model of the III-IV linker, termed "buried-to-exposed conversion" model, is proposed here to explain the molecular mechanism of fast inactivation of Na^+ channel.

Tu-Pos319

PROBING S4-S5 REGIONS OF THE RAT BRAIN SODIUM CHANNEL FOR THE FAST INACTIVATION PARTICLE RECEPTOR SITE. ((M.R. Depp and A.L. Goldin)) Physiology and Biophysics, University of California, Irvine, CA 92717.

The IFM1488-90 amino acid residues in the III-IV linker of the rat brain sodium channel have been shown to be important for fast inactivation, and may form the nucleus of a fast inactivation particle (West et al., 1992, PNAS 89:10910-10914). However, the receptor site for this particle has not been identified. The *Shaker* potassium channel has both structural and sequence homology to the sodium channel. For the *Shaker* channel, the amino terminus functions as an inactivation particle, and the S4-S5 linker forms part of the docking site for the particle (Isacoff et al., 1991, Nature 353:86-90). We have scanned the corresponding S4-S5 regions of the sodium channel for amino acids that might be involved in forming the receptor site for the sodium channel inactivation particle. By making triple amino acid changes to glutamine, we attempted to disrupt hydrophobic interactions with the particle. The mutant channels were co-expressed with the β1 subunit in *Xenopus* oocytes, and the electrophysiological properties of the channels were examined by two-electrode voltage clamping. The mutant channel ALL1329-1331QQQ inactivated more slowly than the wild type channel, with a pedestal of current maintained for more than 200 msec. Single mutations were made to identify the specific residue causing this disruption in inactivation. While L1330Q and L1331Q demonstrated inactivation kinetics similar to those of the wild type channel, A1329Q showed much slower inactivation. Finally, we have constructed compensatory mutations to show a direct interaction between the residues at 1329 and 1489 during inactivation.

Tu-Pos320

Electrophysiological characterization of a novel myotonia causative mutation in the human muscle sodium channel.

((R. Fleischhauer, A.L. George*, H. Lerche, N. Mitrovic, F. Lehmann-Horn)) Dept. of Applied Physiology, University of Ulm, Germany and *Depts. of Medicine and Pharmacology, Vanderbilt University, Nashville, TN, USA. (Spons. by W.Vogel)

Point mutations in the gene encoding the α-subunit of the adult human muscle sodium channel cause three clinically different syndromes: paramyotonia congenita (PC), hyperkalemic periodic paralysis (HyperPP) and potassium-aggravated myotonia (PAM). A mutation at nucleotide position 1473, resulting in the substitution of Ser for Phe located between the fourth and fifth segment in the fourth channel domain, causes PC. Wild type (WT) and Phe1473Ser sodium channels were permanently expressed in HEK293 cells and electrophysiologically characterized using the whole-cell patch-clamp technique. The sodium current decay was best fitted by a double exponential function giving two time constants of inactivation (τ_{s1},τ_{s2}). The inactivation of the mutant channels was significantly slower as compared with WT (e.g. at 0mV Phe1473Ser vs. WT; τ_{h1}, 0.87 ± 0.04 vs. 0.46±0.02ms). The steady-state inactivation curve of the mutant channels was shifted by 17.5mV to depolarizing potentials. As compared with the results on other PC mutants (Yang et al. 1994) a striking difference in recovery from inactivation was observed, being approximately four times faster than the WT (e.g. at -100mV τ_r was 0.46 ±0.04ms for Phe1473Ser and 1.86±0.13ms for WT). The voltage-dependence was the same in the range examined (-60 to -140 mv) and the current-voltage curves for WT and mutant channels were almost identical. The observed changes demonstrate the importance of Phe1473Ser in sodium channel inactivation gating.

Tu-Pos321

Paramyotonia congenita: a study of the R1448P sodium channel mutation in native human skeletal muscle and by expression in HEK cells

((N. Mitrovic, H. Lerche, A.L. George*, F. Lehmann-Horn)). Dept. of Applied Physiology, University of Ulm, D-89069 Ulm and *Depts. of Medicine & Pharmacology, Vanderbilt University, Nashville, TN, USA.

The human sodium channel mutation R1448P in the putative voltage sensor IV/S4 causing paramyotonia congenita was studied in a native muscle biopsy and in an expression system. In-vitro force measurements revealed that weakness upon cooling in paramyotonia occured when the depolarizing sodium inward current reached a certain level, since a hyperpolarizing potassium channel opener was able to antagonize the weakness to a certain degree. Patch clamp on sarcolemmal blebs and HEK293 cells expressing the mutant channel showed a hyperpolarizing shift of the inactivation curve with a reduced steepness and a distinctly slower decay of the sodium current compared to controls. A quantitative analysis of these parameters of native and expressed channels indicated that about 40% of the sodium channels occurring in native muscle were mutated (50% would be expected from the dominant mode of inheritance). Steady-state sodium currents were slightly but significantly increased and increased further upon cooling. Single channel recordings revealed that the slowing of the current decay was induced by an increased number of channel reopenings. The results suggest that the distinctly slowed sodium current decay is responsible for the clinically observed paradoxical myotonia. The weakness might be explained by a combination of a left-shifted inactivation curve and an increased steady-state sodium inward current.

Tu-Pos322

A MINOR CONTRIBUTION OF DIVALENT CATION BINDING SITES IN THE OUTER VESTIBULE TO THE GATING SHIFT IN THE MIDPOINT OF NA-CHANNEL ACTIVATION.

((Y. Sun*, I. Favre†, L. Schild† and E. Moczydlowski*)) *Dept. of Pharmacology, Yale Univ. School of Medicine, New Haven, CT 06520. †Institut de Pharmacologie et Toxicologie, 1005 Lausanne, Switzerland.

External divalent cations have two major effects on voltage-gated Na-channels: a weakly voltage-dependent block and a positive shift in the midpoint of the probability of channel opening, termed the gate-shifting action. Since divalent metal cations exhibit a distinct selectivity or order of effectiveness for shifting activation, specific divalent cations binding sites have been implicated in addition to surface charge screening. In heart Na-channels, Zn^{2+} and Cd^{2+} are among the most effective divalent cations for both the gate shifting and blocking effects, suggesting that the two effects are related. Armstrong and Cota (PNAS 88: 6528, 1991) have also proposed that the gate shifting and blocking action of Ca^{2+} are mediated by the same site in the Na-channel lumen. We examined this hypothesis by measuring the activation gating shift for wild type and mutants Y401C and Y401D of the rat muscle Na-channel (μ1) that have been previously shown to exhibit high affinity sites for Zn^{2+} (K_i = 8 μM) and Ca^{2+} (K_i = 300 μM), respectively, in the external vestibule. Macroscopic Na-currents were measured in oocytes by 2-electrode voltage clamp and also by whole cell recording after stable transfection in HEK293 cells. We analyzed the effect of increasing concentrations of Ca^{2+} and Zn^{2+} on the peak-current voltage relationship. The results indicate that only ~5-10 mV of midpoint gating shift can be attributed to high-affinity Zn or Ca binding in the mutants versus gating shifts of up to 40 mV in the wild type channel titrated over higher concentrations of Ca and Zn. We conclude that divalent cation sites near the pore entrance may exhibit a small electrostatic interaction with the voltage-sensing mechanism , but that large gating shifts characteristic of native Na-channels are mediated by low affinity sites in other locations, presumably outside the vestibule. (NIH, Swiss NSF)

Tu-Pos323

DOMAIN LOCALIZATION OF ISOFORM-SPECIFIC DETERMINANTS OF SITE 3 TOXIN MODIFICATION OF VOLTAGE-GATED Na CHANNELS.

((C.L. Drum, G.R. Benzinger, L-Q. Chen*, R.G. Kallen*, and D.A. Hanck.)) Univ. of Chicago, Chicago, IL 60637 & *Univ. of Pennsylvania, Philadelphia, PA 19104

The high affinity site 3 toxin, Ap-B, produced by the sea anemone, *Anthopleura Xanthogrammica,* binds to the extracellular surface of voltage-gated Na channels and interferes with inactivation from the open state. Ap-B has a similar high affinity for human heart (hH1a) and rat skeletal muscle (rskm1) Na channels, 2.5 ± 1.0 nM and 2.2 ± 1.0 nM, but on-rates and off-rates are 11-12 fold more rapid for the skeletal muscle isoform. We used these differences in on and off-rates to determine the locus of isoform discrimination by constructing chimeric channels that swapped various of the four domains of the human heart and rat skeletal muscle channels. Mammalian cells (tsA-201) were transiently transfected, and they were assayed electrophysiologically using whole-cell patch clamp. After control measurements, cells were transferred to a chamber containing 50 nM Ap-B, and the time course of modification was monitored. Cells were then transferred to a toxin-free bath, and the zeroth order off-rate reaction observed. The current during a 0.4 ms window (7.6-8.0 ms) was taken to reflect channels modified by toxin, since all non-modified current decayed by this time. Chimera donating domain IV from skeletal muscle exhibited rates intermediate between those for cardiac and skeletal muscle, while all chimera donating domain IV from the cardiac isoform exhibited rates typical of that isoform. We conclude that a major structural determinant of the isoform specificity of the binding site for Ap-B is located on domain IV.

Tu-Pos324

MOLECULAR ANALYSIS OF THE NA^+ CHANNEL INACTIVATION GATE

((S. Kellenberger, J.W. West, T. Scheuer and W.A. Catterall)) Dept. of Pharmacology, U. of Washington, Seattle WA 98195 (Spon. by M. Pearson)

The intracellular loop between homologous domains III and IV ($L_{III/IV}$) of the Na^+ channel α subunit is proposed to form a hinged, cytoplasmic inactivation gate that binds to a receptor on the body of the channel. F1489 in this loop is required for stable inactivation and each end of the loop contains pro and gly residues, amino acids that participate in molecular hinges. To test this hypothesis, each gly and pro was mutated individually to ala in $L_{III/IV}$ of the rat brain type IIA Na^+ channel α subunit and co-expressed with rat β1 subunits in *Xenopus* oocytes. Macroscopic inactivation in cell-attached macropatches was slowed in mutants G1484A, G1485A and P1512A but was relatively complete by the end of a 15 ms long pulse (< 2-15% non-inactivating current), consistent with slowed but stable inactivation. Mutants G1505A, P1514A, and P1512A had similar but smaller effects. In contrast, mutation of F1489 to a series of amino acids produced larger fractions of non-inactivating current but little slowing of inactivation. Single channels had open times that were similar to to wild-type but channels reopened throughout the pulse, indicating a destabilized inactivated state. Closed times between reopenings decreased with decreasing hydrophobicity of the substituted residue, suggesting disruption of a hydrophobic interaction. Exposure of the cytoplasmic surface of F1489C to sulfhydryl-modifying reagents disrupted macroscopic inactivation, possibly due to reduction of hydrophobicity or steric hindrance of inactivation gate closure. These findings support $L_{III/IV}$ forming an inactivation gate whose closing involves the gly and pro residues and whose affinity depends on a hydrophobic interaction with its receptor.

Tu-Pos325

A ROLE FOR INTRACELLULAR LOOP IVS4-S5 OF THE NA^+ CHANNEL α SUBUNIT IN FAST INACTIVATION

((J. C. McPhee, D.S. Ragsdale, T. Scheuer and W.A. Catterall)) Dept. of Pharmacology, U. of Washington, Seattle, WA 98195. (Spon. by F. Vincenzi)

Na^+ channel inactivation is thought to involve closure of an intracellular inactivation gate over the channel pore subsequent to voltage-dependent conformational changes in the body of the molecule. S4 segments have been implicated in such changes. The intracellular loops linking S4 to S5 (S4-S5) might also change conformation and could be near the mouth of the channel pore. Thus, they might play a role in Na^+ channel inactivation. To test this hypothesis we replaced each amino acid in S4-S5 of homologous domain IV with ala and expressed the resulting constructs in *Xenopus* oocytes. Mutants F1651A, near the middle of the the loop, and L1660A and N1662A, near the C-terminus, disrupted Na^+ channel fast inactivation as indicated by non-inactivating Na^+ current at the end of depolarizations. The rate of macroscopic inactivation was dramatically slowed for mutant F1651A and inactivation was virtually abolished in N1662A. Unlike wild type (WT), single channels due to each mutant reopened repeatedly during maintained depolarizations, indicating destabilization of the inactivated state. Open times were increased for mutants F1651A and N1662A relative to WT, consistent with a slowed entry into the inactivated state. Macroscopic inactivation was also slowed for mutant L1639A, at the amino terminal end of IVS4-S5 but was complete by the end of the pulse. Most single channel activity for L1639A was WT. However, occasional depolarizations produced bursts of high single channel activity that began at the onset of depolarization, lasted several ms and were terminated by inactivation. This activity was responsible for the slowed macroscopic inactivation. Thus, IVS4-S5 plays a central role in Na^+channel inactivation, perhaps as a conformationally-coupled binding pocket for the inactivation gate.

Tu-Pos326

PHOSPHORYLATION BY PKA AT A SINGLE SITE IN THE I-II LINKER OF THE BRAIN SODIUM CHANNEL IS NECESSARY AND SUFFICIENT FOR CURRENT AMPLITUDE REDUCTION. ((R.D. Smith and A.L. Goldin)) Microbiology & Molecular Genetics, University of California, Irvine, CA 92717.

The rat brain sodium channel is phosphorylated *in vivo* at four PKA consensus sites in the cytoplasmic linker between domains I and II (B.J. Murphy et al., 1993, J. Biol. Chem. 268:27355). PKA phosphorylation modulates sodium channel function by diminishing peak current amplitudes elicited by membrane depolarizations (Li et al., 1992, Neuron 8:1151; Gershon et al., 1992 J. Neurosci. 12:3743). We have constructed mutant channels that 1) completely lack the PKA sites in the I-II linker, 2) lack individual PKA sites, or 3) only have single PKA sites intact in the I-II linker. These mutants were expressed in *Xenopus* oocytes, and were analyzed by two-electrode voltage clamping under conditions of induced PKA activity. PKA was activated by stimulating a co-expressed β_2-adrenergic receptor with isoproterenol, or by perfusing oocytes with a cocktail containing forskolin, IBMX, cpt-cAMP, and db-cAMP. We demonstrate that the I-II linker sites are required for the reduction of current by PKA phosphorylation. Moreover, although phosphorylation at individual sites contributes to the overall reduction in current amplitude, a single site is necessary and sufficient for the reduction in current density to occur.

Tu-Pos327

MOLECULAR DETERMINANTS OF α–SCORPION TOXIN and ANEMONE TOXIN BINDING TO THE NA^+ CHANNEL. J. C. Rogers, Y. Qu, T. Scheuer*, W.A. Catterall. Dept. of Pharmacology, Univ. of Washington, Seattle, WA 98195.

Alpha scorpion (α-ScTx) and sea anemone (ATX) toxins bind to overlapping extracellular receptor sites on the Na^+ channel in a voltage-dependent manner and disrupt fast inactivation. As fast inactivation is thought to be an intracellular process, extracellular binding determinants for these toxins may identify extracellular regions that must change conformational before fast inactivation can occur. Basic residues of α–ScTx have been implicated in binding. Likewise, Na^+ channel domains I and IV are thought to participate in binding. Therefore, extracellular acidic amino acids of the rat brain type IIA Na^+channel α subunit in those domains were converted to neutral or basic residues using site-directed mutagenesis, transiently expressed in tsA-201 cells and tested for ^{125}I-α–ScTx and ^{3}H-saxitoxin binding. Mutation of a glu residue in the extracellular S3-S4 loop in domain IV disrupted α–ScTx binding. Mutations of additional residues disrupted ATX binding. Electrophysiological analysis found that arg and his substitutions gave 100- and 14-fold lower affinities for α-ScTx, respectively. The primary effect of these mutants was to increase α-ScTx dissociation rate while the voltage-dependence of α-ScTx binding was unaffected. This mutation is near the voltage sensing IVS4 segment, suggesting that a conformational change resulting from IVS4 movement may cause voltage-dependent disruption of toxin binding. Mutations causing paramyotonia congenita lie within this loop and modify inactivation, suggesting that this region is important for inactivation and may be the site of functional modulation by α-ScTx.

Tu-Pos328

EXTRACELLULAR pH AFFECTS COCAINE-INDUCED Na^+ CHANNEL BLOCKADE IN RAT VENTRICULAR MYOCYTES. ((T. Chow, Y.-F. Xiao and J.P. Morgan)) The Harvard-Thorndike Laboratory and the Cardiovascular Division, Beth Israel Hospital, Harvard Medical School, Boston, MA 02215.

Sodium channel blockade may play an important role in the etiology of cocaine-related ventricular arrhythmias. Cocaine can cause myocardial acidosis through vasoconstriction and ischemia, and bicarbonate may protect against cocaine-induced ventricular arrhythmias (Beckman HJ et. al. Circulation 1991; 83:1799-807). We therefore investigated the effects of extracellular pH on cocaine-induced Na^+ channel blockade. Cultured neonatal rat ventricular myocytes were clamped using the whole-cell recording method. Application of 50 μM cocaine (at pH 7.4) profoundly inhibited Na^+ current. Lowering the external pH to 6.9 decreased the cocaine-induced Na^+ channel blockade (measured by peak current) by 23 ± 5% ($n=10$, $p<0.05$), while raising the external pH to 7.9 increased the block by 21 ± 9% ($n=10$, $p<0.05$). When 20 μM cocaine was instead applied intracellularly (by adding it to the pipette solution), external acidosis reduced Na^+ current block by 28 ± 12% ($n=5$, $p<0.05$) while alkalosis increased block by 30 ± 13% ($n=5$, $p<0.05$). We found no consistent effect on Na^+ current when altering pH in the absence of cocaine. The above phenomena appear to also hold true for adult rat ventricular myocytes, suggesting generalizability beyond the neonatal period. The pK_a of cocaine is 8.5 in bulk solution and may be 7.1 near its binding site (Nettleton J, Wang GK. Biophys. J. 1990; 58:95-106). Our findings are therefore consistent with the hypothesis that the uncharged form of cocaine diffuses through the cell membrane and reaches its binding site via an intracellular route. However, the observation that extracellular pH affects internal cocaine potency suggests that other mechanisms may also be involved.

Tu-Pos329

A RING OF NEGATIVE CHARGES AT THE Na^+ CHANNEL OUTER VESTIBULE IS INVOLVED IN BINDING GUANIDINIUM-CONTAINING TOXINS. ((J.L. Penzotti, S.C. Dudley, G. Lipkind, H.A. Fozzard)) University of Chicago, Chicago, IL 60637.

The voltage-gated Na^+ channel is encoded by a single polypeptide that consists of four homologous domains (DI-IV). In the current models of the channel, each domain consists of six transmembrane segments (S1-S6), and the linkers between S5 and S6 invaginate into the membrane to form the outer vestibule and selectivity filter. Within this outer vestibule, charged amino acid side chains appear to be arranged in two distinct rings. The inner ring of charge is involved in selectivity, and the role of the outer ring is unclear. Several toxins of known structure have been shown to bind in this region, saxitoxin (STX), tetrodotoxin (TTX), and μ-conotoxin GIIIA (μ-CTX), and therefore they have been used as probes of the channel architecture. Using oligonucleotide-directed mutagenesis of the rat skeletal muscle Na^+ channel (μI), we have investigated the effect of neutralizing the negative charges of the outer ring (DI, DII, DIV) on the binding of these toxins. Messenger cRNA was prepared *in vitro* and expressed heterologously in *Xenopus* oocytes. Recordings were made in the two-electrode voltage clamp configuration in a flowing bath. The effect of neutralization on toxin half maximal block (IC_{50}) and binding kinetics was determined by observing the peak current obtained from voltage steps to 0 mV from a holding potential of -100 mV as the oocytes were exposed to the toxins. The IC_{50} for μI by STX was 3.1 ± 0.5 nM with an on rate (k_{on}) of 5.1e+6 ± 3.1e+6 $M^{-1}s^{-1}$ and an off rate (k_{off}) of 1.3e-2 ± 1.7e-3 s^{-1}. Neutralizations E403Q, E758Q, and D1532N rendered the channel insensitive to 1 μM STX. The IC_{50}s of μI, E403Q, E758Q, and D1532N for TTX were 35 ± 6 nM, 161 ± 14 μM, 5.9 ± 0.3 μM, and 1.5 ± 0.2 μM, respectively. Kinetic analysis suggested that the change in IC_{50} resulted almost exclusively from a change in k_{on} consistent with an electrostatic effect. These results are in qualitative but not quantitative agreement with those from mutations in the rat brain Na^+ channel. The IC_{50}s of μI, E403Q, E758Q, and D1532N for μ-CTX were 17 ± 5 nM, 98 ± 9 nM, 822 ± 105 nM, and 164 ± 32 nM, respectively. E758Q and D1532N affected mostly k_{on} consistent with an electrostatic role for these amino acids. E403Q affects both k_{on} and k_{off} suggesting a mixed electrostatic and short range interaction of this position with the μ-CTX.

Tu-Pos330

TWO PARAMYOTONIA CONGENITA Na CHANNEL MUTATIONS INDUCE AN OPPOSITE AFFINITY CHANGE FOR LIDOCAINE. ((Z. Fan, A.L. George, Jr.[1], J.W. Kyle, J.C. Makielski)) U. of Wisconsin, Madison, WI, [1]Vanderbilt U. Nashville, TN, and [2]U. of Chicago, Chicago, IL

Two paramyotonia congenital mutants (T1313M on the III-IV linker and R1448C on the outside of S4 domain IV) were expressed in a cell line (tsA201) using the recombinant human Na channel α-subunit cDNA hSkM1. Both mutants exhibited similar altered inactivation phenotypes revealed by slower current decay (Fig). Local anesthetics bind primarily to the inactivated state; we therefore assessed lidocaine block for these mutants and the wild type channel. In pulse trains experiments (10 ms to -10 from -120 mV at 10 Hz, 100 μM) T1313M showed reduced phasic block, but R1448C showed increased block (Fig). Tonic block (--120 mV) was also greater for R1448C and less for T1313M, and T1313M showed more rapid recovery from block. Inactivated state block (from drug-induced shifts in steady-state availability) was less for T1313M and greater for R1448C. Neither residue is located at a putative lidocaine binding site in s6, yet both had a considerable effect on lidocaine binding. In addition to having implications for drug therapy of these diseases, these results may give insight into structural requirements for drug affinity.

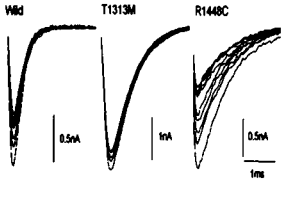

Tu-Pos331

Ibutilide, A Potent Class III Antiarrhythmic Compound, Activates a Slow Na^+ Sensitive Inward Current in Guinea-pig Atrial Cells. Kai S. Lee and Timothy M. Piser. Cardiovascular Pharmacology, Upjohn Laboratories, Kalamazoo, MI 49007. (spon. by JD Petke)

Ibutilide is a potent and effective class III antiarrhythmic compound for the suppression of atrial flutter and fibrillation in man. Earlier studies on guinea-pig ventricular cells reveal that ibutilide prolongs action potential duration (APD) via activation of a Na^+-sensitive, slow inward current. This study further examines the activity of ibutilide on inward current in guinea pig atrial cells under identical conditions. Guinea-pig atrial cells were freshly isolated using standard methods (Lee et al, *Nature* 265:751-753, 1977, *Nature* 278:269-271,1979). Cells perfused internally and externally with Cs^+, K-free solution at 23°C, and held at -40 mV, displayed peak inward current of -497±28 pA and sustained inward current (150 ms) of -200±16.2 pA at 20 mV. Application of 10^{-6}M ibutilide significantly increased the peak and sustained inward current to -550±24 pA and -280±17 pA respectively. Thus, the increase in sustained current is proportionally larger. At 37°C, the drug effect remained similar in that 10^{-6}M ibutilide increased the peak current (measured at 15 ms), at 20 mV, from -412±15 pA to -495±18 pA, and the sustained current, from -45±3 pA to -91±4 pA. Removal of external Na^+ reduced both the peak and the sustained inward current in the presence of ibutilide. We conclude that ibutilide prolongs APD of atrial cells by activating the sodium sensitive inward current, I_{Na+}, described previously in ventricular cells (*JEPT* 262:99-108,1992).

Tu-Pos330a *(See M-Pos276)*

Tu-Pos332

BLOCK OF Na^+ CURRENTS AND ANTIMYOTONIC ACTIVITY ON ADR MOUSE SKELETAL MUSCLE BY ENANTIOMERS OF MEXILETINE ANALOG. ((A. De Luca, F. Natuzzi, S. Pierno, H. Jockusch°, A. Duranti*, G. Lentini*, F. Franchini*, V. Tortorella* and D. Conte Camerino)), Dept. of Pharmacobiology and *Dept. of Medicinal Chemistry, University of Bari, Italy and °Developmental Biol. Unit., University of Bielefeld, Germany.

The enantiomers of mexiletine (Mex), an antimyotonic agent, stereoselectively block the Na^+ currents (I_{Na}) of skeletal muscle fibers, being the R-(-) isomer twice as potent as the S-(+) one (De Luca et al., Naunyn-Schmied. Arch Pharmacol., 1995). The clarification of the structural requirement of the stereospecific receptor on skeletal muscle Na^+ channels can lead to safer antimyotonic drugs. A mexiletine homolog (homo-Mex) with an increased steric hindrance on the chiral carbon atom (methylenamino residue vs. amino group) was synthesized. The enantiomers were tested on Na^+ currents of single fibers of frog semitendinosus muscle by means of three-vaseline gap voltage clamp (holding potential, h.p.=-100mV). The IC_{50} values for the tonic block of the maximum I_{Na} (single 15ms-test pulses from h.p. to -20 mV) were 120μM for R-(-) and 200μM for S-(+) homo-Mex vs. 75μM and 120μM for the R-(-) and S-(+) Mex, respectively. Both enantiomers of each compound produced a use-dependent block of I_{Namax} during a repetitive stimulation at 2Hz. At the steady state, the IC_{50} values for phasic block were 2.5 and 1.5 fold lower than those for tonic block for homo-Mex and Mex enantiomers, respectively, without changes of the eudismic ratios. Both compounds stabilized stereospecifically the Na^+ channels in the inactivated state, being the R-(-) isomers more potent than the S-(+) ones in left-shifting the steady-state inactivation curves. Homo-Mex and Mex also stereoselectively suppressed the hyperexcitability of intercostal muscle fibers of myotonic (ADR) mouse, monitored with the two microelectrode current-clamp technique. In fact 50μM of S-(+) and R-(-) homo-Mex reduced the myotonic repetitive firing by 6% and 32%, respectively; 50μM of R-(-) Mex also produced a 30% reduction of firing capability. The results suggest that slight increase of the hindrance on the chiral carbon atom does not alter the ability of the compound to stereoselectively interact with the receptor. However a change in the pKa of the molecule and thus of the charged/uncharged ratio, can explain the higher use-dependency of homo-Mex with respect to Mex and thus the comparable potency of both compounds during phasic block and antimyotonic action (Telethon-Italy, project # 579).

Tu-Pos333

DIFFERENTIAL EFFECTS OF VOLATILE ANESTHETICS ON THE CARDIAC Na^+ CHANNEL DURING β-ADRENERGIC STIMULATION.
((H.U. Weigt, Z.J. Bosnjak, W.M. Kwok)) Department of Anesthesiology, Medical College of Wisconsin, Milwaukee, WI 53226

The underlying mechanisms of action of volatile anesthetics on cardiac Na^+ channels are poorly understood. Possible sites of action include direct interaction with functional parts of the channel protein, anesthetic-lipid interactions, and second messenger pathways. We investigated the effects of volatile anesthetics on the cardiac Na^+ current (I_{Na}) in ventricular myocytes enzymatically isolated from adult guinea pig hearts. Standard whole-cell configuration of the patch clamp technique was used. I_{Na} was elicited by depolarizing test pulses from a holding potential of -80 mV. Halothane (*HAL*) and isoflurane (*ISOFL*) depressed peak I_{Na} by 42.1±3.4% (n=9) and 21.3±1.9% (n=10), respectively. Isoproterenol (3μM) potentiated the effects of *HAL*, further decreasing peak I_{Na} by 34.7±4.1% (n=9). Isoproterenol alone depressed peak I_{Na} by 14.6±1.7% (n=11), thus indicating synergy between *HAL* and isoproterenol. The depressant effect of *HAL* was less effective in the presence of GDPβS and a PKA inhibitor (PKA inhibitor fragment 6-22 amide), reducing peak I_{Na} by 24.2±3.3% (n=10) and 24.0±2.4% (n=11), respectively. The effect of isoproterenol on *ISOFL* inhibition of I_{Na} was less pronounced, decreasing current by an additional 12.6±3.9% (n=10). GDPβS also reduced the inhibitory effect of *ISOFL*. In contrast, the PKA inhibitor had no effect on *ISOFL* inhibition of I_{Na}. Our results suggest 2 different pathways for volatile anesthetic actions on the cardiac Na^+ channel: 1) involvement of a cAMP mediated pathway for *HAL* and 2) a membrane-delimited G protein pathway for *ISOFL*.

Tu-Pos334

HETEROLOGOUSLY EXPRESSED *DROSOPHILA para* SODIUM CHANNELS ARE HIGHLY SENSITIVE TO PYRETHROIDS AND NATURAL TOXINS ((C. J. Cohen, M. M. Smith, R. Reenan*, V. Garsky,, P. Wang, J. Wang, B. Ganetzky*, and J. W. Warmke)) Merck Res Labs, Rahway, NJ 07065; *University of Wisconsin, Madison, WI 53706

Voltage-gated Na channels are a common target of animal and plant toxins and commercially useful insecticides. At least 6 distinct drug binding sites for these toxins exist on mammalian Na channels. *Drosophila para* and rat brain IIA Na channels were heterologously expressed in the same oocyte system to better understand why many of these agents are more toxic to insects than mammals. Rat brain IIA was co-expressed with rat brain β1; *para* was expressed with and without *tipE* (see accompanying abstr.). Para/TipE Na channels are >10-fold more sensitive than mammalian Na channels to block by TTX or to slowing of inactivation by toxin II from *Anemonia sulcata*. The peptide toxin μ-Aga-IV, originally isolated from spider venom, was synthesized and found to specifically modify Para/TipE Na channels. Furthermore, modification by the pyrethroid insecticide permethrin is >100-fold more potent than rat brain type IIA Na channels expressed in the same oocyte system. The pharmacological properties of *para* at the 4 sites defined by these toxins are little effected by co-expression with *tipE*. While the basic biophysical properties of the insect and mammalian Na channels examined in this study are similar, the pharmacology is quite different. The selective toxicity of pyrethroid insecticides is due at least in part to the greater affinity of pyrethroids for insect Na channels than for mammalian Na channels.

Tu-Pos335

FUNCTIONAL EXPRESSION OF *DROSOPHILA para* NEURONAL SODIUM CHANNELS IS MODULATED BY THE MEMBRANE PROTEIN *tipE* ((J. W. Warmke, R. Reenan*, P. Wang, J. Arena, J. Wang, D. Wunderler, K. Liu, G. Kaczorowski, L. Van der Ploeg, B. Ganetzky*, and C. J. Cohen)) Merck Res Labs, Rahway, NJ 07065; *University of Wisconsin, Madison, WI 53706

The *para* locus encodes the predominant class of Na channels in *Drosophila* neurons. We have constructed a composite *para* cDNA clone and shown that it encodes a 240 kDa protein by *in vitro* translation. This α subunit expresses poorly in *Xenopus* oocytes. Classical genetic and biochemical analyses of the *tipE* locus suggested that this gene encodes a regulatory or structural component of neuronal Na channels. Indeed, co-expression with *tipE* greatly enhances and accelerates expression of *para* (studies with G. Feng and L. Hall, SUNY-Buffalo). *tipE* is not homologous with mammalian Na channel β1 or β2 subunits and is not functionally equivalent: 1) rat β1 does not cause similar acceleration of expression of *para*; 2) coexpression of β1, but not *tipE*, with rat brain αIIA results in currents that inactivate more rapidly than with αIIA alone. *Para* Na channels inactivate rapidly with or without *tipE*, whereas expressed mammalian neuronal Na channels inactivate rapidly only when the α and β1 subunits are coexpressed. Expression of *para* alone results in Na channels that activate more slowly than those due to *para* plus *tipE*. Para/TipE sodium channels have biophysical and pharmacological properties similar to those of native Drosophila channels.

Tu-Pos336

A HETEROLOGOUS MAMMALIAN EXPRESSION SYSTEM THAT PERMITS MEASUREMENT OF SODIUM CHANNEL GATING CURRENTS
((Michael F. Sheets, John W. Kyle*, Stephanie Krueger, Dorothy A. Hanck*)) Departments of Medicine, Northwestern University Medical School and University of Chicago*, Chicago IL

A mammalian expression system offers two advantages over the *Xenopus* oocyte expression system for the study of Na current (I_{Na}) and ion channel gating currents (I_g); (1) mammalian cells have been shown to express Na channels with kinetics similar to those of native Na channels, and (2) high quality voltage clamp is more easily achieved. We have developed an approach to the measurement of Na channel I_g in which polyethylene glycol is used to fuse tsA201 cells into large, multinucleated cells with diameters up to 150-200 μm. Immediately after fusion cells exhibit complex capacitive properties, however after 48-78 hours the plasma membrane has undergone remodelling and produces single, large spherical cells with simple RC properties. We have successfully transfected fused cells and obtained expression of high numbers of Na channels. Fig. A shows typical records from a voltage-clamped fused cell internally perfused with 200 mM TMA-F through a single large suction pipette. Extracellular Na^+ was only 45 mM (12°C). Peak I_{Na} in a step from -120 to -10 mV was -67 nA. Fig. B shows the integrals of the Na channel I_g in the same cell; maximal charge was 4 pC. Approximately 30% of fused cells express Na channels in sufficient numbers for measurement of Na channel I_g. Fused cells may be useful in the study of other ion channels or other membrane proteins where high expression levels are required.

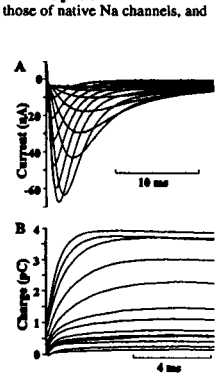

Tu-Pos337

A NOVEL TYPE OF SODIUM CURRENT EXPRESSED IN VITRO IN CULTURED HUMAN CORONARY MYOCYTES.
JF. Quignard, F. Ryckwaert, B. Albat, MC. Harricane, J. Nargeot & S. Richard (spon.: P. Mollard) CRBM, Route de Mende, BP 5051, 34033 - Montpellier - F.

Human coronary myocytes were enzymatically isolated from the left descending coronary artery of the failing heart (ischemic cardiopathies) of seven patients undergoing cardiac transplantation. Sodium currents (I_{Na}) were studied using the whole-cell patch clamp technique (18-22 °C) in conditions optimized to suppress Ca^{2+} and K^+ currents. I_{Na} was absent in freshly isolated myocytes but appeared after several days of culture. Cultured cells were identified as smooth muscle (SM) cells, based on expression of SM α-actin. I_{Na} was dependent upon extracellular Na^+ and was highly sensitive to the Na^+ channel-specific antagonist tetrodotoxin (TTX; see figure; $IC_{0.5}$: 10 nM) and to agonists such as veratridine and the polypeptide toxin ATX V from the sea anemone *Anemonia sulcata* (figure). I_{Na} activated at -40 mV , peaked at 0 mV and had a bi-exponential decay with a fast inactivating (tau: 5 ms) component and a sustained (tau > 200 ms) component. In conclusion, human coronary myocytes grown *in vitro* express a new type of TTX-sensitive I_{Na} with unusual electrophysiological properties. This current probably appears in relation to cell dedifferentiation and proliferative activity ot vascular SM cells.

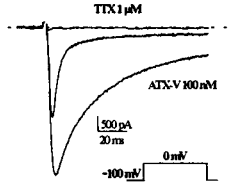

Tu-Pos338

DIFFERENTIAL EFFECTS OF PROTEIN KINASE C ACTIVATORS ON THE VOLTAGE-DEPENDENT SODIUM CURRENT IN NEONATAL RAT VENTRICULAR MYOCYTES. ((Cheryl L. Watson and Michael R. Gold)) Dept. of Medicine, University of Maryland, Baltimore, MD.

Phosphorylation of the sodium channel has marked effects on gating. To assess the modulation of the inward sodium current (I_{Na}) by phosphorylation with protein kinase C (PKC), we compared the action of a direct activator of the PKC catalytic subunit with membrane activation by oleic acid (OA). Whole cell patch clamp recordings of neonatal rat cardiac cells were performed with intracellular perfusion of a synthetic peptide corresponding to the PKC catalytic subunit (530-558, PKCP) or with extracellular superfusion of OA (40μM). There was a 9 mV depolarizing shift of steady-state inactivation with 2 nM PKCP (n=17; $p< 0.01$) and reactivation was accelerated ($\tau_f = 34.8 \pm 6.6$ ms vs 13.0 ± 4.2 ms and $\tau_s = 117.9 \pm 19.2$ ms vs 52.6 ± 10.0 ms; n=14, p=0.01). In contrast, with OA there was a 6 mV hyperpolarizing shift of inactivation (n=11, p=0.01) and reactivation was slowed. Peak current was reduced by OA at a holding potential of -90 mV, but currents were unaffected by either substance at -125 mV. We conclude that the modulation of I_{Na} is not uniformly affected by PKC activators. This is likely due to different isoform stimulation or to stimulation of other PKC mediated cellular events.

Tu-Pos339

POLARIZED OPTICAL SIGNALS SENSITIVE TO THE DIRECTION OF IMPULSE PROPAGATION IN THE SQUID GIANT AXON ((D Landowne and H Duclohier)) U Miami Medicine, Miami FL 33101 and URA 500 CNRS-U. Rouen, 76821 Mont-Saint-Aignan, France

Two different optical polarization measurements (linear and circular) indicate a transient change in nerve structure which precedes the voltage-dependent sodium permeability change of the action potential. Watanabe '93 (*JPhysiol*466:55) reported the sense or handedness of the optical rotation signals in the lobster leg nerve bundle reverses when the site of stimulation is changed from proximal (P) to distal (D) with respect to the optical recording site. To investigate this signal in a single motor fiber we used squid giant axons looking for optical signals which are sensitive to propagation direction

Axons were mounted on a rotary stage of a polarization microscope with the P-D axis oriented towards lab 0°, the polarizer at -45° and the analyzer at +45°. Changes in light intensity from a 3 mm length of axon were measured with Pt-Pt foil barriers in the chamber to form a 1 mm slit.

Axons at angles near the analyzer gave an optical response with a different timecourse in right and left handed arrangements. Thus with P stimulation the rising phase of the response recorded at 35-41° lagged the rising phase recorded at 51-56° by about 1 msec at 10°C in six axons. The opposite effect (51° lags 39°) was seen with D stimulation. Experiments on squid fin nerve bundles produced similar results except the sense was reversed (51° lagging 39° with P stimulation). At 45° no change in light intensity was detected over the noise level. At 0° axons showed an optical response to D stimulation up to 10% larger in amplitude than for P stimulation.

The above results suggest a non-random orientation of excitable molecules along the membrane; the sodium channel, assuming only a pseudo-symmetry

Supported by NIH Grant NS26651 and CNRS GDR 1153

Tu-Pos340

DOES AN ELECTROGENIC TRANSITION IN THE S4 SEGMENTS DRIVE THE CLOSED-OPEN CONFORMATIONAL CHANGE OF THE Na CHANNEL?
((H. Richard Leuchtag)) Department of Biology, Texas Southern University, Houston, TX 77004.

Calculations show (*BJ* 66:217-224, 1994) that the S4 segments can not be stable as transmembrane α helices without an external force (e.g., resting potential) to compress them. Thus if the S4s are α helices in the closed state, a threshold depolarization will allow them to expand by the electrostatic repulsion of their positive charges. Work by Zundel et al. (*J. Molec. Structure* 300:573-592, 1993) demonstrates the existence of $O^- Na^+ \ldots {}^-O$ bonds, $O^- Na^+ \ldots ON$ bonds and their equivalents with Li^+. The integrated intensities of the IR continuum spectra are less for these than for the corresponding H bonds, decreasing with increasing ion mass. I postulate that the threshold depolarization breaks the H bonds connecting the loops of the S4 α helices, and that their H's are displaced by Na's from one of the aqueous phases, forming a new type of helix, one that is stabilized by N Na ... O bonds instead of N H ... O bonds. Li^+ would produce a similarly modified helix. The metal ions in the four modified S4 helices can then form a membrane-spanning salt bridge that would function as a conductive pathway.

Tu-Pos341

TRIPLE-BARREL MULTIMERIC STRUCTURE OF ENaC, A CLONED EPITHELIAL Na^+CHANNEL. ((Iskander I. Ismailov[1], Mouhamed S. Awayda,[1] Bakhram K. Berdiev[1], James K. Bubien[1,2], Joseph E. Lucas[1] Catherine M. Fuller[1] and Dale J. Benos[1])) [1]Depts. of Physiology and Biophysics, and [2]Medicine, University of Alabama at Birmingham, Birmingham, Alabama 35294

Channels produced by the α subunit, and by α, β, and γ subunits of a cloned rat epithelial Na^+ channel (rENaC), were studied in planar lipid bilayers. Both *in vitro* translated or heterologously expressed in *Xenopus* oocytes plasma membranes α-rENaC alone, or α- in combination with β- and γ-rENaC, produced highly Na^+ selective (P_{Na}/P_K = 10), amiloride-sensitive (K_i^{amil} = 170 nM), and mechanosensitive cation channels in planar bilayers. α-rENaC displayed a complicated gating mechanism: there was a nearly constituitively open 13 pS state and a second 40 pS level that was reached from the 13 pS level by a 26 pS transition. α, β, γ-rENaC showed primarily the 13 pS level. α-rENaC and α, β, γ-rENaC channels studied by patch clamp displayed the same gating pattern albeit with >2-fold lowered conductance levels, i.e., 6 pS and 18 pS, respectively. Upon treatment of either channel with the sulfhydryl reducing agent dithiothreitol (DTT), both channels fluctuated between three independent 13 pS sublevels. Bathing each channel with a high salt solution (1.5 M NaCl) produced stochastic openings of 19 and 38 pS in magnitude between all three conductance levels. Different combinations of α, β, γ-rENaC in the reconstitution mixture did not produce channels of intermediate conductance levels. These findings suggest that functional ENaC is composed of three identical conducting elements, and that their gating is concerted. Supported by NIH grant DK 37206.

TRANSMEMBRANE SIGNALING - CALCIUM

Tu-Pos342

MODULATION OF AGONIST-EVOKED CALCIUM OSCILLATIONS IN HUMAN VASCULAR ENDOTHELIAL CELLS. ((F.Viana, L. Missiaen, G. Droogmans and B. Nilius)) KULeuven, Laboratory of Physiology, B-3000 Belgium. (Spon. by J. Parys)

We used fluorescence imaging and the patch-clamp technique to investigate the effects of extracellular nucleotides on the membrane conductance and the free intracellular Ca^{2+} concentration of a human endothelium cell line (EAhy926). Submaximal concentrations of agonist (0.5 to 2 μM) evoked sinusoidal oscillations (0.5-2/min) in most cells. At higher agonist concentrations the response was biphasic, a fast initial transient followed by a sustained plateau in all cells. The pharmacological profile was UTP=ATP>ADP>>α,β-methylene-ATP=2-Methylthio-ATP=adenosine, suggesting the involvement of P_{2U} receptors. Oscillations persisted for >8 min in Ca^{2+}-free solutions or after replacing external Na^+ with NMDG. La^{3+} (100 μM) blocked the oscillations but this effect was independent of Ca^{2+} influx. Increasing the external divalent concentration diminished the agonist sensitivity. In normal external Ca^{2+} (1.5 mM), application of the SERCA-type ATPase inhibitor BHQ (10 μM) modified the oscillations into an elevated plateau. In Ca^{2+}-free conditions, thapsigargin (1 μM) produced a transient elevation of Ca^{2+} and suppressed the oscillations. The active phorbol ester PMA (500 nM) abolished the oscillations in less than 30s. Intracellular dialysis with 2,4,5 IP_3 and GTPγS produced sustained elevations in Ca^{2+} rather than oscillatory changes. Ca^{2+} elevations were accompanied by periodic hyperpolarizations of the membrane potential due to activation of a strongly outwardly-rectifying TEA- and charybdotoxin-sensitive Ca^{2+}-activated K^+ conductance, but oscillations persisted in voltage-clamped cells or in 55 mM K^+.

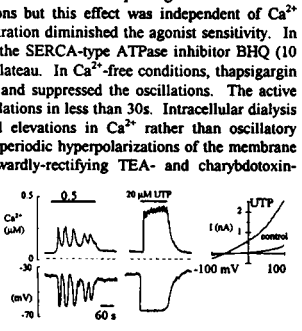

Our results suggest that cyclic mobilization of Ca^{2+} from IP_3-sensitive stores and a PKC-sensitive feedback mechanism are essential requirements for generation of oscillatory calcium signals in EAhy926 cells.

Tu-Pos343

TEMPERATURE DEPENDENCY OF CALCIUM RESPONSES IN MAMMARY TUMOR CELLS. ((Yoshio Oosawa[1], Chiharu Imada[1] and Kishio Furuya[2])) [1]International Institute for Advanced Research, Matsushita Electric Industrial Co., Ltd., 3-4 Hikaridai, Seika-cho, Kyoto-fu, 619-02, JAPAN; [2]Department of Cell Physiology, National Institute for Physiological Sciences, Okazaki, 444, JAPAN.

Changes of intracellular calcium activity (Ca^{2+}_i) by ATP and bradykinin in mouse mammary tumor cells (MMT060562) were investigated by image analysis of fluo-3 fluorescence at 24°C and 35°C. ATP and bradykinin increased Ca^{2+}_i at both temperature and Ca^{2+}-depletion did not affect these Ca^{2+}_i responses. Bradykinin-induced Ca^{2+}_i response became more sensitive at 35°C than at 24°C, although ATP-induced Ca^{2+}_i response was similar at both temperature. Latency between drug application and peak of response changed with the drug concentrations. At higher concentrations of ATP or bradykinin, the latency became shorter and approached to a constant value. At lower concentrations, the latency became longer at 24°C. However, the latency did not change so much at 35°C.

Tu-Pos344

PHENYLALKYLAMINE (PAA) ACTION ON CHIMERIC CALCIUM CHANNELS IS DEPENDENT ON CURRENT KINETICS ((V.E. Degtiar, E.N. Timin, F. Döring, M. Grabner, H. Glossmann, S. Hering,)) Institut für Biochemische Pharmakologie, Peter Mayr Straße 1, A-6020 Innsbruck, Austria (Spon. by H. Schindler)

Kinetics of cumulative barium current (I_{Ba}) inhibition by 50 μM (-)devapamil during trains of 800 ms-pulses from -80 mV to 10 mV were compared in two Ca^{2+} channels chimeras: AL23 (consisting of the α_{1A} subunit with transmembrane segment IVS6 replaced by a L-type skeletal muscle sequence of α_{1S}) and L_h ($\alpha_{1C\text{-}a}$ with the amino terminus replaced by α_{1S}). I_{Ba} of chimera L_h inactivated at 10 mV with τ_h = 1.45 ± 0.32 s. Peaks of I_{Ba} of L_h declined in (-) devapamil during the pulse train with significantly slower time course compared to the peak I_{Ba} decay of chimera AL23 (see figure) which inactivates with faster kinetics (τ_h = 44 + 8 ms at 10 mV). There was evidence that block development during a train correlates with the time constant of current inactivation.
The time course of block development was evaluated and analysed in terms of channel state models which enable a quantitative estimation of drug-binding rate constants to the open channel and account for possible drug trapping in the closed and inactivated channel.

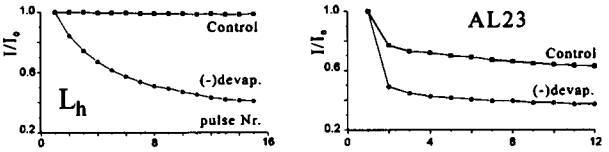

Supported by FWF grants S6601-MED (H.G.) and S6603-MED (S.H.)

Tu-Pos345

FUNCTIONAL COUPLING OF RAT GROUP I METABOTROPIC GLUTAMATE RECEPTORS TO A STABLY EXPRESSED HUMAN ω-CONOTOXIN GVIA-SENSITIVE CALCIUM CHANNEL IN HEK 293 CELLS. ((B.A. McCool[1], P.F. Brust[2], M.M. Harpold[2], J-P. Pin[3], and D.M. Lovinger[1])) Dept. Molec. Physiol./ Biophys.,Vanderbilt Univ. Sch. Med., Nashville TN 37232[1]; SIBIA Inc., La Jolla CA 92037[2]; UPR-9023 CNRS, 34094 Montpellier Cedex 05, France[3]

Metabotropic glutamate receptors (mGluRs) perform a variety of modulatory functions in the central and peripheral nervous systems. Among them, the modulation of voltage gated calcium channels has been proposed as an essential component of the inhibitory effects of mGluR agonists on synaptic transmission. The quisqualate/dihydroxyphenylglycine(DHPG)-sensitive mGlu receptors (rat Group I receptors) are known to modulate both synaptic transmission *in vivo* and voltage-gated, N-type calcium channels in acutely isolated neurons. These receptors can also couple to phosphatidyl inositol metabolism/Ca^{2+}, mobilization in both neurons and in heterologous systems, like HEK 293 cells. To determine whether a given rat Group I mGluR (rmGluR) can couple to multiple signal transduction pathways, we have transiently expressed rmGluR1a & 5a in a HEK 293 cell line (G1A1) which stably expresses the human $\alpha_{1B\text{-}1}$, α_{2b}, $\beta_{1\text{-}3}$ calcium channel subunits. Both rmGluR1a and rmGluR5a mediate robust and reversible inhibition of the ω-conotoxin GVIA-sensitive barium currents in G1A1 cells in response to application of L-glutamate (100μM) and the Group I-"specific" agonists quisqualate (0.1-10μM) and DHPG (1-100μM). Inhibition is characterized by slowing of the macroscopic current activation kinetics, voltage dependence, and partial relief by a depolarizing prepulse. These characteristics are reminiscent of a membrane-delimited, G protein-coupled signal transduction pathway we have previously described for the modulation of these channels by rat Group II mGluRs (rmGluR2 & 3) when transiently expressed in G1A1 cells. Because HEK 293 cells express both pertussis toxin-sensitive and -insensitive G proteins, this heterologous system will allow us to better understand the molecular aspects of receptor/G protein/effector coupling for the rat Group I mGlu receptors. Supported by NS09719 (B.A.M.) and NS30470 (D.M.L.).

Tu-Pos346

IONOMYCIN REVERSIBLY ACTIVATES AN INWARD Ca^{2+} CURRENT IN RAT BASOPHILIC LEUKEMIA CELLS (RBL-1). ((M.J. Mason and G.G Schofield)) Dept. of Physiol., Tulane Univ., New Orleans, LA 70112.

Dialysis of the cell interior with internal solutions devoid of Ca^{2+} and containing high concentrations of Ca^{2+} chelator activates an inwardly rectifying Ca^{2+} current in RBL-1 cells. To confirm the requirement of depletion of Ca^{2+}_i-stores for the activation of this current we have measured whole cell currents following addition of 14 μM ionomycin while employing an internal solution designed to minimize passive depletion of Ca^{2+}_i-stores. Subsequent depletion of Ca^{2+}_i-stores induced by ionomycin resulted in the activation of an inwardly rectifying current of 10.1 ± 1.2 pA at -120 mV (n=10) in solutions containing 1.5 mM free Ca^{2+}. Representative ramp IV relationships (-125 to +60 mV from a holding potential of -40 mV) before and after ionomycin application and the kinetics of the generation of the whole cell current measured at -120 mV are shown in the accompanying figure. Maintenance of the inward current was dependent upon the sustained application of ionomycin. Removal of the ionophore was accompanied by a time dependent decrease of the current which was reversed by re-application of ionomycin. Consistent with the characteristics of the inward current activated by passive depletion, changes of $[Ca^{2+}]_o$ altered the magnitude of the current and the reversal potential. Interestingly, the inward current activated by ionomycin was irreversibly inhibited by 8 mM extracellular Ni^{2+} whereas the current activated by passive depletion displayed reversible inhibition.

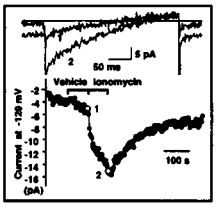

Tu-Pos347

Ca^{2+} CHANNEL β SUBUNITS REGULATE NEUROTRANSMITTER MODULATION OF VOLTAGE-GATED Ca^{2+} CHANNELS. ((S.M. Cibulsky and W.A. Sather)) Department of Pharmacology, Univ. of Colorado Health Sciences Center, Denver, CO 80262.

The activity of voltage-gated Ca^{2+} channels can be modulated by a variety of neurotransmitter receptors, including those for somatostatin (SOM), serotonin (5-HT) and adenosine. We have studied the modulation by these transmitters of two distinctly different Ca^{2+} channels heterologously expressed in *Xenopus* oocytes. SOM modulation of either class A (BI-2) or class C (L-type) Ca^{2+} channels depends upon the species of β subunit co-expressed. The degree of modulation by SOM is in general greater for BI-2 than for the L-type clone. 5-HT_{2a} receptors express functionally in oocytes but do not modulate BI-2 Ca^{2+} channels incorporating any of betas 1-3. Endogenous adenosine receptors were present in some oocytes. In preliminary studies, the adenosine receptor agonist 2-chloroadenosine produced a potent but transient inhibition of $\alpha_{1C}\alpha_2\beta_{2b}$ channels but little or no inhibition of $\alpha_{1C}\alpha_2\beta_{2a}$ channels.

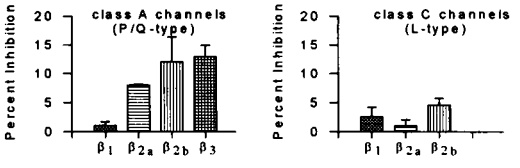

Tu-Pos348

MODULATION OF CALCIUM LEVELS IN LEUKEMIA CELLS BY FREE AND LIPOSOME-ASSOCIATED ETHER LIPID, ((Andrew C. Peters., A.S. Janoff and Eric Mayhew)) The Liposome Company Inc., Princeton, NJ 08540.

Ca^{++} mediated mechanisms may be involved in the anticancer effects and/or the non-specific toxic effects of the ether lipid, 1-O-octadecyl-2-*sn*-O-methyl-glycero-3-phosphocholine (EL) and an optimized liposome formulation of EL, ELL-12 (DOPC : Cholesterol : DOPE-GA : EL, in a 4 : 3 : 1 : 2 molar ratio). In vitro, ELL-12 is at least 20 times less hemolytic than EL. In vivo, ELL-12 has reduced toxicity and maintained or increased therapeutic effects against several murine tumors, compared to EL. The effects of EL and ELL-12 on changes in $[Ca^{++}]$ in murine leukemia L1210 cells loaded with a fluorescent $[Ca^{++}]$ dependent indicator (Fluo3AM) were compared. An external concentration of 1.25 μM EL in phosphate buffer (Ca^{++}, Mg^{++} 'free') caused an immediate, transient $[Ca^{++}]$ increase in L1210 cells (Ca^{++} could become available from intra- or extracellular sources) which decreased after 100-200 seconds. If the EL concentration was increased to 5 μm, there was a rapid irreversible increase in $[Ca^{++}]$. In contrast, 1.25 or 5.0 μM ELL-12 (EL concentration) did not cause any significant increase in $[Ca^{++}]$. The improved therapeutic effects of ELL-12 are related to decreased availability of 'free' EL from liposomes, necessary to cause rapid changes in $[Ca^{++}]$. The decreased availability of EL may be due to the strong association of EL with the components of the ELL-12 formulation.

Tu-Pos349

INCREASED THAPSIGARGIN-MEDIATED CALCIUM UPTAKE IN CLUSTERS OF APLYSIA BAG CELL NEURONS. ((S. Levy, D. Utheza and A. Levine)) Dept. of Physiology, Boston Univ. Sch. Med., Boston, MA 02118.

The purpose of the present experiments was to characterize calcium fluxes following depletion of intracellular calcium stores by thapsigargin. We have previously shown a thapsigargin-mediated Ca^{2+} uptake in single isolated bag cells neurons. To better quantify the Ca^{2+} uptake, we have used calcium-sensitive minielectrodes to measure extracellular calcium (Ca_o) at the plasma membrane of intact clusters of bag cell neurons. The calcium-sensitive minielectrode was made out of polyethylene tubing (O.D. 1.09 mm, I.D. 0.38 mm). The tubing was made calcium-sensitive by dipping its tip in a PVC-based calcium sensor; after evaporation, a 80-100 μm thick membrane was formed. The minielectrode was bevelled by cutting the tip at a 30 degrees angle, resulting in a sensing area of about 15.10^4 μm^2, large enough to cover and measure from about 70 cells. To follow the electrical activity, a separate microelectrode was used to measure the membrane potential in a neighboring cell (bag cell neurons are electrically coupled). Ca_o in the seawater was lowered to 1 mM to improve the signal-to-noise ratio. A brief stimulus train to the afferent input induced a transient Ca_o decrease of about 12 μM, indicating a Ca^{2+} influx. This Ca^{2+} influx is believed to induce Ca^{2+} release from intracellular stores (J. Neurophys. 71:3). Following bath application of thapsigargin (1 μM), the transient Ca_o decrease increased by about 50%, suggesting an increased Ca^{2+} uptake brought about by depletion of intracellular calcium stores.
Supported by NIH grant NS 30672.

Tu-Pos350

INVESTIGATION OF CALCIUM REGULATION USING SERCA PUMP INHIBITORS ((M.A. Albrecht and D.D. Friel)) Department of Neuroscience, Case Western Reserve University, Cleveland, OH 44106.

The role of intracellular Ca^{2+} pumps in $[Ca^{2+}]_i$ regulation was studied using the reversible SERCA pump inhibitor 2,5-di(*tert* -butyl-)-1,4-hydroquinone (BHQ). $[Ca^{2+}]_i$ was measured in fura-2 AM loaded bullfrog sympathetic neurons. BHQ application elicited a $[Ca^{2+}]_i$ rise consisting of transient and steady components that were graded with [BHQ] (1-100 μM). The transient rise was observed both in the presence (50 μM: 227±87 nM, N=9) and absence of external Ca^{2+} (108±28 nM, N=3) (no added Ca^{2+} and 0.2 mM EGTA) indicating that BHQ releases Ca^{2+} from an internal store, presumably by inhibiting intracellular Ca^{2+} uptake and unmasking an ongoing Ca^{2+} leak. Following BHQ removal $[Ca^{2+}]_i$ underwent a transient undershoot, which in the absence of external Ca^{2+} was maintained. This suggests that recovery from the undershoot reflects replenishment of the store via the cytosolic compartment at the expense of external Ca^{2+}. The steady elevation of $[Ca^{2+}]_i$ in the presence of BHQ required external Ca^{2+} (N=3), suggesting that it reflects Ca^{2+} entry from the extracellular medium. However, thapsigargin (TG), another SERCA pump inhibitor presumed to have a similar mechanism of action, had no detectable effect on resting $[Ca^{2+}]_i$ (N=3), suggesting that some actions of BHQ and TG may be different. The transient responses to BHQ application and removal can be described by the difference between two decaying exponential functions, consistent with a model that has been proposed to describe Ca^{2+} homeostasis in these cells over the range $[Ca^{2+}]_i$<~500 nM (Friel, 1995).

Tu-Pos351

ACTION OF NITRIC OXIDE ON CALCIUM CURRENT IN NON-VASCULAR SMOOTH MUSCLE CELLS. ((Zima A.V. & *Shuba M.F.)) Bogomoletz Institute of Physiology and *Shevchenko University of Kiev, Bogomoletz St.4, Kiev-24 GSP, 252601, Ukraine.

The whole-cell patch-clamp method was used to study the action of nitric oxide (NO) donors, nitroglycerin (NG) and sodium nitroprusside (SNP), on the basal L-type Ca^{2+} current (I_{ca}) in isolated myocytes from taenia coli guinea pig. I_{ca} was markedly reduced during exposure to NG in a concentration-dependent manner with IC_{50} of 1μM and maximum inhibition of 38%. This effect was partly blocked by 20μM methylene blue (MB), an inhibitor of guanilate cyclase. 8-bromo-3'5'-cyclic GMP (8-br-cGMP) also reduced the amplitude of I_{ca}. NG and 8-br-cGMP decreased I_{ca} without significantly altering the current-voltage curve and steady-state inactivation of I_{ca}. SNP (0.1-10μM) caused increase of I_{ca} (by 23% for 10μM), although high concentration (0.1-1mM) reduced current (by 27% for 1mM). MB (20μM) abolished the inhibitory action of SNP, but did not attenuate the stimulatory action. SNP did not change I_{ca} in the presence of oxyhemoglobin. $NaNO_2$-containing solution mimicked the effects of SNP on I_{ca}. These results suggest that NO can produce cGMP-dependent inhibition and cGMP-independent activation of L-type Ca^{2+} channels in taenia coli smooth muscle cells.

Tu-Pos352

EXPRESSION OF LVA Ca CHANNELS FROM RAT HYPOTHALAMUS IN *XENOPUS* OOCYTES. ((I.P. Dzhura, V.G. Naidenov, O.P. Lyubanova, P.G. Kostyuk and Y.M. Shuba)) Bogomoletz Institute of Physiology, National Academy of Sciences of Ukraine, Bogomoletz Str., 4, 252024 Kiev, Ukraine.

Ca-channel currents expressed in *Xenopus* oocytes following injection of mRNA purified from rat thalamohypothalamic complex were studied using double microelectrode technique. In Cl^--free extracellular solutions containing 40 mM Ba^{2+} as a charge carrier through the Ca channels depolarizations from very negative holding potential (V_h = -120 mV) elicited inward Ba^{2+} current (I_{Ba}) with voltage-dependence typical of low-voltage-activated (LVA) Ca channels, i.e., I_{Ba} activated around -80 mV, reached maximal amplitude at -30 - -20 mV and reversed at +50 mV. The time-dependent inactivation of the current during prolonged depolarization to -20 mV was slow and followed a single exponential decay with time constants of 1550 ms and a maintained component of about 30% of the maximal amplitude. As expected for LVA-type current, steady-state inactivation curve was shifted towards the negative potentials and could be described by Boltzmann equation with half inactivation potential -78 mV, slope factor 15 mV and steady-state level 0.3. Current couldn't be completely inactivated at any holding potential. Expressed Ba^{2+} current could be blocked by flunarizine with K_d = 0.42 μM, nifedipine, K_d = 10 μM, and amiloride at 500 μM concentration. Among the inorganic Ca-channel blockers the most potent was La^{3+} (K_d = 0.48 μM) while Cd^{2+} and Ni^{2+} had similar potency and were almost thousand fold less effective than La^{3+} (K_d = 0.52 mM and K_d = 0.62 mM respectively). Our data show that mRNA purified from thalamo-hypothalamic complex induces expression in the oocytes of almost exclusively LVA Ca^{2+} channels with voltage-dependent and pharmacological properties very similar to those observed for T-type Ca^{2+} current in native hypothalamic neurons, though kinetic properties of the expressed and natural currents are somewhat different. Supported in part by International Science Foundation no. U5L000 (YMS).

Tu-Pos353

MITOCHONDRIAL CONTRIBUTIONS TO $[Ca^{2+}]_i$ REGULATION IN SYMPATHETIC NEURONS ((D.D. Friel)) Dept. of Neurosciences, Case Western Reserve University, Cleveland, OH 44106

In a variety of neurons, stimulus-evoked elevations in $[Ca^{2+}]_i$ approaching ~500 nM are followed by a slow and complex recovery. Since the slow recovery is speeded by mitochondrial uncouplers such as FCCP, it has been interpreted as reflecting Ca^{2+} release from mitochondria which accumulate Ca^{2+} during the stimulus. To test for an intracellular compartment whose Ca^{2+} content rises reversibly during membrane depolarization, fura-2 AM-loaded bullfrog sympathetic neurons were exposed to 10 μM FCCP in low Ca^{2+} media (no added Ca^{2+} + 0.2 mM EGTA) under resting conditions, and during the slow recovery following depolarization with 50 mM K^+. FCCP had little effect on $[Ca^{2+}]_i$ at rest, but elicited a large transient $[Ca^{2+}]_i$ elevation when applied during the slow recovery, demonstrating that there is an internal store whose Ca^{2+} content rises during depolarization. To learn more about the identity of the store, effects of other mitochondrial inhibitors were examined. Antimycin A_1 (1 μM), a respiratory chain inhibitor, abolished the slow recovery, but unlike FCCP, had little or no effect on the $[Ca^{2+}]_i$ level reached during depolarization, as reported previously in rat sensory neurons (Werth and Thayer, 1994). However, depolarization in the combined presence of antimycin A_1 and oligomycin (1 μM), an ATP synthase inhibitor, elicited a $[Ca^{2+}]_i$ response closely resembling that observed in the presence of FCCP. These results confirm the presence of an FCCP-sensitive store that shapes $[Ca^{2+}]$ responses to membrane depolarization (Friel and Tsien, 1994), and provide additional support for the conclusion that the store is mitochondrial.

Tu-Pos354

LACK OF INVOLVEMENT OF PROTEIN KINASE A PHOSPHORYLATION SITES IN VOLTAGE-DEPENDENT FACILITATION OF THE ACTIVITY OF HUMAN CARDIAC L-TYPE CALCIUM CHANNELS. ((J. Eisfeld[1], G. Mikala[2], A. Schwartz[2], G. Varadi[2] and U. Klöckner[1])) [1]Department of Physiology, University of Cologne, 50931 Cologne, Germany and [2]Institute of Molecular Pharmacology and Biophysics, University of Cincinnati, OH 45267-0828, USA.

Phosphorylation by protein kinase A is thought to be involved in the voltage-dependent facilitation of calcium channel activity. Here we demonstrate that the subunit complex of a cloned human cardiac L-type calcium channel, as expressed in *Xenopus* oocytes, responds to voltage-dependent facilitation by an approximately 40 % increase of calcium channel peak current. Further, we have tested whether the protein kinase A consensus sites on the α_1 subunit are involved in the facilitation process. The removal of all five protein kinase A consensus sequences by site-directed mutagenesis diminished the extent and frequency of response to prepulse facilitation, however, Rp-cAMP-S, an inhibitor of of protein kinase A, did not influence facilitation either of the wild-type- or of the phosphorylation-multi-mutant-evoked calcium channel currents. Similarly, the individual substitution of the consensus sites showed no effect on the extent of facilitation, as well as on the inhibition by Rp-cAMP-S. We conclude that voltage-dependent facilitation of calcium channel currents is due to voltage-induced conformational changes of the channel rather than to enhanced cAMP-dependent phosphorylation.

Tu-Pos355

CARDIAC Ca^{2+} CHANNELS EXPRESSED IN *XENOPUS* OOCYTES ARE NOT SUSCEPTIBLE TO PHOSPHORYLATION/DEPHOSPHORYLATION. ((Y. M. Shuba, V. G. Naidenov and M. Morad)) Department of Pharmacology, Georgetown University, Washington, DC 20007. (Spon. by I. Dukes)

Rat heart mRNA was used to express cardiac Ca^{2+} channel in *Xenopus* oocytes to examine its β-adrenergic regulation. To record membrane currents and to apply drugs, the glass-funnel technique permitting fast voltage clamp and effective intracellular dialysis was used. Even though cardiac mRNA-injected oocytes expressed L-type Ca^{2+} channels, we failed to augment corresponding Ba^{2+} current (I_{Ba}) with either external application of β-agonist isoproterenol (ISO, 10 μM), adenylate cyclase (AC) activator forskolin (FSK, 10 μM), phosphodiesterase inhibitor IBMX (200 μM) or their mixtures. I_{Ba} was also unaffected by application of membrane permeable cAMP analog CPT-cAMP (500 μM) or intracellular infusion of cAMP (300 μM). Block of cAMP-dependent phosphorylation pathway by intracellular dialysis of Rp-cAMPS (200 μM) plus synthetic protein kinase A (PKA) inhibitor peptide (200 μM) also failed to alter the basal level of I_{Ba}, suggesting that absence of cAMP effect on the expressed Ca^{2+} channels could not result from an already maximally phosphorylated resting state. Measurements of cAMP levels in control and mRNA-injected oocytes using enzyme-immunoassay system showed that they have similar basal cAMP concentration (2-2.5 μM). On the other hand, in mRNA-injected, but not control oocytes, cAMP level increased 2 to 3 fold in response to stimulation by either ISO+FSK or IBMX. Our data show that injection of heart mRNA into *Xenopus* oocytes leads to the expression of receptor-stimulated AC, and a cAMP-insensitive L-type Ca^{2+} channels. The absence of cAMP-dependent phosphorylation/dephosphorylation reponse may be due to either inaccessibility of PKA-dependent phosphorylation site or lack of some necessary cofactor(s). In light of these findings previous reports on cAMP-dependent regulation of the expressed cardiac Ca^{2+} channels in the oocytes remain puzzling. Supported by AHA Washington, DC Affiliate (YMS) and NIH HL16152 (MM).

Tu-Pos356

A NOVEL Cd^{2+}-INSENSITIVE Ca^{2+} CHANNEL IN CARDIAC MYOCYTES. ((C.M. Ko, M. MacCormack, and M. Morad)) Institute for Cardiovascular Sciences and Department of Pharmacology, Georgetown University Medical Center, Washington, DC, 20007. (Spon. by T. Panavelil)

The L-type Ca^{2+} channel is the primary Ca^{2+} transporting protein in cardiac myocytes. This channel is blocked most effectively by inorganic cations Cd^{2+} (K_d1-10μM), Co^{2+}, Ni^{2+}, and Mn^{2+}. In this report we have examined the effectiveness of Cd^{2+} block of L-type Ca^{2+} channel, as well as the possible existence of Cd^{2+}-insensitive Ca^{2+} currents. In whole cell clamped rat or guinea-pig ventricular myocytes dialyzed with Cs^+, 14mM EGTA, and 0.2mM cAMP, the L-type Ca^{2+} channel was maximally activated from holding potentials of -50 mV by step depolarization to zero or +10 mV. The current density was 34.6±2.1 (n=30) pA/pF in rat and 18.2±3.1 (n=9) pA/pF in guinea-pig myocytes. 100 μM Cd^{2+} blocked this current by 97% rapidly (<100 ms). In the presence of100μM Cd^{2+} we could identify an inward, slowly inactivating current which was independent of extracellular Ca^{2+}, Mg^+, or Na^+ concentrations, and was enhanced by increases of $[Cd^{2+}]_o$, reaching a maximal value of 3.7 pA/pF (n=7) in 3.0 mM Cd^{2+} (at 0 mV, rat). The Cd^{2+} current had a Kd ≈ 200μM, a voltage-dependence similar to I_{Ca}, and was present even when Ba^{2+} was the charge carrier through the L-type Ca^{2+} channel. The Cd^{2+} current was enhanced in the presence of BayK8644 and was blocked by 1 μM nifedipine, verapamil, and diltiazem, as well as 5 mM Co^{2+} or Ni^{2+}. Our results are consistent with the existence of either a novel sub-type of Cd^{2+}-insensitive Ca^{2+} channels, or a Cd^{2+}-permeant sub-population of L-type Ca^{2+} channels heretofore unreported in cardiac myocytes. Supported by NIH HL16152.

Tu-Pos357

EFFECTS OF MICROCYSTIN AND ISOPROTERENOL ON L-TYPE Ca^{2+} CURRENT AND cAMP-REGULATED Cl^- CURRENT IN GUINEA PIG VENTRICULAR MYOCYTES. ((Y.Hirayama and H.C.Hartzell)) Dept. Anatomy & Cell Biology, Emory University, Atlanta, GA 30322.

We have reported that in frog ventricular myocytes, regulation of L-type Ca^{2+} current (I_{Ca}) by β-adrenergic agonists involves two phosphorylation sites (J. Gen. Physiol. 106, 1-22:1995). One site is dephosphorylated by phosphatase 2A and the other site by a phosphatase having low sensitivity to microcystin (MC). One site can be phosphorylated by a novel protein kinase (PKX) that is basally active and may play a role in setting the basal amplitude of I_{Ca}. It is not known whether a similar protein kinase regulates ion channels in mammalian cardiomyocytes. The present experiments suggest that PKX also contributes to the regulation of I_{Ca} and cAMP-activated Cl^- current (I_{Cl}) in guinea pig cardiomyocytes. 1μM isoproterenol (Iso) increased I_{Ca} from 3.1±0.3 pA/pF to 9.1±0.7 pA/pF and activated I_{Cl} 1.5±0.1 pA/pF. The effect of Iso on I_{Cl} was twice as rapid as the effect on I_{Ca} [for I_{Ca} and I_{Cl}, respectively, activation t/2 = 25.8±0.6s and 12.0±0.2 s; deactivation t/2 =3.6±0.2 m and 2.2±0.2 m]. Low concentrations (<3μM) of MC alone had no effect on either current, but partially inhibited the washout of the effect of Iso. This suggested that both currents are regulated by multiple phosphorylation sites. In contrast, high concentrations of MC (>10μM) stimulated I_{Ca} and I_{Cl} in the absence of Iso: I_{Ca} was stimulated 6.5pA/pF and I_{Cl} was stimulated 1.6pA/pF. In contrast to the effect of Iso, MC had a much slower effect on I_{Cl} than I_{Ca}. The effects of MC on I_{Ca} and I_{Cl} were not attenuated by PKA inhibition, suggesting that PKA was not responsible for the MC effect. This suggests that PKX exists in guinea pig ventricular myocytes and can phosphorylate I_{Ca} and I_{Cl}.

Tu-Pos358

P_{2X} PURINOCEPTORS IN HUMAN PLATELETS. ((Amanda B. MacKenzie, Stewart O. Sage & Martyn P. Mahaut-Smith)) The Physiological Laboratory, Downing Street, Cambridge. CB2 3EG, U.K. (Spon. by Prof. R. Thomas)

We have investigated purinoceptor subtypes underlying calcium signalling in human platelets. $[Ca^{2+}]_i$ was measured in fura-2-loaded platelet suspensions in the presense of 20 μg ml^{-1} apyrase to minimise desensitization. In the presence of 1mM $Ca^{2+}{}_o$, a rapid rise in $[Ca^{2+}]_i$ was induced by 40μM ADP (basal to peak, 313±12nM, n=9) and 40μM ATP (138±45nM, n=8). 10μM α,β-meATP elicited an increase in $[Ca^{2+}]_i$ of 90±8nM (n=4) in 1mM external Ca^{2+} which was abolished in Ca^{2+}-free saline. In Ca^{2+}-free saline, ADP caused a peak $[Ca^{2+}]_i$ increase of 164±14nM (mean±S.E, n=4) while ATP caused only a gradual rise in $[Ca^{2+}]_i$ of 57±37nM (mean±S.E., n=6). Pre-addition of α,β-meATP did not alter the $[Ca^{2+}]_i$ response to ADP in Ca^{2+}-free saline. Under nystatin whole-cell patch clamp in 150mM NaCl saline, at negative potentials, ATP evoked a transient inward current with a delay of < 20ms, a peak current of 25.5-101pA and a decay time constant ranging from 47 to 107ms. Single channel chord conductance (at -70mV) was 11.5±0.4pS in 150mM NaCl and 10.7±0.7pS in 110mM $BaCl_2$. From the peak currents, we estimate at least 100 channels per platelet. This non-selective cation channel was also activated by the non-hydrolysable analogues of ATP, ATPγS (40μM) and α,β-meATP (10μM). This channel has been previously shown to be activated by ADP and to involve a receptor-operated (rather than a second messenger-operated) mechanism (Mahaut-Smith et al, *J.Biol.Chem.* 267, 3060-65). We conclude that human platelets possess at least two purinoceptors subtypes; an α,β-meATP-sensitive P_{2X} purinergic receptor which is coupled to a non-selective cationic channel and a second ADP-selective purinoceptor, linked to phospholipase C.

Funded by the British Heart Foundation and the BBSRC.

Tu-Pos359

NPPB BLOCKS VOLUME-REGULATED CHLORIDE CURRENT AND CAPACITIVE CALCIUM CURRENT IN JURKAT CELLS. ((K. T. Spence, P. G. Dargis, and E. P. Christian)) Department of Pharmacology, Zeneca Pharmaceuticals, Wilmington, DE 19850.

The Cl^- channel blocker NPPB (5-nitro-2-(3-phenylpropylamino)benzoic acid also blocks capacitive calcium entry in mast cells (Reinsprect, et al., *Molecular Pharm.* 47:1014-1020, 1995). Using standard whole-cell techniques, we show that NPPB inhibits both Cl^- current and ICRAC (Ca^{2+} release-activated Ca^{2+} current) in E6-1 Jurkat T-lymphocytes. Solutions were as follows (in mM). **Extracellular Cl^-:** NaCl 160, KCl 4.5, $CaCl_2$ 2, $MgCl_2$ 1, HEPES 5, pH 7.4, ~305 mOsm. **Intracellular Cl^-:** Cs-aspartate 160, $MgCl_2$ 2, $CaCl_2$ 0.1, EGTA 1.1, Na_2ATP 4, HEPES 10, pH 7.2, ~309 mOsm. **Extracellular Ca^{2+} :** NaCl 160, KCl 4.5, $CaCl_2$ 2, $MgCl_2$ 1, HEPES 5, glucose 5, pH 7.4, ~325 mOsm. **Intracellular Ca^{2+}:** Cs-aspartate 140, $MgCl_2$ 2, HEPES 10, EGTA 10, pH 7.2, ~305mOsm. Activation of volume-regulated Cl^- current was induced by diluting the extracellular Cl^- solution by 20% with distilled water. Steady-state Cl^- current was reversibly blocked by NPPB (IC_{50} ~10.5 μM). NPPB showed similar potency and reversibility on ICRAC (IC_{50} ~8 μM). In other experiments, Michaelis-Menten analysis is being applied to the ICRAC current density generated by various extracellular Ca^{2+} concentrations in the absence or presence of fixed NPPB concentrations to evaluate the mechanism of NPPB inhibition (i.e., competitive, noncompetitive or uncompetitive).

Tu-Pos360

SWELLING-ACTIVATED WHOLE-CELL CURRENTS IN MOUSE THYMOCYTES. ((Paul E. Ross and Michael D. Cahalan)) Department of Physiology and Biophysics, UC Irvine, CA 92717.

We have previously studied a swelling-activated Ca^{2+} (SWAC) influx pathway in immature thymocytes using fura-2 imaging (Ross and Cahalan, *J. Gen. Phys.* 106: 415–444, 1995). Here we describe swelling-induced currents in thymocytes using the whole-cell patch-clamp technique. Perfusion with hyperosmotic Cs^+ glutamate pipette solutions elicits a SWAC transient after a delay of ≈ 40 s. Measurements at +/- 80 mV show that the transient consists of both outward and inward currents (*left Figure*). Voltage ramp traces exhibit pronounced outward-rectification at early stages of the transient. Midway through the 8 s long event, the outward component subsides, revealing an inwardly-rectifying current. Outward current development always precedes the inward component (*right Figure*). Two lines of evidence suggest that non-selective channels open during

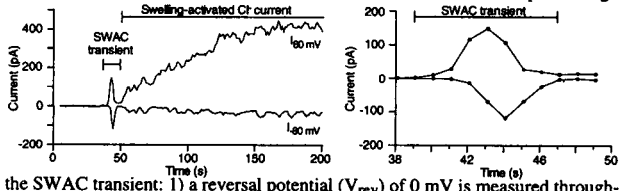

the SWAC transient: 1) a reversal potential (V_{rev}) of 0 mV is measured throughout the event; and 2) a prominent inward current, probably carried by Na^+, is still observed in the absence of extracellular Ca^{2+}. After the SWAC transient, swelling-activated Cl^- currents shift V_{rev} to ≈ -40mV. Our data support the idea that the SWAC transient is generated by non-selective channels which carry multiple ionic species. Supported by NIH grants NS14609 and GM41514.

Tu-Pos361

TNP-ATP BINDING TO Na^+/K^+ ATPase MEASURED BY FLUORESCENCE QUENCHING. ((E.H. Hellen, C.P. Collier, A. Palit, B.C. Yacono, J.M. Fox, and P.R. Pratap)) Dept. of Physics and Astronomy, UNC-Greensboro, Greensboro, NC 27412.

Trinitrophenyl-ATP (TNP-ATP) is a useful probe of the ATP binding site of the IAF labeled Na^+/K^+ ATPase enzyme. This nonhydrolyzable ATP analogue binds to the ATP binding site of the enzyme with concomitant quenching of the IAF fluorescence. TNP-ATP has been used in distance studies and in ATP binding kinetics studies of the IAF labeled enzyme. Here we examine the steady-state fluorescence of membrane fragments of IAF labeled Na^+/K^+ ATPase titrated with TNP-ATP as a function of ATP, Na^+, and Mg^{2+} concentrations. Binding affinities and amounts of specific and non-specific binding are determined. In experiments where TNP-ATP and ATP compete for sites on the enzyme, we find that with no Na^+ and no Mg^{2+} present, K_d for ATP is 2 μM, and K_d for TNP-ATP is 0.3 μM. For [Na^+] greater than 1 mM, the affinity of ATP increases, with K_d dropping to 0.5 μM, while the affinity of TNP-ATP has little or no change. The affinity of TNP-ATP does increase in the presence of 1 mM Mg^{2+} (with no Na^+). At 0.5 μM TNP-ATP, approximately 20% of the quenching is due to nonspecific binding. Supported by a grant from the NIH.

Tu-Pos362

KINETICS OF TNP-ATP BINDING TO Na^+,K^+-ATPASE MEASURED BY QUENCHING OF IAF-ENZYME FLUORESCENCE. ((P. R. Pratap†, A. Palit†, E. H. Hellen†, and J. D. Robinson*)) †Physics and Astronomy, UNC-Greensboro, Greensboro, NC 27412 and *Pharmacology, SUNY-HSC, Syracuse, NY 13210.

Fluorescence quenching of the Na^+-form of a dog kidney Na^+, K^+-ATPase preparation labeled with 5-iodoacetamidofluorescein (IAF) by the ATP analog, trinitrophenyl ATP (TNP-ATP) was used as a measure of TNP-ATP binding to the Na^+,K^+-ATPase. The time-course of quenching was followed with a stopped-flow fluorimeter: IAF-enzyme in 25 mM imidazole-HCl, pH 7, 1 mM EDTA, 155 mM choline chloride was rapidly mixed with varying concentrations of TNP-ATP in the same buffer. The fluorescence changes $\Delta F(t)$ were described well by a "stretched exponential" function: $\Delta F(t) = \Delta F_0 \cdot \exp[-(k_0 t)^\alpha]$, where ΔF_0 is the magnitude of quenching, α is the stretch factor, and $1/k_0$ is an "effective" lifetime for the fluorescence change. ΔF_0 increased with [TNP-ATP], while the constant k_0 was independent of [TNP-ATP]. The stretch factor, α, decreased from 0.7 at 0.2 μM [TNP-ATP] to about 0.3 at 5 μM [TNP-ATP]; the half-maximal [TNP-ATP] for this decrease was estimated to be greater than 1.5 μM. α was not affected by replacing choline with Na^+, but decreased with increasing [Mg^{2+}] ($K_{1/2}$ = 0.55 mM) at constant [TNP-ATP]. Heat-inactivation of the enzyme (9 hours at 37°C, 50% residual activity) reduced the magnitude of the quenching, but did not change the dependence of α on [TNP-ATP]. Ethanol (10% by volume) inactivated the enzyme but had no effect on quenching. These results indicate the existence of a spectrum of activation energies for TNP-ATP binding to the enzyme. This poster will discuss further the implications of these and other results. [Supported by grants from NIH]

Tu-Pos363

INSULIN CAN INDUCE A NEGATIVE SLOPE IN THE Na^+-K^+ PUMP'S VOLTAGE DEPENDENCE. ((P.S. Hansen, D.F. Gray and H.H. Rasmussen)) Department of Cardiology, Royal North Shore Hospital, Sydney, AUSTRALIA.

Previous studies in adipocytes suggest that insulin stimulates the Na^+-K^+ pump by increasing its apparent Na^+ affinity. To further explore this we voltage clamped cardiac myocytes with wide-tipped patch pipettes containing either 10 or 80 mM Na^+. Pipette solutions and extracellular solutions eliminated time dependent currents. Pump current (I_p), identified as the shift in holding current induced by 50 μM ouabain, was measured at membrane voltages (V_m) from -100 to +60 mV. I_ps for each cell were normalised to the I_p at 0 mV ($I_{p\text{-}0mV}$). When pipette solutions contained 10 mM Na^+ and extracellular solutions contained 5.6 mM K^+ and 140 mM Na^+ insulin reduced the positive slope of a near-linear I_p-V_m relationship from 0.49 $\%I_{p\text{-}0mV}$/mV to 0.11 $\%I_{p\text{-}0mV}$/mV ($p<0.05$) while it had no effect on the relationship when pipette solutions contained 80 mM Na^+. We reduced extracellular Na^+ to 1.5 mM by isosmolar substitution of NaCl with NMG.Cl to minimize effects of voltage-dependent extracellular Na^+ release from the pump. The I_p-V_m slope of 8 control myocytes patch clamped with pipettes containing 10 mM Na^+ was 0.28 $\%I_{p\text{-}0mV}$/mV. The slope for 6 myocytes exposed to insulin was -0.27 $\%I_{p\text{-}0mV}$/mV ($p<0.05$). The findings are consistent with insulin-regulated, voltage-dependent binding of Na^+ at intracellular pump sites.

Tu-Pos364

VOLTAGE-DEPENDENT INACTIVATION OF THE ION CHANNEL IN THE NA,K-ATPASE AND ITS REMOVAL BY PRONASE. ((T. Blackmer, P. A. Yates, J. K. Hirsh and C. H. Wu)) Dept. Mol. Pharmacol. & Biol. Chem., Northwestern University, Chicago, IL 60611.

The Na,K-ATPase pumps ions by a mechanism currently thought to involve a channel structure. We reconstituted purified dog kidney Na,K-ATPase in planar lipid bilayer. Single channel currents were induced by palytoxin. When a voltage ramp from -60 to +80 mV at 20 mV/s was applied to the bilayer, two types of single channel conductance were observed. One exhibited a linear I-V relationship, while the other showed inward rectification. The inward rectification was not due to block by Mg^{2+} or polyamines but rather an intrinsic voltage-dependent inactivation. The ohmic channels inactivated at positive potentials over a range of +30 to +80 mV. The curve relating open probability to membrane potential was fitted to a Boltzmann distribution with a $V_{½}$ of +50.4 mV and a slope factor of 6.6 mV. After treatment with pronase (1 mg/ml) at the cytoplasmic face, the inactivation was removed. The Na,K-ATPase has a cluster of basic residues in the N-terminus homologous to the *Shaker* B K^+ channel, which may have been removed by pronase. This suggests a mechanism similar to the N-type inactivation of *Shaker* B in which the N-terminus functions as a ball-and-chain to block the ion pore. Supported by Northwestern Medical School IRG8673.

Tu-Pos365

NaK-ATPase: PROTEOLYTIC FRAGMENTS LACKING THE CATALYTIC ATP SITE RETAIN ATP-REGULATED Rb^+ ACCESS CHANNELS. ((L. Liu and A. Askari)) Dept. Pharmacology, Med. Coll. of Ohio, Toledo, OH 43699

Extensive trypsin digestion of purified NaK-ATPase in the presence of Rb^+ removes large portions of the cytoplasmic domains of α-subunit. The remaining α fragments and β ("19-kDa membranes") do not contain the high-affinity ATP catalytic site but retain the ability to occlude Rb^+ (Karlish et al, PNAS, 87, 4566, 1990). Using the procedures we have used before on the native enzyme (Hasenauer et al, JBC, 268, 3289, 1993) we found that the access channels connecting the occlusion sites of "19-kDa membranes" to the medium, like those of the native enzyme, are regulated by nucleotides. In "19-kDa membranes" containing less than 1% intact α, both occlusion and deocclusion rates were significantly increased by ATP ($K_{0.5}$ = 0.4 mM) and CTP, but not by GTP and AMP. Pretreatment with FITC did not affect occlusion, but blocked the effect of ATP on occlusion rate. Presence of 5 mM ATP during pretreatment, partially antagonized the FITC effect. Of the large number of α residues that have been implicated in high-affinity ATP binding to the native enzyme, only K766 remains in the "19-kDa membranes". These data show that catalytic and allosteric ATP sites are distinct entities, and that the residues involved in the latter site must be close to the intramembrane domains of α. Supported by NIH grant HL36573.

Tu-Pos366

REGULATORY PHOSPHORYLATION-DEPHOSPHORYLATION OF THE Na^+/K^+-ATPase FROM MAMMALIAN KIDNEYS AND *XENOPUS* OOCYTES BY PROTEIN KINASES AND PHOSPHATASES. ((L.A.Vasilets[1,2], E.-M.Gärtner[1], H.Fotis[1])) [1]Max-Planck-Institute f. Biophysics, Frankfurt/M, FRG; [2]Inst. of Chemical Physics, Chernogolovka, Moscow reg., Russia. (Sponsored by W. Stoeckenius)

Modulation of transport activity and phosphorylation-dephosphorylation of the Na^+/K^+-ATPase have been studied in *Xenopus* oocytes and in enzymes purified from pig, dog, sheep, and rat kidneys. Microinjections into the *Xenopus* oocytes of exogenous PKA lead to an increase of ouabaine-sensitive ^{86}Rb-uptake by 25-140%, microinjections of PKC produced 50% of inhibition. PKA phosphorylated the α-subunits of all tested animal species. PKC phosphorylated only the α-subunit from rat kidney Na^+/K^+-ATPase. Comparison of amino acid sequences indicates that enzymes from pig, dog, and sheep kidneys do not contain N-terminal Ser-23 which can form a phosphorylation site for PKC. None of the α-subunits from mammalian kidney Na^+/K^+-ATPase was phosphorylated by casein kinase and Ca^{2+}/calmodulin-dependent protein kinase. Microinjections into the *Xenopus* oocytes of serine-threonine phosphatases PP-1, PP-2A, and PP-2B lead to an increase of ^{86}Rb-uptake by 94%, 62%, and 95% respectively, while alkaline phosphatase was without effect. Phosphorylation of the α-subunit by PKA increased if PP-2A was present in incubation buffer in small concentrations. High concentrations of PP-2A reduced phosphorylation signal. PP-1 did not effect phosphorylation by PKA. The data indicate that regulatory effects of phosphatases may be attributed not only to dephosphorylation of the pump protein but also to a prevention of inhibitory autophosphorylation of protein kinases. (Supported by HHMI grant 75195-547101).

Tu-Pos367

INFLUENCE OF RADIATION-INDUCED FREE RADICALS ON PARTIAL REACTIONS OF THE NA,K-ATPASE ((M. Mense*, R. Buehler, G. Stark, H.-J. Apell)) Dept. of Biology, University of Konstanz, Postfach 5560 M635, D-78434 Konstanz, Germany, and *Dept. of Physiology, Yale School of Medicine, New Haven, CT 06511

The effect of free radicals, produced by X-ray radiolysis of water, upon partial reactions of the Na,K-ATPase was studied by a fluorescence method using the potential-sensitive dye RH 421. Under standard conditions (histidine buffer, 10 mg/ml of rabbit-kidney ATPase in membrane fragments, and 1 μM RH 421; Schwappach et al., J. Biol. Chem. 269:21620,1994) addition of 10 mM Na^+ reduced RH 421 fluorescence by ~15%, and further addition of 0.5 mM ATP increased the fluorescence by about 50%. Using this basic assay on control enzyme, we determined the K_m for the Na^+-driven fluorescence shift to be ~6.9 mM, corresponding to the accepted value for sodium binding constant of the enzyme in presence of 5 mM Mg^{2+} (Stein, Acad. Press, 1986). Measurements on enzyme pre-reacted with free radicals revealed only a slight change (increase) of the sodium binding affinity, at least up to doses (~1600 Gy), sufficient to inactivate 99% of ATP hydrolysis. In the ATP-driven process, both the rate constant and the amplitude of the fluorescence shift (ΔF) produced by fast addition of ATP (flash photolysis of caged ATP) were conspicuously decreased by free-radical treatment. We have interpreted the reduction of *rate constant* to mean that free radicals inhibit the $E_1 \rightarrow E_2$ conformational transition in the enzyme, which is the rate-limiting step for ATP-driven ΔF. The reduced *amplitude* measures the fraction of ATPase molecules still capable of undergoing the conformational change. Free-radical effects on several reaction substates (as judged from a detailed examination of fluorescence shifts in steady-state measurements) were compared with the observed ATPase activity after same free-radical treatment. The results support the conclusion that loss of enzyme function results from (1) slowing of the conformational transition ($E_1 \rightarrow E_2$), and (2) destruction of the enzyme.

The work was financially supported by the Deutsche Forschungsgemeinschaft (Sonderforschungsbereich 156).

Tu-Pos368

POTASSIUM DEPENDENT pNPP HYDROLYSIS AND AND INDUCED CONFORMATION CHANGES IN NaK-ATPASE

((I. Kovacs, M. H. Garner)) Dept. of Anatomy and Cell Biology, UNT HSC, 3500 Camp Bowie Blvd. Fort Worth, Texas 76107. (Sponsored by M.H.Garner)

The potassium induced pNPPase activity of NaK-ATPase from rabbit kidney was studied at different sodium and potassium concentrations. The temperature dependence of the kinetics also was measured in the temperature range from 278°K to 313°K by applying a fast linear temperature scan. Without Na the pNPPase activity increases with increasing K concentration and saturates at about 8 mM [K]. There is an intermediate plateau from 8 to 80 mM [K]. At higher potassium concentration the activity gradually drops. Beyond 300°K the temperature dependence of the kinetics could be described by the Arrhenius relationship. Below the saturation potassium concentration both the activation enthalpies and the relative entropies are small. Beyond the saturating potassium concentration the entropy increases considerably. The drop of the activity at high potassium concentration is associated with an increase of the activation enthalpy. Below 300 °K the temperature dependence is different from that of Arrhenius and the rate decreases fast with decreasing temperature.

Tu-Pos369

GAB: A NOVEL PROTEIN THAT INTERACTS WITH THE γ SUBUNIT OF THE NA,K-ATPASE. ((N. Minor and R.W. Mercer)) Washington University, St. Louis, MO 63110

The Na,K-ATPase consists of two major subunits, α and β, both of which are required for normal enzymatic activity. In addition, there is a third small protein, termed γ, that is associated with α and β. At present, the role of the γ subunit is unknown. Although not required for catalytic activity, it is plausible that γ may act as a modulator of the kinetic properties of the Na,K-ATPase. This modulation could occur directly, or through interaction with another molecule. We have used the two hybrid screen to explore the role of the γ subunit in Na,K-ATPase function. This screen is a yeast-based genetic assay that detects functional protein-protein interactions *in vivo*. Yeast cells were transformed with the cDNA corresponding to the cytoplasmic tail of the γ subunit, fused to a lex A DNA binding domain. Cells containing γ were transformed with a rat muscle cDNA library fused to the activation domain of Gal 4. Interaction of the γ peptide with a cDNA directed peptide results in Gal 4 promoter activity. Using these techniques, several positive clones were isolated by β galactosidase assays. One of these cDNA clones encodes a 26 amino acid peptide corresponding to the carboxy terminus of a novel protein. This polypeptide, termed GAB (gamma binding peptide) may represent one of the effectors by which Na,K-ATPase function is regulated. The interaction between GAB and γ is being characterized using glutathione *S*-transferase as well as 6-His fusion vectors.

Tu-Pos370

SUBSTITUTION OF Na,K-ATPase $Glu^{779}Ala$ CHANGES ELECTROGENIC ION TRANSPORT BY THE Na PUMP. ((JM Arguello*, RD Peluffo, J Feng*, JB Lingrel* and JR Berlin)) Bockus Research Inst., Philadelphia, PA and *Dept. of Molec. Genetics, Univ. of Cincinatti, Cincinatti, OH.

The effect of changing Glu^{779}, located in the 5th transmembrane segment of the α-subunit of the Na,K-ATPase, on the ion transport properties of the Na pump was investigated. HeLa cells were transfected with cDNA coding for the $Glu^{779}Ala$ substitution (9A) in an ouabain (OUA)-resistant sheep α1 subunit (RD). Cells were voltage-clamped using patch electrodes filled with a solution that included (mM) 85 Na, 35 Cs, 20 TEA, 10 MgATP and superfused at 37°C by solutions containing (mM) 145 Na plus K, 2 Ba, 0.2 Cd, 0.5 DIDS and 0.001 OUA. In RD cells, increasing extracellular K (K_o) from 0 to 0.2 - 50 mM activated a 10 mM OUA-sensitive membrane current (I_m) that decreased at negative V_m. The $K_{0.5}$ for K_o in RD cells also decreased from 2.1 ± 0.4 mM (n=4) at 0 mV to 1.2 ± 0.2 mM at -40 mV. In 9A cells, K_o-activated, OUA-sensitive current was V_m-independent, but the $K_{0.5}$ for K_o was increased to 5.5 ± 0.6 mM. Thus, $Glu^{779}Ala$ altered extracellular ion affinities and binding kinetics during electrogenic ion transport. In K_o-free solutions, addition of 10 mM OUA produced no significant change of I_m in RD cells but caused an inward shift of I_m in 9A cells that was 40 ± 5 % (n=7) of maximal K_o-activated, OUA-sensitive I_m. In membrane fractions prepared from RD and 9A cells, the stability of the Na,K-ATPase (RD and 9A) phosphoenzymes (EP) formed in the presence of imidazole, Mg and ATP was similar. Thus, $Glu^{779}Ala$ dramatically increased electrogenic Na-Na exchange without destabilizing EP. These results are consistent with the $Glu^{779}Ala$ substitution changing the selectivity for ions that promote interconversion between Na,K-ATPase conformations.

Tu-Pos371

KINETICS OF THE PHOSPHORYLATION BY P_i OF THE Na,K-ATPase DETECTED BY A FLUORESCENCE METHOD. ((H.-J. Apell, M. Roudna, J.E.T. Corrie* & D.R. Trentham*)) Dept. of Biology, Univ. Konstanz, D-78434 Konstanz, Germany and *Natl. Inst. for Med. Res., London NW7 1AA, U.K.

Phosphorylation of the Na,K-ATPase by P_i in the absence of Na^+ ions but presence of Mg^{2+} ions is possible according to the reaction $E + P_i \rightarrow P\text{-}E$. In the enzyme from rabbit kidney, the states E and P-E in the absence of K^+ ions cause different fluorescence levels to be generated by the potential-dependent dye RH421. Therefore transitions between E and P-E can be detected in equilibrium and kinetic experiments. For kinetic studies the above reaction was initiated by rapid photochemical release of P_i from 1-(2-nitrophenyl)ethyl phosphate (caged P_i) using laser flash photolysis at 308 nm. Equilibrium studies of the overall reaction showed that the apparent K_m for P_i was 23.0 ± 0.3 μM (mean ± s.e.m.) at pH 7.0 and 21°C. The reaction exhibited first order kinetics in P_i up to 60 μM P_i. Fluorescence records vs. time were exponential with rate constant k_{obs}. A plot of k_{obs} vs. $[P_i]$ had a slope of $1.47 \times 10^5\ M^{-1}s^{-1}$ and ordinate ($[P_i] = 0$) intercept of 3.1 s^{-1}, consistent with the equilibrium data. The equilibrium reaction was studied over the pH range 6 to 8.5. Fluorescence was greatest at pH 8.5, dropping to 50% at pH 6.0 in a simple binding isotherm with pK 7.5. The K_m for P_i rose cooperatively with increasing pH, with a good fit of the data with pK 8.6 and a Hill coefficient of 2. In the absence of monovalent cations the occupation of the binding sites by protons promotes phosphorylation by P_i. (Supported by the Deutsche Forschungsgemeinschaft, Sonderforschungsbereich 156)

Tu-Pos372

CONFORMATIONAL CHANGES AS DETERMINANTS OF THE SENSITIVITY OF THE SODIUM/POTASSIUM ATPase TO THE CARDIAC GLYCOSIDES. ((D.M. Balshaw and W.J. Ball, Jr.)) Department of Pharmacology & Cell Biophysics, University of Cincinnati College of Medicine, Cincinnati, OH 45267

It has long been known that the Na/K-ATPase of rodent kidney is 2000 times less sensitive to inhibition by the cardiac glycosides than that of other eukaryotes. An explanation for this difference is that the conformational changes occurring in the rodent enzyme following ligand binding are altered. We investigated this hypothesis using fluorescein isothiocyanate (FITC) labeled enzymes to probe the conformational transitions of the Na/K-ATPase from rat and lamb kidney. Our results show that both enzymes are labeled and inhibited to the same degree by bound FITC. In addition, in both species the conformational changes induced by Mg^{2+}, Na^+,K^+, and Pi show essentially the same extent of FITC fluorescence changes, affinities, and cooperativities. Finally, the nature of the interactions between Mg, Pi, and the cardiac glycosides appear the same for both enzymes. We conclude that the enzyme's conformational changes, as reported by FITC, are unaltered in the insensitive rat enzyme.

Supported by the American Heart Association, *Ohio Affiliate* and NIH training grant T32-HL07382.

Tu-Pos373

SUBSTITUTIONS OF GLU781 IN THE NA,K-ATPASE α SUBUNIT DEMONSTRATES REDUCED CATION SELECTIVITY . ((J.C. Koster, G. Blanco, and R.W. Mercer)) Department of Cell Biology and Physiology, Washington University School of Medicine, St. Louis MO. 63110.

The intramembrane Glu781 residue of the Na,K-ATPase α-subunit has been postulated to interact directly with the cations. To ascertain the role of Glu781, the residue was replaced with either an Asp, Ala, or Lys residue and the mutant Na,K-ATPases were expressed with the β1 subunit in *Sf*-9 insect cells. All α mutants efficiently assemble with the β1 subunit to produce functional Na,K-ATPase molecules with activities comparable to the wild-type enzyme. Analysis of enzyme kinetics showed a decrease in affinity for K^+ for the mutants compared to wild-type Na,K-ATPase, with the Lys and Ala substitutions displaying the greatest reduction. All Na,K-ATPase mutants demonstrated an increase in affinity for ATP while the sensitivity to the cardiotonic inhibitor, ouabain, was unchanged. The dependence on Na^+ differs among the enzymes with both the E781D and E781A mutants displaying a decrease in the affinity for the cation, while the E781K mutant exhibits a modest increase. In the absence of K^+, the E781A mutant displays a Na^+-ATPase activity and a cellular Na^+ influx suggesting that Na^+ is substituting for K^+ at the extracellular binding sites. The observations that trypsin digestion of the E781A mutant in Na^+ medium produces a K^+-stabilized tryptic fragment and that the mutant displays similar affinities for both K^+ and Cs^+ also intimates a decreased cation selectivity at the extracellular loading sites. These data implicate Glu781 of the Na,K-ATPase as an important coordinate of cation selectivity and activation, although the modest effect of E781K substitution precludes a direct role for the residue in the cation binding. In addition, Glu781 may be an important communicative link between the ATP and cation binding domains of the Na,K-ATPase.

Tu-Pos374

Ca^{2+} STIMULATES Na,K-PUMP RATE IN SHEEP CARDIAC PURKINJE FIBERS. ((S.O. Semb and O.M. Sejersted)) Inst Exp Med Research, University of Oslo, Ullevaal Hospital, N-0407 Oslo, Norway.

We examined whether Ca^{2+} exerts an effect on Na,K-pump rate in intact sheep cardiac Purkinje fibers impaled with single and double-barreled H^+- and Na^+-selective microelectrodes. Fibers were loaded with Na^+ in a K^+ -and Mg^{2+} -free medium (containing 140 mM Na^+ and a free Ca^{2+} concentration of 10^{-8} M). Mg^{2+} (6 mM) was then added and extracellular Na^+ lowered to 24 mM before the Na,K-pump was reactivated by 30 mM Rb^+. This load/recovery cycle was repeated twice in 10 fibers and did not affect the ATP content. During one of the cycles Ca^{2+} (0.1 to 1.0 mM) was added before Rb^+, so that a contracture developed. During both cycles, reactivation of the Na,K-pump caused the membrane potential to hyperpolarize from -30 to -70 mV. Subsequently, a^i_{Na} started to fall almost linearly and reached a stable level in 10-20 min whilst the fibers became depolarized again. The transient hyperpolarization was not significantly affected by Ca^{2+}. However, a^i_{Na} which fell from 62.8 ± 3.0 to 6.5 ± 1.0 mM in control cycles and from 55.9 ± 3.0 to 3.7 ± 1.1 mM in the Ca^{2+} cycles, fell significantly faster in the Ca^{2+} cycle. The time integral of the a^i_{Na} curve from points of identical a^i_{Na} was 25.7 % smaller during Ca^{2+} (p=0.009). Fitting the data to the Hill equation showed that Ca^{2+} increased maximum Na,K-pump rate by 31.5 % and decreased the a^i_{Na} which caused half maximal pump stimulation from 17.7 to 12.8 mM. We conclude that the Na,K-pump is stimulated during contracture in Ca^{2+} exposed Purkinje fibers probably through increases of both maximum pump rate and the pump affinity for intracellular Na^+.

Tu-Pos375

LIGANDS MODULATE THE IRREVERSIBLE INACTIVATION OF (Na,K)-ATPase BY HIGH PRESSURE. ((Paul DiGregorio and P. A. George Fortes)). Dept. of Biology, University of California San Diego, La Jolla, CA 92093-0116.

High pressure has two general effects on (Na,K)-ATPase. In the range 1 bar to 1.5 kbar pressure effects are fully reversible and include stimulation or inhibition of the activity depending upon the reaction pathway. Above 1.5 kbar, pressure inhibits catalysis irreversibly. We now report that ligands of the enzyme that stabilize certain conformations modulate the rate and pressure-dependence of the inactivation process. (Na,K)-ATPase from dog kidney was incubated at 23°C for various times and pressures in 12 mM histidine, 1 mM EDTA, pH 7.0, ± ligands. K (10 mM), but not Na, decreased the rate constant of inactivation at 2.5 kbar from 0.34 min^{-1} to 0.068 min^{-1} and the apparent volume change of inactivation from 160 ml/mol to 80 ml/mol. After 60 min at 2 kbar <2% activity was seen with no ligands, 10 mM Na, or 1 mM ATP. Increasing [K] protected up to 80% of the activity and this protection was blocked competitively by the K-occlusion inhibitor Br-TITU (Hoving, *et al.*, J. Biol. Chem., in press). The [K]-dependence was consistent with K binding to two sites with *Kapp* ≈ 0.4 and 4 mM. Phosphorylating ligands also protected: Mg+Pi 35% and MgATP+16 mM to 2 M Na 64 to 100% activity after 60 min at 2 kbar. If we assume that resistance to pressure inactivation reflects a decreased volume of the enzyme (the membrane domain?) these results indicate that the relative volumes of (Na,K)-ATPase intermediates are: $E \approx E(Na_n) \approx E{\cdot}ATP >> EP > EP(Na) > EP(Na_2) \approx E(K_2) > EP(Na_3)$. (Supported by NIH GM 47165)

Tu-Pos376

H_2DIDS INACTIVATES NA/K-ATPASE BY MODIFICATION AT K480 & K501: EVIDENCE FOR CROSS-LINKING. ((C. Gatto, S. Lutsenko, J.H. Kaplan)) Dept. of Biochemistry & Molecular Biology, Oregon Health Sciences University, Portland, OR 97201-3098.

The negatively charged amino-reactive reagent H_2DIDS (dihydro-4,4'-diisothiocyanostilbene-2,2'-disulfonate) covalently labels and irreversibly inhibits the Na/K-ATPase; both inactivation and labeling are protected by the presence of ATP or K (Pedemonte & Kaplan, Biochem. 27: 7966, 1988). In the present study, purified canine Na/K-ATPase was treated with 50 μM $^3H_2$DIDS (60 min, 37°C) in a medium containing: 60 mM imidazole (pH = 7.6, 25°C), 1 mM EDTA, and either 2 mM NaCl or 2 mM KCl. Ouabain-sensitive ATPase activity and incorporation of ^3H into the alpha subunit confirmed that K protected against inactivation and labeling. The H_2DIDS-labeled enzyme was extensively digested with trypsin (1:10, 4 h, 37°C); the insoluble fraction was removed by centrifugation and the soluble fraction further digested with trypsin (1:50, 16 h, 25°C). All of the K-protectable radioactivity was associated with the soluble fraction. The digested enzyme fragments were separated on a 16% Tricine gel and electroblotted onto a PVDF membrane. K-protectable radioactive bands were analyzed by N-terminal amino acid sequencing. The prominent radioactive peaks in 3 experiments revealed the same two sequences, 1) IVEIPFNSTNxYQL and 2) HLLVMxGAPE. The "x's" correspond to K480 and K501 respectively. The fact that these sequences always co-localized and were relatively resistant to trypsin treatment, suggest that the two isothiocyano groups of H_2DIDS crosslink K480 with K501. Consistent with this idea are the findings that all other aromatic isothiocyanates which inactivate the Na/K-ATPase label only K501, including the single isothiocyano substituted stilbene, SITS. Supported by NIH GM39500 (JHK) & Am Heart Assoc OR affl. (CG).

Tu-Pos377

KINETICS OF THE PHOSPHOENZYME INTERCONVERSION REACTION IN BIPM-LABELED PIG KIDNEY Na, K-ATPase. ((Jeffrey P. Froehlich, R. Wayne Albers, Takeshi Yokoyama and Kazuya Taniguchi)) NIA, NIH, Baltimore, MD 21224; NINDS, NIH, Bethesda, MD 20892; Dept. of Chemistry, Hokkaido U., Sapporo, Japan

The fluorescent probe, N-(p-(2- benzimidazolyl) phenyl) maleimide (BIPM), was used to monitor Na^+ translocation coupled to the conversion of E1P to E2P in pig kidney Na, K-ATPase. At 24°C, the addition of 10 μM ATP to BIPM-labeled Na, K-ATPase suspended in a medium containing 16 mM NaCl, 1 mM $MgCl_2$ and 25 mM imidazole (pH 7.45) gave an increase in fluorescence intensity with an apparent rate of 137 s^{-1}. This signal corresponds to the accumulation of $E2P(Na_3)$, which is rate-limited by ATP binding in this experiment. Under identical conditions, phosphorylation of the BIPM-labeled enzyme measured by rapid acid quenching had an apparent rate of 119 s^{-1}. Control experiments revealed that BIPM labeling did not alter the kinetics of ATP binding, E1P formation, K^+-dependent E2P hydrolysis or the conformational transitions, E1P to E2P and E2 to E1. These results show that the BIPM signal and phosphoenzyme formation have similar kinetics and that, consequently, the conversion of E1P to E2P is very fast (> 1000 s^{-1}). At physiological (saturating) [ATP], Na^+ release from $E2P(Na_3)$ is rate-limited by phosphorylation (k_{app} = 327 s^{-1} at 200 μM ATP) and/or the conformational transitions involving Na^+ deocclusion. These results are similar to those obtained with eel electric organ Na, K-ATPase, which exhibits a very high rate of conversion of E1P to E2P.

Tu-Pos378

THE PLASMA MEMBRANE CA PUMP (PMCA) FLUX IN HUMAN ERYTHROCYTES IS MEMBRANE POTENTIAL DEPENDENT. ((W.-Y. Xu and M.A. Milanick)) Dept. of Physiology & Dalton CRC, Univ. of Missouri, Columbia, MO 65212.

The Ca pump mediates Ca/H exchange (see e.g., Milanick, AJP 258:C552, 1990) and is electrogenic under some conditions (Hao, Rigaud, & Inesi, J.B.C, 269:14268, 1994). ^{45}Ca efflux was determined from $[Ca]_{in}$ -preloaded cells (100 μM). The cells were loaded using the A23817 technique. The extracellular media contained either 1 mM KCl, 2 μM valinomycin, the appropriate buffer, and 130 mM NaCl (Em ≈ 0 mV) or 130 mM KCl (Em ≈ -70 mV). pH_{in} was clamped at 7.4 by addition of 125 μM DIDS. The Ca efflux was the same at both potentials pH_{out} = 7.4 (Flux ≈ 125 μmol/l cells/min). We next studied the effect of Em at H_{out} << $K_{1/2}$ (≈500 pM). At 32 pM H_{out}, negative Em inhibited Ca efflux by almost 2 fold: from 9.0±0.8 to 5.1±1.1 μmol/l cells/min. This flux probably represents uncoupled Ca efflux mediated by the Ca pump: eosin inhibited the flux by 85% at both pH 7.4 and 10.5 (cf. Gatto et. al., Biochem. 34:965, 1995). The flux was independent of H_{out} from 5 to 20 pM. For a completely coupled Ca/H exchanger, the flux would be proportional to [H] when [H] < K1/2. These data are consistent with Em altering the slow step in uncoupled Ca efflux. We next characterized the inhibition by Ca_{out}. At pH_{out} = 7.4, Ca_{out} was a weak inhibitor of Ca efflux and even in the presence of Ca_{out} the flux was the same at the two potentials. At pH_{out} 8.4, Ca_{out} was a more potent inhibitor and the IC50 was the same at the two potentials. Surprisingly, at pH 9.7, the IC50 was increased about 2 fold by negative potential; i.e., at moderate Ca_{out}, negative Em stimulated Ca efflux. We conclude that the effect of membrane potential on the Ca pump depends upon the extracellular proton and calcium concentrations. Supported by NIH DK37512, AHA-Missouri Affiliate, and an RDCA to MAM.

Tu-Pos379

DIFFERENTIAL EFFECTS OF LOCAL ANESTHETICS ON THE Ca-ATPASE AND Na,K-ATPASE ((P.A. Singleton, L.L. Probert, and J.E. Mahaney)) Department of Biochemistry, West Virginia University.

We have measured the effects of procaine, lidocaine, benzocaine and diphenhydramine (which has some local anesthetic properties) on the protein-protein and lipid-protein interactions of the rabbit skeletal Ca-ATPase and sheep kidney Na,K-ATPase. These local anesthetics exist in both charged and uncharged forms, depending on their pK_a and the medium pH. In general, both enzymes are stimulated by the uncharged forms of the anesthetics, while the charged forms are inhibitory. However, the Ca-ATPase is stimulated to a greater extent and is more susceptible to inhibition relative to the Na,K-ATPase. Cross-linking either enzyme using DSP (dithiobis (succinimidyl propionate)) resulted in a disappearance of monomeric Na,K-ATPase (α and β subunits) and Ca-ATPase and the formation of higher molecular weight species as confirmed by SDS-PAGE and Western blots. Increased cross-linking correlated with increased inhibition of enzyme activity. At a constant concentration of DSP, increasing the amount of the charged form of these anesthetics also reduced the monomeric form of each enzyme in favor of increased molecular weight species. In contrast, the uncharged form of these anesthetics inhibited cross-linking relative to the charged form. We propose that the charged form of these anesthetics aggregates each enzyme, whereas the uncharged form favors enzyme disaggregation. EPR studies are underway to physically test this model.

Tu-Pos380

BLOCKING THE Ca^{2+}-INDUCED CONFORMATIONAL TRANSITION IN CALMODULIN IMPAIRS ITS ABILITY TO ACTIVATE Ca^{2+}-ATPase. ((I.Fomitcheva,* Z. Grabarek,# and D. Kosk-Kosicka*)), Johns Hopkins University, School of Medicine, Baltimore, MD 21287 and Boston Biomedical Research Institute, Boston, MA 02114.

CaM mutants containing intramolecular disulfide bonds have been generated using site directed mutagenesis to introduce Cys either at positions 41 and 75 (CaM 41/75) or 85 and 112 (CaM 85/112). The mutants displace decreased affinity for Ca^{2+} and loss of ability to activate PDE and calcineurin, indicating that disulfide bridges at the strategic positions block the Ca^{2+}-induced conformational transition that is critical for regulatory properties of CaM (Tan et al.,1995 submitted). In agreement with these conclusions, neither of the mutants activates Ca^{2+}-ATPase at physiological Ca^{2+} and CaM concentrations. Upon reduction of the disulfide and blocking SH groups the regulatory properties are fully restored in CaM 41/75 but not in CaM 85/112. In addition, the two mutants differed in their behavior at nonphysiological micromolar concentrations at which CaM 41/74 fully activates the Ca^{2+}-ATPase, similar to the C-terminal CaM half tested in parallel. We have shown previously that Ca^{2+}-ATPase activation by CaM is significantly more impaired by amino acid alterations in the C-terminal than N-terminal domain (Biochemistry 30, 65; JBC 267, 4394). The present study demonstrates that the Ca^{2+}-induced opening at the helical interfaces in the C-terminal domain is crucial. AHA 9201190 (DKK) and AR 41156 (ZG)

Tu-Pos381

EFFECTS OF SUBSTITUTING Asp^{672} BY Glu IN THE PLASMA MEMBRANE Ca^{2+} PUMP.((H.P.Adamo#, A.G. Filoteo*, A. Enyedi* and J.T. Penniston*)) , Instituto de Química y Fisicoquímica Biológicas (UBA-CONICET),1113 Buenos Aires, Argentina# and Dept. Biochem. & Molec. Biology, Mayo Clinic, Rochester, MN 55905 *.

A site-directed mutant of the plasma membrane Ca2+ pump with Asp^{672} changed to Glu was constructed and expressed in COS-1 cells. Asp^{672} is part of the highly conserved region of the P-type ATPases which has been associated with nucleotide binding. The rate of Ca^{2+} transport of the Asp^{672}Glu mutant was 15 % of that of the wild-type enzyme. High concentrations of ATP (25 mM) did not change the percentage of inhibition, suggesting that effects not related with the binding of ATP where causing the inhibition.

To see if the mutant was able to form acylphosphate (EP), membranes from transfected COS-1 cells were incubated with (γ ^{32}P)-ATP and then submitted to slightly acidic SDS-PAGE. The radioactivity was detected by autoradiography. As judged by the intensity of the bands, both the mutant and the wild-type enzyme formed about the same amount of EP. When chased with cold ATP, the EP formed by the Asp^{672}Glu mutant decomposed at slower rate than that of the wild-type. The results indicate that the substitution of Asp^{672} by Glu inhibits the plasma membrane Ca^{2+} pump by reducing the rate of the dephosphorylation step of the enzyme cycle. Supported by grants GM28835, INT 93-02981, CONICET and Fundacion Antorchas.

Tu-Pos382

MAPPING THE TWO FIRST TRANSMEMBRANE DOMAINS OF THE RED BLOOD CELL Ca^{2+}-PUMP ((Juan Pablo F.C. Rossi, Pablo R. Castello, F. Luis González Flecha, Ariel J. Caride, José M. Delfino and Horacio N. Fernández)) Instituto de Química y Fisicoquímica Biológicas, Facultad de Farmacia y Bioquímica, Junín 956, 1113 Buenos Aires, Argentina (Spon. by Silvia Alonso-Romanowski).

The erythrocyte Ca^{2+} pump is a monomeric integral membrane protein that actively transports Ca^{2+} from the cytosol to the external milieu. The ion translocation machinery should be localized in the extensive transmembrane domain of this protein. Between 8 to 12 putative transmembrane segments have been predicted from the aminoacid sequence of the protein. We have employed reagents like [^{3}H]DIPETPD, a photoactivatable bipolar phospholipid probe designed to label deeply into the lipid bilayer to identify transmembrane peptides in the pump *(Biochem. Biophys. Res. Commun. 201, 194, 1994)*. After having unambiguously identified membrane-spanning stretches with [^{3}H]DIPETPD, for recent labeling experiments, we have taken advantage of the superior specific radioactivity provided by [^{125}I]TID. In the end, this generic hydrophobic probe will facilitate peptide sequencing and, therefore, achieve aminoacid resolution of the labeling site(s). Controlled proteolysis of the photoadduct with V8 protease and further SDS-PAGE analysis, identified the same set of fragments as that labeled with [^{3}H]DIPETPD. Furthermore, the similarity among the labeled peptide patterns with V8 protease after labeling of the Ca^{2+}-pump with [^{125}I]-TID in (a) isolated red blood cell membranes, (b) in reconstituted proteoliposomes and (c) in the purified enzyme, validates the conclusion that the conformation of the enzyme is preserved after solubilization, purification and reconstitution. Results presented here show evidence for the existence of M1 and M2, the two first transmembrane segments of the pump. These findings are consistent with the current model for the topography of the Ca^{2+}-pump.

Tu-Pos383

PHOSPHORYLATED CALMODULINS AND THE PLASMA MEMBRANE Ca^{2+}-ATPase . ((M.M. Lopez[*] ; D.B.Sacks[$] ; A. Wang[#] ; D. Kosk-Kosicka[*])) +Johns Hopkins University, School of Medicine, Dept. Anesthesiology, Baltimore, MD 21287. *Brigham and Women's Hospital and Harvard Medical School, Dept. Pathology, Boston, MA 02115. # Boston Biomedical Research Institute, Boston, MA 02114.

Phosphorylation is one of the main mechanisms for the regulation of intracellular signalling. We studied the effect of phosphorylation of calmodulin on its ability to activate the human erythrocyte Ca^{2+}-ATPase. Phosphorylation of mammalian CaM on Ser/Thr residues by casein kinase II decreased its affinity for Ca^{2+}-ATPase by two-fold. In contrast, Tyr phosphorylation by the insulin receptor kinase did not have a significant effect. Two other CaMs, with only one Tyr, were examined: wheat germ CaM with Tyr-139 and a mutant CaM (Y138F) with Tyr-99. The concentrations of those calmodulins required for half-maximal activation of the Ca^{2+}-ATPase were four- and ten-fold higher respectively, than mammalian CaM. Phosphorylation at Tyr-139 of wheat germ CaM had no effect on its interaction with Ca^{2+}-ATPase, whereas phosphorylation at Tyr-99 in the Y138F mutant partially reversed the effect of mutation by shifting its affinity towards that of mammalian CaM. We conclude that, introduction of phosphate affects CaMs affinity for Ca^{2+}-ATPase, but not the V_{max}. The most significant effect of phosphorylation is revealed when phosphate is exclusively incorporated in Tyr-99. Supported by NIH DK43682 (to DBS) and AHA 92010190 (to DKK).

Tu-Pos384

HALOTHANE BINDING TO PLASMA MEMBRANE Ca^{2+}- ATPase. ((Maria M. Lopez and Danuta Kosk-Kosicka)), Johns Hopkins University, School of Medicine, Department of Anesthesiology, Baltimore, MD 21287.

Volatile anesthetics at clinical concentrations inhibit the Ca^{2+}-ATPase activity and the presumptive Ca^{2+}-induced conformational change of the plasma membrane Ca^{2+} pump (Lopez and Kosk-Kosicka, J.Biol.Chem. 1995, in press). In the present study we are investigating halothane binding to the purified dimeric Ca^{2+}-ATPase using quenching of the intrinsic tryptophan fluorescence. The fluorescence intensity decreases in a dose-dependent manner and saturates with 80% of the initial fluorescence quenched. Several controls are included to determine the specificity of the halothane-protein interaction. Contributions from collisional quenching, halothane binding, and conformational changes in the protein are analyzed. The calculated $K_{halothane}$ (a measure of the overall effect) was 0.20 mM, in good agreement with the halothane concentration which produces half-maximal inhibition of the Ca^{2+}-ATPase activity (0.26 mM). From Hill analysis, no cooperativity (n=1.04±0.02) is observed for the halothane-Ca^{2+}-ATPase interaction. The reversibility of the halothane binding is assesed by competition studies with diethyl ether. At saturating halothane concentrations (0.7 mM), addition of ether reverses the decrease in Trp fluorescence almost completely, suggesting that halothane can be displaced from its sites in the protein. The results concur with our hypothesis that volatile anesthetics inhibit the Ca^{2+}- ATPase by interacting with nonpolar sites in the protein interior. Such binding is expected to modify the enzyme conformation and perturb its function. Supported by NIH GM 447130.

Tu-Pos385

Enhancement of Ca^{2+} uptake by the Sarcoplasmic Reticulum in isolated myocytes through Ca^{2+}-ATPase activation or via Phospholamban inhibition.

((I. Bertrand, V. Lahouratate, J.-C. Camelin, J. Guibert, A. Bril and P. Lahouratate)) SmithKline Beecham Laboratoires Pharm, BP 58, 35762 Saint Grégoire, France.

The Ca^{2+} ATPase of the sarcoplasmic reticulum (SR) plays a key role in the regulation of $[Ca^{2+}]_i$ in cardiac myocytes and can be affected by the direct modulation of the Ca^{2+} pump or by removing the inhibitory effect of dephosphorylated phospholamban (PLB). We investigated the role of these mechanisms in the enhancement of SR-Ca^{2+} uptake using ellagic acid (EA) or 1-(3,4-dimethoxyphenyl)-3-dodecanone (DMPD). Both compounds (30μM) enhance ATP dependent SR-Ca^{2+} uptake either in rabbit cardiomyocytes and in dog cardiac SR-microsomes. We used the fluorescent Ca^{2+} dye, fluo-3, to measure the oxalate supported SR-Ca^{2+} uptake. For concentrations higher than 1 μM a marked stimulation (26% for both EA and DMPD at 10 μM) of Ca^{2+} uptake was observed for both compounds in myocytes. However, the action of the two compounds was clearly different. The effect of DMPD occurred mainly at high Ca^{2+} and resulted in a 56% increase of the V_{max}. EA stimulated Ca^{2+} uptake at low Ca^{2+} and produced a leftward-shift of the pCa-ATPase activity relationship (ΔpCa=0.24). The effect of these two compounds was further examined on Ca^{2+} ATPase activity. EA produced a Ca^{2+} sensitising effect in cardiac (ΔpCa=0.3), but not in fast skeletal muscle SR-microsomes. The effect of DMPD consisted mainly in an increase of the ATPase activity at high Ca^{2+}, both in cardiac and in fast skeletal muscle (50% at 30μM in cardiac and 31% at 3 μM in skeletal muscle vesicles). These results show that SR-Ca^{2+} uptake can be increased either by mimicking the effect of PLB phosphorylation as observed with EA, or by directly affecting the SR-Ca^{2+} pump as observed with DMPD.

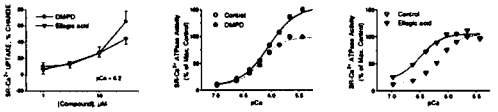

Tu-Pos386

NUCLEOTIDE BINDING BY STRUCTURAL DOMAINS OF NA,K-ATPASE EXPRESSED IN E. COLI. ((C.M.Tran, E. Hrouda, C.M. Grisham, and R.A. Farley)) U. Southern California, Los Angeles CA 90033 and U. Virginia, Charlottesville, VA 22901.

Many amino acids involved in ATP binding or hydrolysis by ion-transport ATPases are located in a cytoplasmic domain of approximately 400 amino acids. In order to identify the minimum region that is required for ATP binding, we have expressed this domain from Na,K-ATPase (NKA) in E. coli as a fusion protein with glutathione-S-transferase (GST), beginning at M344 and ending any of several different amino acids up to E779. Fusion proteins were purified by affinity chromatography on glutathione-Sepharose, and the NKA domains were cleaved from the GST by proteolytic digestion. The ability of fusion proteins or isolated domains to bind ATP was measured by photolabeling with [32P]-2-N_3-ATP (2N3) in the presence and absence of ATP. Quantitation of labeling was done by scintillation counting of excised bands from SDS-PAGE. Both fusion proteins and isolated domains of NKA ending at E779 and G731 were labeled by 2N3; neither the fusion protein nor the isolated domain ending at G518 were labeled. For the domain ending at G731, the EC50 for 2N3 labeling was 0.2-0.3 mM; the IC50 for ATP protection was 0.2-0.4 mM. The fusion protein and the isolated domain had similar characteristics, and GST was not labeled by 2N3. Cleavage of the domain ending at G731 from GST generated the expected fragment of approximately 43 kDa, and also a fragment of approximately 29 kDa that was also labeled by 2N3 and protected by ATP. These results suggest that the minimum size of the ATP binding region of NKA is between 19 kDa and 29 kDa. (Supported by NIH)

Tu-Pos387

A ROLE IN ENERGY TRANSDUCTION AND KINETIC REGULATION FOR THE PEPTIDE SEGMENT CONNECTING PHOSPHORYLATION AND CATION BINDING DOMAINS IN TRANSPORT ATPases. ((C. Garnett, F. Fernandez Belda, C. Sumbilla and G. Inesi)) Depart. of Biological Chemistry, University of Maryland School of Medicine, Baltimore, MD 21201. (Spon. by G. Inesi)

The sarcoplasmic reticulum Ca^{2+} ATPase segment connecting the extramembranous phosphorylation domain to the preceding transmembrane helix (which is an integral component of the Ca^{2+} binding domain), retains a high degree of sequence homology with other cation transport ATPases. Single non-conservative mutations of any of the homologous residues within this segment, interfere with enzyme activity (Zhang et al., J. Biol. Chem. 270:16283-16290, 1995). We have now produced single and multiple mutations of non homologous residues in the Ca^{2+} ATPase, to match the corresponding residues of the Na^+,K^+ ATPase. We find that the main characteristics of the ATPase mechanism are retained even when the entire peptide segment (Ile315-Leu356) of the Ca^{2+} ATPase is rendered identical to the corresponding segment of the Na^+,K^+ ATPase by simultaneous mutations of fourteen amino acids. However, the phosphoenzyme turnover is progressively reduced as the number of simultaneous mutations is increased. The experimental findings indicate that the peptide segment connecting phosphorylation and cation binding domains sustains a mechanistic role in energy transduction by transport ATPases, and its conformation has a strong influence on the rate limiting step of the catalytic and transport cycle. (Supported by NIH).

Tu-Pos388

DO PARVALBUMIN AND CALMODULIN HELP DELIVER CALCIUM TO A MICROSOMAL Ca^{2+}-PUMP? ((J.E. Moore and R.F. Abercrombie)) Emory University, Department of Physiology, Atlanta, GA 30322.

In previous studies, we demonstrated that EGTA and other calcium chelators enhance ATP-dependent calcium uptake of isolated rat brain microsomes (*Biophys. J.*, 1995, *68*: A395) by facilitating Ca transfer to the pump. This study examines whether two *endogenous* calcium-binding proteins, parvalbumin and calmodulin, are also capable of increasing ^{45}Ca transport. Isolated microsomes were incubated in an EGTA-free intracellular ionic medium at pH 7.4, 37°C, ± 3mM ATP for up to 300 seconds in the presence or absence of either 8μM parvalbumin or 5μM calmodulin. Free calcium, measured with calcium-sensitive mini-electrodes, was adjusted to 0.6μM. ATP-dependent ^{45}Ca uptake was ten times greater in microsomes when parvalbumin or calmodulin was present (3.21 ± 0.22 μmol/g protein) compared to chelator-free controls (0.30 ± 0.02 μmol/ g protein). BSA (100μg/ml) did not significantly enhance ^{45}Ca uptake. When the increased Ca transport was supported by 100 μM of the chelator EGTA, ionic strength had a significant effect: increasing ionic strength by adding 150mM KCl or 40mM $MgCl_2$, in the presence of chelator, reduced ^{45}Ca uptake 40-60% while having no effect on chelator-free controls (0.6μM free Ca). Mannitol, at similar osmolarity, reduced ^{45}Ca transport by less than 15% in the presence of chelator. Our interpretation is that calcium-binding proteins, by acting as mobile calcium chelators, may enhance Ca uptake through interactions at the microsomal membrane. The chelator interaction, which facilitates Ca transfer to the microsomal pump, may be weakened under increased ionic strength. Supported by NIH NS-19194

Tu-Pos389

PHOSPHORYLATION OF PHOSPHOLAMBAN DECREASES THE ROTATIONAL DYNAMICS OF THE Ca-ATPase IN CARDIAC SR MEMBRANES. ((Sewite Negash, Linda Chen, Diana J. Bigelow, and Thomas C. Squier)) Dept. of Biochemistry, University of Kansas, Lawrence, KS 66045-2106.

We have used saturation transfer electron paramagnetic resonance (ST-EPR) spectroscopy to examine possible alterations in protein-protein interactions that accompany the activation of the cardiac sarcoplasmic reticulum (SR) Ca-ATPase following the phosphorylation of phospholamban (PLB). Cardiac and skeletal Ca-ATPase isoforms in native SR membranes were specifically spin-labeled and directly compared using ST-EPR to measure the rotational dynamics of the Ca-ATPase (Negash et al., 1995; Biophys. J., 68: A314). We report that the phosphorylation of PLB in cardiac SR results in a two-fold reduction in the apparent rotational mobility of the Ca-ATPase. Identical experimental conditions associated with the activation of the cardiac Ca-ATPase result in no change in the apparent rotational dynamics of the skeletal Ca-ATPase, indicating that the observed changes in protein rotational mobility in cardiac SR membranes result from the phosphorylation of PLB. Measurements of the rotational dynamics of stearic acid spin labels (SASL) with a nitroxide at the 5 and 12 position relative to the carboxylate using conventional EPR indicate that there is virtually no difference in the lipid acyl chain dynamics in cardiac SR membranes upon the phosphorylation of PLB. These results indicate that the decrease in rotational dynamics of the cardiac Ca-ATPase associated with the phosphorylation of PLB is due to i) an alteration in the spatial arrangement of cardiac Ca-ATPase polypeptide chains within a defined oligomeric state or ii) increased protein-protein associations.

Tu-Pos390

CONFORMATIONAL COUPLING BETWEEN NUCLEOTIDE BINDING SITES ON ADJACENT Ca-ATPase POLYPEPTIDE CHAINS. ((Shaohui Huang and Thomas C. Squier)) Department of Biochemistry, University of Kansas, Lawrence, KS 66045-2106.

We have reinvestigated the biphasic dependence of Ca-ATPase activity with respect to ATP concentration using erythrosin 5-isothiocyanate (ErITC) to selectively label the nucleotide site on the Ca-ATPase (Huang et al., 1995; Biophys. J. 68: A314). Fluorescence depolarization measurements indicate that ErITC labeling sites are not located on the neighboring Ca-ATPases (Huang et al., 1994; Biophys. J. 66: A200). Labeling with ErITC displays negative cooperativity such that the low-affinity class of ATP binding sites are not labeled, indicating that the high- and low-affinity class of ATP binding sites are conformationally distinct. Binding of the nonhydrolyzable nucleotide analog AMPPNP results in a fluorescence and phosphorescence enhancement of ErITC, with a corresponding 40% increase in the average phosphorescence lifetime of Er-ITC. Subsequent to the solubilization of the SR membranes we observe no change in Er-ITC fluorescence or phosphorescence upon the addition of AMP-PNP. We conclude that the high and low affinity classes of nucleotide binding sites are i) located on different Ca-ATPase polypeptide chains and ii) undergo conformational coupling associated with occupancy of the low affinity class of nucleotide binding sites.

Tu-Pos391

EXPRESSION AND PURIFICATION OF PHOSPHOLAMBAN FROM *E.coli* CELLS. ((Q. Yao, J. L. Beven, R. F. Weaver, and D. J. Bigelow)) Department of Biochemistry, University of Kansas, Lawrence, KS 66045.

Phospholamban is a membrane protein which regulates active calcium transport catalyzed by the cardiac sarcoplasmic reticulum Ca-ATPase by a mechanism involving phospholamban's phosphorylation and dephosphorylation. We have used the polymerase chain reaction to amplify the phospholamban gene from the genomic DNA of porcine heart. The phospholamban gene was inserted into the pGEX-2T plasmid expression vector which expresses the gene product fused to glutathione S-transferase (GST) in *E. coli* cells (Y1089). After cell lysis, the expressed fusion protein was found predominantly in the insoluble fraction. Most of the fusion protein was extractable with 4% SDS. Phospholamban was subsequently purified by a three-step process consisting of: (1) isolation of the fusion protein by preparative electrophoresis, (2) thrombin-mediated cleavage of the fusion protein and (3) a second electrophoretic separation of phospholamban from GST. The yield of the purified phospholamban was 3-4 mg per liter of cells.

Tu-Pos392

MEMBRANE TARGETING AND PROTEIN FOLDING FOLLOWING SERCA ATPase GENE TRANSFER IN CULTURED CELLS. **((C. Sumbilla, D. Lewis, C. Garnett, A. Hussain, Z. Zhang, M. Klein and G. Inesi.)) Depart. of Biological Chemistry, University of Maryland, School of Medicine, Baltimore MD. 21201.**

We have introduced SERCA1 and SERCA2 cDNA constructs (including promoters and 3' end kits) into various cultured cells such as COS1, chinese hamster lung (DC3F) and insect (Sf9 and Sf21) cells. Transfection of COS1 cells with cDNA (using a SV40 promoter) by the DEAE-Dextran method results in transient overexpression in 10-15% of the cells. It can be shown by high resolution immunofluorescence that the SERCA protein is targeted to the endoplasmic reticulum, and can be recovered with the microsomal fraction of the disrupted cells. The microsomal vesicles sustain high rates of Ca^{2+} transport and ATPase activity. Mutated cDNA generally yields protein which is either functionally active or inactive. However, some mutations interfere with folding and membrane assembly of the expressed protein. This effect is very specific since mutations A331 to E or R interfere while A331 to C or L do not; also, the mutation S338G interferes, while S338 to A or R do not. Infection of Sf9 or Sf21 cells with recombinant Baculovirus results in high yield of expressed protein. However, the protein is targeted to a ring near the plasma membrane, and the activity of the isolated protein is very much dependent on the multiplicity of infection. Stable expression was obtained in DC3F cells cotransfected with SERCA and a dehydrofolic reductase mutant permitting selective pressure with methotrexate. In these cells the protein was targeted to the endoplasmic reticulum, producing intracellular organelles which display ATP dependent Ca^{2+} transport in situ. (Supported by NIH).

Tu-Pos393

A NOVEL PREPARATION OF PURE ACTIVE SR CA^{2+}-ATPASE: FUNCTIONAL RECONSTITUTION USING NEW SHORT CHAIN LIPID DETERGENT DHPC **((Bannikuppe D. Shivanna and Elizabeth S. Rowe)) Department of Biochemistry and Molecular Biology, University of Kansas Medical School, and VA Medical Center, Kansas City, MO 64128.**

The short-chain phospholipid diheptanoyl-*sn*-phosphatidylcholine (DHPC) has been shown to be a superior detergent in solubilizing and preserving the biological activity of membrane proteins compared to most detergents commonly used for this purpose (Kessi, et al., 1994, Biochemistry **33** 10825). Using this new detergent we have developed a preparation method for solubilization and reconstitution of rabbit skeletal muscle sarcoplasmic reticulum (SR) Ca^{2+}-ATPase and compared it to the most commonly used procedure with $C_{12}E_8$. DHPC is more effective than $C_{12}E_8$ in SR solubilization at a wide range of detergent concentrations, and gave higher specific activity compared to $C_{12}E_8$. The sucrose gradient purified Ca^{2+}-ATPase from DHPC solubilization had higher specific activity, higher recovery and exhibited more native conformational features compared to the $C_{12}E_8$ preparation. Detergent dissociation, followed by gel filtration of the two Ca^{2+}-ATPase preparations on a Sepharose CL-6B column in buffer containing Tween-80, resolved higher aggregates from oligomer and monomeric species. The profile indicated monomer Ca^{2+}-ATPase as the predominant species in both preparations, however the monomer from DHPC had ~10 fold more ATPase activity than the monomer from $C_{12}E_8$. Purified Ca^{2+}-ATPase preparations from $C_{12}E_8$ and DHPC were reconstituted into the exogenous lipid DOPC exchanging greater than 80% of the endogenous lipid for DOPC. The DHPC reconstituted ATPase preparation had significantly higher specific activity compared to that from $C_{12}E_8$. These results show that DHPC is superior to $C_{12}E_8$ as a detergent for solubilization, purification and functional reconstitution of Ca^{2+}-ATPase from skeletal SR. (Supported by the Department of Veterans Affairs.).

Tu-Pos394

MUTATION LYS758→ILE OF THE SR Ca^{2+}-ATPase UNCOUPLES ATP HYDROLYSIS FROM Ca^{2+} TRANSPORT. ((Thomas Sørensen and Jens Peter Andersen)) Department of Physiology, University of Aarhus, DK-8000 Aarhus C, Denmark.

Site-directed mutagenesis was used to substitute isoleucine for residue Lys758 located in the stalk sector near the cytoplasmic end of transmembrane segment M5 of the Ca^{2+}-ATPase of sarcoplasmic reticulum. This mutant catalyzed a high rate of Ca^{2+}-activated ATP hydrolysis without corresponding accumulation of Ca^{2+} in the microsomal visicles. The ATPase activity of the mutant, like that of the the wild type, was stimulated by Ca^{2+} in the micromolar range, and the mutant was able to occlude Ca^{2+} in the presence of CrATP. However, there was no significant accumulation of Ca^{2+}. While the ATPase activity of the wildtype was enhanced 2-3 fold by incorporation of the calcium ionophore A23187 in the vesicles, relieving "backdoor inhibition" by accumulated Ca^{2+}, the mutant ATPase activity was fully activated in the absence of ionophore. In the absence of K^+ and at pH 8.35 the phosphoenzyme was very stable in the wild type whereas a rapid dephosphorylation was observed with the mutant, suggesting an alternative route for dephosphorylation in the mutant, which was not associated with Ca^{2+} translocation. A salt bridge between Lys758 and a negatively charged residue may play a crucial role in the gating mechanism or in the mechanism of energy transduction.

Tu-Pos395

LUMINAL CA^{2+} DISSOCIATION FROM THE PHOSPHORYLATED SARCOPLASMIC RETICULUM CA^{2+}-ATPASE IS SEQUENTIAL. ((D. Canet, E. Mintz, V. Forge and F. Guillain)) SBPM/DBCM, CEA and CNRS URA1290, CE Saclay, 91191 Gif-sur-Yvette Cedex France (Spon. E. Nabedryk)

It was already shown that when the two transport sites of Ca^{2+}-ATPase face the cytoplasm, Ca^{2+} dissociation is sequential. To examine by rapid filtration, the mechanism of Ca^{2+} dissociation when the transport sites face the SR lumen, an ADP-sensitive phosphorylenzyme having 2 Ca^{2+} bound should be stabilized. We found that at 3°C, pH8 and 300mM KCl, $Ca_2.E$-P is stable for at least 10s. Working on leaky SR vesicles, we show that rapid perfusion of $Ca_2.E$-P with EGTA induces both dephosphorylation and dissociation of the two Ca^{2+} bound with the same kinetics. In contrast, when an excess of Ca^{2+} is perfused, the phosphorylenzyme is stable and remains ADP-sensitive whereas half of the bound Ca^{2+} is exchanged. Therefore luminal Ca^{2+} dissociation from the transport sites of the Ca^{2+}-ATPase is sequential as on the cytoplasmic side. Results will be presented about the conservation of the order during Ca^{2+} transport from cytoplasmic binding to luminal dissociation.

Tu-Pos396

Characterization of Bovine Heart Mitochondrial ATPase as an Iron Transporter. *C-Y Li, J.A Watkins, and J.Glass. Section of Hematology/Oncology, Department of Medicine, and Center for Excellence in Cancer Research, Treatment, and Education, LSUMC-Shreveport, LA., 71130.*

We have previously shown that the vaculolar H^+-ATPase both binds iron and transports iron when reconstituted in liposomes. To determine if the mitochondrial ATPase also acts as an iron transporter, partially purified bovine mitochondrial ATPase was reconstituted into liposomes composed of soybean phospholipid or mixed phospholipid [PS:PE:PC(1:2:9)]. In proteoliposomes containing 150 mg/ml protein and 5 mg/ml soybean phospholipid with 34 mM ^{59}FeNTA(1:4/Fe:NTA) the ATPase-dependent ^{59}Fe transport proceeded at an initial rate of 1.76 ± 0.3x10^{-2} mmoles Fe(III)/mg ATPase/min. During 2.5 hours about 44.0±1.8% of ^{59}Fe(II) and 51.0±0.8% of ^{59}Fe(III) of total internal iron was transported out of the liposomes. The passive ^{59}Fe transport from liposomes was 4.5 ± 1.0% for ^{59}Fe(II) and 5.6 ± 2.0 for ^{59}Fe(III). ^{59}Fe transport from mixed phospholipid proteoliposomes was about 32.9% for Fe(II) and 32.6% for Fe(III). The ATPase showed ^{59}Fe binding activity. When the ATPase was separated by nondenaturing polyacrylamide gel electrophoresis ^{59}Fe binding coincided with ATPase activity. Heat treatment of the ATPase at 60° C for 10 min before reconstitution decreased ATPase-dependent iron transport by 2.5-3.7 fold. Other small molecules did not exhibit ATPase-dependent transport as ^{14}C-dextran (MW=5000) and ^{14}C-sucrose trapped in proteoliposomes had an efflux of only 7.7 ± 1.1% and 7.1 ± 1.7% respectively. Intriguingly when ^{59}Fe,^{125}I-transferrin was trapped in proteoliposomes, 56..9 ± 1.6% of the ^{59}Fe was transported compared to only 11.2 ± 0.5% of the ^{125}I.

Tu-Pos397

MAPPING PROTEIN-PROTEIN CONTACTS WITHIN THE YEAST VACUOLAR ATPase
((Walter H. Kahr, C. Landolt-Marticorena and M. F. Manolson)) Division of Cell Biology, Hospital for Sick Children, Toronto, Ontario, Canada.

Vacuolar-type H^+ - ATPases (V-ATPases) are multimeric complexes that mediate the lumenal acidification of various organelles (*e.g.*, yeast and plant vacuoles, endosomes, lysosomes and clathrin-coated vesicles). The V-ATPase complex contains two distinct sectors; a membrane-associated complex (V_0) which functions as the proton channel proper and a peripheral catalytic domain (V_1) responsible for ATP hydrolysis. In *Saccharomyces cerevisiae*, the V_1 sector contains two major polypeptides; the 69 kDa catalytic subunit and the 60 kDa regulatory subunit. Vph1p, the hydrophobic 100 kDa V_0 subunit is required for complex assembly but has not been ascribed a catalytically relevant function. Antibodies directed against the extreme N-terminus of Vph1p have been utilized to localize the hydrophilic domain of the 100 kDa subunit to the cytosol. We have previously demonstrated that ATP•Mg protects the catalytic subunit (69 kDa) from trypsin degradation (range 0.1 to 2.5 µg/mL) in isolated vacuolar membranes. Under comparable treatment conditions (range 0.05 to 2.5 µg/mL), ATP•Mg renders the regulatory domain (60 kDa) and the Vph1p (100 kDa) more sensitive to trypsin proteolysis. These observations suggest that the non-catalytic subunits undergo conformational changes as a consequence of ATP binding and/or hydrolysis and that Vph1p might establish direct contacts with regions of the catalytic sector. Dithiobis(succinimidylpropionate) has been utilized to generate a unique product which reacts with antibodies directed against the 60 and 100 kDa subunits of the V-ATPase. These results suggest that the two proteins are in close proximity in the native V-ATPase complex. Further studies involving chemical (CNBr) and enzymatic (trypsin) cleavage and multidimensional mapping will be utilized to localize this specific protein-protein contact site. In addition, similar studies will be performed to determine whether contact sites are retained or modified in a catalytically active state.

Tu-Pos398

SYNTHESIS AND USE OF A pH-SENSITIVE SPIN-LABEL-CARBODIIMIDE-DERIVATIVE FOR PROBING PROTON-FLUX IN PROTON-PUMPING ENZYMES
((John G. Wise, Thomas Schanding, Wolfgang E. Trommer and Pia D. Vogel)) FB Chemie der Universität, 67663 Kaiserslautern, Germany. Tel.: 49-631-205-4254 Fax.: x3419.

The synthesis of a pH-sensitive spin-label-cyclohexylcarbodiimide derivative (N-cyclohexyl-N'-[(1-oxyl-2,2,3,5,5-pentamethyl)- 4-imidazolidinyl]-methylcarbodiimide, CIMCD) and its initial use in labeling the ATP synthase from *Escherichia coli* is described. Several imidazolidine nitroxyl radicals have been previously synthesized (Volodarsky, L.B., Grigor'ev, I.A. *Imidazoline Nitroxides*, vol. I & II, CRC Press, 1988) that have shown a protonation-dependent line splitting of the high field ESR signal that could be used to report intracellular and intravesicular pH as well as membrane surface potential and polarity (Khramtsov, V.V., Marsh, D., Weiner, L., Rezinkov, V.A. (1992) Biochim. Biophys. Acta *1104*, 317-24). Dicyclohexylcarbodiimide (DCCD) and other lipophilic carbodiimides have been shown to react specifically with the membrane-embedded carboxyl residue of the proteolipid subunit of the ATP synthase F_0-sector (Asp-61 in the *E. coli* F_0 subunit c protein). Covalent modification of F_0 by DCCD inhibits oxidative phosphorylation and ATP-driven proton-pumping in the ATP synthase, as well as proton-translocation through F_1-depleted F_0-containing membranes. We thought it of interest to synthesize a pH-sensitive imidazolidine cyclohexylcarbodiimide-derivative to investigate the environment of the subunit c DCCD-reactive Asp-61 residue in the ATP synthase. Such a compound might also be of interest with other presumptive proton-pumps. CIMCD was shown to react specifically with the proton-translocating portion of the ATP synthase, inhibiting its enzymatic activities. In addition to CIMCD, the use of non-protonatable analogs should enable us to separate conformational effects from protonation effects.

ERYTHROCYTES

Tu-Pos399

ATOMIC FORCE MICROSCOPY OF THE ERYTHROCYTE MEMBRANE SKELETON
((A.H.Swihart,J.M.Mikrut,J.B.Ketterson and R.C.MacDonald)) Dept. BMBCB, Northwestern University, Evanston IL 60208.

The human erythrocyte membrane inner surface was examined using AFM, either in air or aqueous buffer. Erythrocytes on mica were lysed with hypotonic solutions, allowing AFM probe access to the cytoplasmic membrane face. The topography after lysis in 5 mM NaPi resembles a honeycomb of 40-50 nm high ridges, with a lattice constant of 300-400 nm. These ridges may be due to the clustering of band 3 and/or spectrin molecules, which would force spectrin and associated proteins to loop tens of nm away from the bilayer. Crossing the valleys are filaments of about the length of extended spectrin tetramers (≈200 nm). The meshwork is less ordered when solutions of higher ionic strength are used for lysis. Results after low ionic strength extraction or detergent treatment both support the identity of these structures. These data are consistent with a model of membrane skeletal elasticity in which clustering of components plays a critical role. Further studies are now in progress to obtain images of the skeleton at near physiological conditions. The ability to change imaging conditions during scanning is expected to allow direct observation of dynamic structural changes in response to experimental manipulations. (Supported by the American Heart Association and NIH).

Tu-Pos400

CONFORMATIONAL ORDER AND DOMAIN FORMATION OF DMPC AND DMPS INCORPORATED INTO HUMAN ERYTHROCYTES AS STUDIED BY FTIR SPECTROSCOPY.
((David J. Moore[1,2], Richard H. Sills[2], Neeta Patel[1] and Richard Mendelsohn[1])) [1]Department of Chemistry, Rutgers University, Newark, N.J. 07102 and [2]Department of Pediatrics, the Childrens Hospital of N.J./University of Medicine and Dentistry of N.J., Newark, N.J. 07107

Acyl chain perdeuterated dimyristoylphosphatidylcholine (DMPC-d_{54}) and dimyristoylphosphatidylserine(DMPS-d_{54}) were incorporated by incubation into human erythrocytes. Light microscopic analysis demonstrated that erythrocytes incubated with DMPC-d_{54} became echinocytic while those incubated with DMPS-d_{54} became stomatocytic. This indicates that DMPC-d_{54} was incorporated preferentially into the outer monolayer whereas DMPS-d_{54} was selectively incorporated into the inner monolayer. Fourier transform infrared (FTIR) spectroscopy was used to monitor the conformational order of the incorporated phospholipids. The asymmetric CD_2 stretching frequency of the inserted perdeuterated acyl chains was measured in both isolated membranes and intact erythrocytes as a function of temperature. DMPC-d_{54} incorporated into erythrocytes exhibited a cooperative phase transition at 19-20 °C, i.e., at the same temperature as pure DMPC-d_{54} vesicles. In contrast, DMPS-d_{54} incorporated into red cells exhibited no phase transition, but possessed conformational order similar to that of the liquid crystalline state. These results suggest that DMPC-d_{54} persists in domains in the outer monolayer while DMPS-d_{54} is dispersed in the inner monolayer. These experiments are the first to demonstrate that FTIR spectroscopy can be used to isolate and monitor directly a specific lipid molecule from the entire phospholipid population in the modified erythrocyte membrane.

Tu-Pos401

ANALYSIS OF ROTATIONAL DIFFUSION MEASUREMENTS OF EOSIN-5-MALEIMIDE-LABELED BAND 3 IN TERMS OF THE UNIAXIAL ROTATIONAL DIFFUSION MODEL.
((S.M. Blackman, E.J. Hustedt, C.E. Cobb, D.W. Piston, and A.H. Beth)) Dept. of Molecular Physiology & Biophysics, Vanderbilt University, Nashville, TN 37232.

The micro- to millisecond rotational dynamics of the erythrocyte anion exchange protein, band 3, have been measured via phosphorescence and delayed fluorescence anisotropy, and analyzed according to the uniaxial rotational diffusion (URD) model using an independently measured chromophore orientation. According to the URD model, data are fit by two exponential decay terms and a nonzero residual anisotropy (r_∞), whose amplitudes are related to the orientation of the probe with respect to the diffusion axis. Independent measurement of probe orientation therefore provides important constraints on interpretation of anisotropy data, potentially distinguishing between a multiple-oligomers model and other models of band 3 dynamics. Polarized steady-state fluorescence images of single erythrocyte ghost membranes were obtained on a confocal microscope. These data have been analyzed in terms of an orientation distribution (produced by independent fast motion), which predicts the preexponential amplitudes and r_∞ of the URD model, assuming the diffusion axis coincides with the membrane normal axis. These results predict the average orientations of the absorption (~61° to the membrane normal) and fluorescence emission (~72°) dipoles, and that the amplitude of one of the exponential decay terms, the e^{-4Dt} term, is about 3 times larger than that of the other, e^{-Dt} term. Trypsin treatment does not significantly alter the orientation, which indicates that the large anisotropy changes produced by trypsin treatment represent a dynamic rather than orientational process; also, the r_∞ observed after trypsin treatment is close to the value predicted by the orientation. The orientation of the absorption and fluorescence emission dipoles is being used to simultaneously analyze delayed fluorescence and phosphorescence anisotropy decay data, to determine if these data sets are consistent with a model including multiple uniaxially rotating populations. *Supported by HL34737 and DK07563.*

Tu-Pos402

EFFECT OF MEMBRANE PERTURBATION, PROTEIN CLUSTERING AGENTS, AND TRYPSIN TREATMENT ON THE ROTATIONAL DYNAMICS OF HUMAN ERYTHROCYTE BAND 3.
((C.E. Cobb, E.J. Hustedt, D.J. Scothorn, and A.H. Beth)) Dept. of Molecular Physiology & Biophysics, Vanderbilt University, Nashville, TN 37232.

Saturation Transfer EPR (ST-EPR) and time-resolved optical anisotropy techniques can both be used to measure the rotational dynamics of integral membrane proteins, such as the human erythrocyte anion exchange protein (band 3). In principle, these two independent techniques should provide complementary quantitative information. However, it has been difficult to resolve apparent discrepancies between time-resolved phosphorescence anisotropy decay (TPA) measurements of eosin-5-maleimide labeled band 3 and ST-EPR measurements of [$^{15}N,D_{13}$]-SL-H_2-DADS-maleimide labeled band 3 [Hustedt & Beth, **Biophys. J. 69:1409**]. In an effort to develop a single model which predicts both the TPA and ST-EPR results, we have used chemical agents, temperature, and proteolysis as perturbants of band 3 rotational motion. Increasing temperature from 2 to 37 °C or addition of the volatile anesthetic diethyl ether progressively increases band 3 rotational motion in both ST-EPR and TPA measurements, as expected for effectors which decrease the lipid bilayer viscosity. Two agents which have been shown to promote integral membrane protein clustering in erythrocyte membranes, Zn^{+2} and acridine orange [Clague & Cherry, **BBA, 980:93**; Turrini et al., **JBC, 266:23611**], cause an apparent decrease in the rotational mobility of band 3 as measured by ST-EPR. The corresponding TPA experiments with these two agents are now being conducted. Trypsin treatment of band 3, which removes its cytoplasmic domain and releases its attachment to the membrane cytoskeleton, only subtly alters the ST-EPR spectrum, but very significantly increases the amplitude of the fast TPA decay component and concomitantly decreases the slow (millisecond) anisotropy decay amplitude. These results will be discussed in the context of current interpretations of band 3 ST-EPR and TPA results in the literature, and the sensitivity of the two techniques to the rate of rotational motion and restriction of rotational amplitude. *Supported by HL34737, RR04075, and T32DK07563.*

Tu-Pos403

SHAPE STABILIZING AGENTS PROTECT RED BLOOD CELLS AGAINST FREEZE-THAW DAMAGE. ((I. Bakaltcheva[1], A. Rudolph[2] and B. Spargo[2])) Geo-Centers, Inc., 10903 Indian Head Hwy, Ft. Washington, MD 20744[1]; Center for Biomolecular Science and Engineering, Code 6910, Naval Research Laboratory, Washington, DC 20375[2]

It has been recently shown that lectins protect thylakoid membranes against freeze-thaw damage (Hincha et al. (1993) Plant. Physiol. 103, 59-65). In this work we show the cryoprotective action of WGA and Con A on RBCs. The lectins WGA and Con A are known as RBC shape stabilizing agents. A basic question arises from this fact: do shape stabilizing agents act as cryoprotectants? We tested three different types of shape stabilizing agents: lectins, the sulfhydryl oxidizing agent diamide and the fixitative glutaraldehyde for their cryoprotective action. They all reduced the freeze-thaw damage after freezing RBCs at -20 °C in a concentration and time dependent manner. The ability of those agents to protect RBCs against freeze-thaw damage is compared with their ability to stabilize RBC shape and decrease the membrane deformability. We determined the concentration of each shape stabilizing agents needed to block lysolecithin-induced echinocytosis. At those equieffective concentrations both lectins, diamide and glutaraldehyde showed similar cryoprotection after 15 min incubation at -20 °C. However after prolonged incubation highest survival was observed in glutaraldehyde treated RBCs followed by diamide and the two lectins. All shape stabilizing agents induced significant decrease in the membrane deformability measured by a "gravity-driven" filtration assay. Shape stabilization or decreased deformability in the presence of the tested agents is acountable for their cryoprotective action? The monoclonal antibody to glycophorin A (R-10) causes membrane rigidity but does not impair lysolecithin-induced echinocytosis. R-10 does not protect RBCs against freeze-thaw damage. The ability of the lectins, diamide and glutaraldehyde to stabilize the RBC shape accounts for their cryoprotective action. Decreased deformability itself does not protect against freeze-thaw damage.

CYTOSKELETON

Tu-Pos404

SARCOMERE DOMAIN BEHAVIOR IN PASSIVELY STRETCHED SHR & WKY CARDIAC MYOCYTES. ((R.E. Palmer and K.P. Roos)) Cardiovascular Research Lab. and Dept. of Physiology, UCLA Medical School., Los Angeles, CA., 90095-1760.

Three-dimensional striation pattern analysis of resting cardiac myocytes suggested that the sarcomeres are organized into domains (Roos, Biophys, J. 52:317, 1987). The domains are bound together by the intermediate filament network (primarily desmin). We now report on the mechanical behavior of these domains in single cells enzymatically dissociated from the left ventricle of SHR and WKY rat hearts. Passive stretches (1.9μm to > 3.0μm SL) of chemically skinned cells attached between two pipettes in relaxing solution were analyzed from digital images. Adjacent domains usually varied in average sarcomere length (SL) at any given length or at rest. The domains had the ability to behave independently at short SL (<2.0 μm), however, at extended lengths the slope of their strain-extension relationship was identical. At short sarcomere lengths the domains may slide relative to each other, however at longer lengths there is no slack in the interdomain intermediate filament network and the domains behave in synchrony. Sarcomeric homogeneity was greater within a domain than between domains. A yield point was reached at sarcomere lengths greater than 2.6 μm. These data suggest a strong mechanical coupling of sarcomeres within a domain and a looser coupling between domains. There was no difference in this behavior in the hypertrophied SHR myocytes. *Supported by HL-47065 (KPR) and AHA-LA Affiliate (REP).*

Tu-Pos405

BENDING ELASTICITY OF INDIVIDUAL CYTOSKELETAL POLYMERS MEASURED BY APPLYING CALIBRATED FORCES WITH OPTICAL TWEEZERS.
((M. W. Allersma, D. R. Stom, C. F. Schmidt)) Dept. of Physics and Biophysics Research Division, University of Michigan, Ann Arbor, MI 48109.

Optical tweezers can be used to three-dimensionally trap μm-sized dielectric particles under a microscope and exert calibrated forces on the trapped particle. We developed a dual trap scheme which allows us to set and manipulate two traps independently in the field of view of a high resolution video microscope. In our assay, we attached 0.5 μm silica spheres to the ends of *in vitro* reconstituted taxol stabilized microtubules (from bovine brain). The spheres serve as "handles" for the optical trap to capture and bend the microtubules. With less than 3 pN of force applied to each end, microtubules between 5 and 15 μm in length were bent to large angles (40% - 60% relative deformations). Modeling the microtubules as elastic rods, their flexural rigidity is calculated from the force necessary to reach a measured deformation. The force can be measured with high resolution using sub-nm position detection optics. We measured an average flexural rigidity of $0.40 \pm 0.1 \times 10^{-23}$ Nm^2, corresponding to a persistence length of 940 ± 250 μm at 300K. The same method can also be applied to actin filaments. (Supported by a grant from the Whitaker Foundation)

Tu-Pos406

RIGIDITY ANALYSIS OF ACTIVATED PMN LEUKOCYTES. ((Ralph Nossal)), Phys. Sci. Lab., DCRT, National Institutes of Health, Bethesda, MD 20892.

Upon noting that the cortical cytoskeletal matrix of activated leukocytes has characteristics of a transient polymer network, one can show that the transit time measured by a cell transit analyzer varies linearly with the instantaneous shear modulus, G, of the cortical matrix. It thus follows that measurements of cell deformability can be analyzed in terms of a mathematical theory [1] that relates the time-dependent elasticity of complex actin networks to changes in crosslinking, rates of actin polymerization, nucleation kinetics, capping dynamics, etc. Derived expressions have been used to examine data obtained when leukocyte stiffening is brought about by immersing PMN cells in solutions containing differing concentrations of chemoattractants [2]. Quantitative analysis of the dependence of cell rigidity on the actin content of the network suggests that the crosslinking is primarily that of tetrafunctional junctions -- e.g., entanglements or ABP (filamin) links. Further, it appears that the rigidity increase noted upon stimulation is due solely to an increase in f-actin concentration and not to changes in the nature of matrix crosslinking. Additional analysis of the early time increase of rigidity after stimulatin allows us to determine the functional dependence of rigidity on network kinetic parameters, thereby enabling us to distinguish between several models of cell physiologic response.

[1] Nossal, R. 1988. *Biophys. J.*, **53**: 349-359.
[2] Pecsvarady, Z. et al., 1992. *Blood Cells*, **18**:333-352.

Tu-Pos407

ROLE OF THE CYTOSKELETON IN LEUKOCYTE MECHANICAL PROPERTIES. ((M. A. Tsai and R. E. Waugh)) Department of Biophysics, University of Rochester Medical Center, Rochester, NY 14642

Leukocyte mechanical properties play an important role in cell trafficking in the microvasculature and cell egress from the bone marrow into the peripheral blood. In this study, we investigated the role that the cytoskeleton plays in leukocyte mechanical properties, using a human promyelocytic cell line (HL-60) as a model. Fractions of proliferating HL-60 cells in G_1 and S phases of the cell cycle were prepared by centrifugal elutriation. To alter the cytoskeleton, 30 μM dihydrocytochalasin B (DHB) and 100 μM colchicine were used to disrupt microfilaments (F-actin) and microtubules respectively. Cell rheological properties were evaluated by single-cell micropipette aspiration (Tsai et al, *Biophys. J.*, **65**: 2078-88,1993), and tested at similar geometry of deformation, i.e., same ratio of cell to pipette radii. When compared at the same aspiration pressure, both reagents significantly softened G_1 and S cells, and the effect of DHB was more pronounced. Furthermore, HL-60 cells exhibited power-law fluid behavior as neutrophils: $\mu = \mu_c(\gamma_m/\gamma_c)^{-b}$, where μ is cytoplasmic viscosity, γ_m is mean shear rate, μ_c is characteristic viscosity at characteristic shear rate γ_c, and b is a material constant. Treatment with DHB reduced both the characteristic viscosity (~ 65%) and shear rate-dependence (20–30%) of G_1 and S cells. Colchicine had only a slight effect on G_1 cells, but reduced the characteristic viscosity of S cells by ~ 25% without significant changes in shear rate-dependence. These results support the view that F-actin plays the predominate role in determining leukocyte mechanical properties. Moreover, this study provides the first evidence that microtubules may also make a significant contribution to the mechanical properties of proliferating leukocytes in a cell cycle-dependent fashion. (Supported by NIH grant No. HL-18208 and Am. Heart Assoc. grant No. F93-219).

Tu-Pos408

BARRIER-FREE PATHS OF DIRECTED PROTEIN MOTION IN THE ERYTHROCYTE PLASMA MEMBRANE. ((David H. Boal and Seng K. Boey)) Dept. of Physics, Simon Fraser University, B.C. Canada. (Spon. by D. Boal)

A model is presented for the steric interaction between a plasma membrane protein and the membrane cytoskeleton in the human erythrocyte. The cytoskeleton is treated as a network of polymer chains attached to a flat bilayer, and the membrane protein is a hemisphere of radius R with center on the bilayer edge. The simulation is used to investigate the barrier-free path L for linear guided motion of a protein in the bilayer plane. It is shown that the barrier-free paths of small proteins can be used to extract the effective in-plane diameter of cytoskeletal components.

Tu-Pos409

THREE DIMENSIONAL DISTRIBUTION AND ACTIN LOCALIZATION OF ACTIVATED PROTEIN KINASE C IN STIMULATED GASTRIC MYOCYTES. ((D. J. Schmidt and F.S. Fay)) Univ. of Mass., Prog. in Molecular Medicine, Biomedical Imaging Group, Worcester, Ma. 01605. (Spon. by Elaine F. Etter.)

Since activation of protein kinase C (PKC) modulates key aspects of smooth muscle contractile function and myocytes express multiple isoforms of PKC, localization of specific PKCs is required to assess putative roles in contraction-related processes. Indirect immuno-fluorescence staining was performed on fixed cryosections of agonist and phorbol ester stimulated toad stomachs with mAb1.9, an antibody shown to selectively bind to *active* PKCs (Moore et al, Biophys.J., 64 (2P2), pA32, 1993) Results confirmed that report's localization of active PKC continuously along filamentous structures in stimulated cells . To identify the PKC-associated filament, high resolution 3D subcellular colocalization of PKC(s) and cytoskeletal markers was performed on fixed cryosections of toad stomach using digital imaging fluorescence microscopy including image de-blurring with constrained iterative mathematical deconvolution. Probes included pan-PKC 'active-kinase-selective' mAb 1.9, monoclonal anti- α–PKC, monoclonal anti-α–actin, labelled phalloidins. A modified filterset allowed the additional measurement of fluorescence resonance energy transfer (FRET) between fluorescein and rhodamine-labelled probes. With appropriate calibration and ratioing of donor and transfer images, this technique allows identification of image voxels where fluorescent labels were located only tens of nanometers apart in the cell. Both statistical colocalization analysis of restored images and analysis of FRET images determined that the activated PKC detected following agonist and phorbol stimulation of visceral and vascular myocytes was associated with actin, and also that it consists, at least in part, of the α–PKC isoform. Since resting myocytes show a beadlike distribution of this isoform along filaments, it may rapidly and locally activate and translocate along actin during initiation of contraction. α–PKC's association with actin indicates that it may play a role in phosphorylation of actin-asociated proteins putatively involved in regulation of contraction. (Support by NIH HL 14523 and Fellowship DK09226).

Tu-Pos410

CHARACTERIZATION OF TWO HIGH MOLECULAR WEIGHT TRITON-INSOLUBLE PROTEINS SPECIFICALLY ALTERED IN *MDX* SKELETAL MUSCLE. ((K.M. McCutcheon and B.H. Bressler)) Department of Anatomy, University of British Columbia, Vancouver, B.C., Canada.

Triton X-100 insoluble protein compositions of skeletal muscle membranes from *mdx* C57Bl/10ScSnMdx and normal C57Bl/10SnJ mice were compared at 2, 6 and 20 weeks of age. It has been previously reported that the cytoskeleton of the *mdx* mouse is not compromised by the absence of dystrophin. Relative to other proteins seen on reducing SDS-PAGE, we have observed a significant upregulation of an unknown Mr 370 kDa Triton-insoluble protein in *mdx* soleus, extensor digitorum longus and diaphragm at 6 and 20 weeks of age. Also, an unknown Mr 240 kDa Triton-insoluble protein is downregulated. This change in protein composition is skeletal muscle specific. Relative to other proteins, these proteins are present but unchanged in *mdx* cardiac muscle and in non-muscle tissues such as lung. We have biochemically localized the 240 and 370 kDa proteins to the same Triton-insoluble fraction as dystrophin in the presence of high or low salt. Treatment of this Triton-insoluble fraction with RNase and DNase has shown our interpretation of protein compositions to be free of nucleic acid contamination. Indirect evidence suggests the 240 and 370 kDa proteins are posttranslationally modified: they are trypsin resistant; they stain weakly with Coomassie Blue and Alcian Blue; they stain a reddish-brown colour with silver; and they migrate in a dumbell-shape on SDS-PAGE. The presence and amounts of the 240 and 370 kDa proteins relative to other proteins are affected by the developmental stage and vary between tissues and species. Our results show a new and significant alteration in a biochemically defined cytoskeletal protein fraction of *mdx* skeletal muscle. We hope to identify the 240 and 370 kDa proteins and implicate a role for their co-ordinate regulation in muscle regeneration.

MEMBRANES - CELLULAR

Tu-Pos411

DIELECTROPHORETIC MANIPULATION OF CELLS USING SPIRAL ELECTRODE ARRAYS ((X.-B. Wang, Y. Huang, F.F. Becker and P.R.C. Gascoyne)) Department of Molecular Pathology, Box 89, University of Texas MD Anderson Cancer Center, 1515 Holcombe Boulevard, Houston, TX 77030 USA

Methods for cell manipulation using a spiral microelectrode array having four electrode elements excited by phase-quadrature signal excitation are presented. Electrokinetic responses of human breast cancer (MDA 231) cells are demonstrated for suspension conductivities from 28 to 406 mS/m over the frequency range 10 kHz to 100 Mhz as an example. Individual cells could be selectively transported towards or away from the center of the spiral array or trapped at the electrode edges depending on the applied excitation frequency. Cell radial transportation velocity was found to be a function of the suspension medium conductivity and the frequency and voltage of the applied electrode signals. The observed cell kinetic behaviors are analyzed with the aid of generalized dielectrophoresis theory, simulated electric field distributions close to the the spiral array, and the measured cell dielectric properties. It is shown that the vertical components of the electrical field distribution plays an important role in determining the overall cell kinetics by generating a levitation force that affects cell equilibrium height and thereby influences the height-dependent radial force that is experienced by the cells. Applications of the spiral electrode array to the isolation of rare or dilute cells of clinical relevance is discussed.

Tu-Pos412

CELL SEPARATION BY CONVENTIONAL DIELECTROPHORESIS COMBINED WITH FIELD-FLOW-FRACTIONATION ((P.R.C. Gascoyne, Y. Huang, X.-J. Wang, J. Yang, G. DeGasperis and Xiaobo Wang)) Department of Molecular Pathology, Box 89, University of Texas MD Anderson Cancer Center, 1515 Holcombe Boulevard, Houston, TX 77030 USA

We demonstrate the principle of cell fractionation by conventional dielectrophoresis (cDEP) applied in conjunction with field-flow fractionation (FFF) and present preliminary demonstrative results. Our fractionation device takes the form of a thin chamber in which the bottom wall supports an array of microelectrodes. These generate a non-uniform AC electrical field and induce conventional dielectrophoretic forces on cells suspended in the chamber thereby levitating them. A parabolic flow profile is established so that fluid flows faster with increasing height above the chamber bottom wall. A cell in the flow stream will attain an equilibrium height (and corresponding velocity) depending upon the dielectrophoretic, gravitational and hydrodynamic lift forces it experiences. Cells of differing density, size or dielectric properties will therefore exhibit different transit times as they traverse the chamber at characteristic heights; mixtures of cells can thereby be fractionated. This principle is demonstrated using human leukemia (HL-60) cells in a thin chamber equipped with an array of parallel electrodes. Transit times are shown to be a function of cell suspension conductivity, fluid flow rate, and magnitude and frequency of the applied voltage signals. A theoretical analyses of the cell behavior is provided based on the dielectrophoretic and hydrodynamic forces on the cells and this is found to be in very good agreement with the experimental observations. Optimization of the electrode and chamber designs and applications of cDEP/FFF cell separations are discussed.

Tu-Pos413

APPLICATION OF AC ELECTROKINETICS FOR CELL CHARACTERIZATION AND MANIPULATION ((Y. Huang, P.R.C. Gascoyne, F.F. Becker and X.-B. Wang)) Department of Molecular Pathology, Box 89, University of Texas MD Anderson Cancer Center, 1515 Holcombe Boulevard, Houston, TX 77030 USA

Cells become electrically polarized when subjected to an alternating electrical field and the interaction between this induced polarization and the applied field can give rise to various electrokinetic effects. An inhomogeneous field will exert a translational dielectrophoretic (DEP) force on cells while a rotating field will induce cell electrorotation (ROT). The frequency responses of these effects are functions of the intrinsic cellular dielectric properties and there is a growing interest in the exploitation of these phenomena for cell characterization and manipulation. We report here ROT measurements for a number of cell types and demonstrate that the dielectric properties of cells constitutes a component of phenotype that reflects their biological function. We go on to demonstrate DEP manipulations using several different electrode geometries, a range of cell suspension conductivities and applied field frequencies, and different excitation modes. Several characteristic cell behaviors are identified including linear motion, trapping, levitation and circulation. The findings are rationalized using generalized dielectrophoresis theory, simulated electrical field distributions, and measured cell dielectric properties. Finally, dielectrophoretic separation of cells having different dielectric properties is demonstratetdd including the removal of human breast cancer and leukemia cells from blood using a dielectric affinity chamber. The separation principles and efficiency of the affinity chamber are discussed.

Tu-Pos414

A FEEDBACK MODIFIED OPTICAL TRAP FOR PROBING LOCAL VISCOSITY AND EXAMINING DIFFUSIVE BEHAVIOR ON CELL MEMBRANES. ((Neil A. Switz, Jerome Mertz, and Watt W. Webb)) Dept. of Applied and Eng. Physics, Cornell University, Ithaca, NY 14853.

The traditional methods of probing molecular mobility on membranes, fluorescence photobleaching recovery (FPR) and single particle tracking (SPT), are incapable of providing direct information on the local forces affecting the particles. FPR provides only ensemble averaged information, and SPT yields limited information on the localized membrane properties. To measure local interaction restraints and active forces, we use an optical trap consisting of a strongly focused infrared laser combined with a simple position sensing device and computer controlled stage, providing both picoNewton-level tensiometry and nanometer-scale position detection. This combination of optical force microscope (OFM) and SPT system provides the additional capacity for dynamical, continuous force measurements on the tracked particle. Such a configuration requires the use of tunable feedback to modify the trap position in response to displacements of the tracked particle; our analysis indicates that by varying the feedback transfer function one may also obtain information about the local constraints on particle motion, making this a potentially powerful tool for the investigation of anomalous diffusion on cell membranes. We present a theoretical analysis of the necessary feedback scheme, experimental details of its implementation, and some preliminary results.

Funded by NSF(BIR9419978) and NIH(RR04224) at the Developmental Resource for Biophysical Imaging and Opto-Electronics.

Tu-Pos415

SINGLE-PARTICLE TRACKING: NEW METHODS OF DATA ANALYSIS ((Michael J. Saxton)) Institute of Theoretical Dynamics, University of California, Davis, California 95616.

Single-particle tracking experiments make it possible to observe motion of membrane proteins over submicroscopic distances, to try to see whether the motion is diffusive, directed, or confined. Interpreting the observed trajectories may be difficult because, simply by chance, a random walk can look like nonrandom motion. It is useful to define parameters characterizing the trajectory, and evaluate the probability distribution of those parameters for pure random walks and other modes of motion. Three approaches to the analysis of trajectories are discussed. The first is based on the convex hull of the trajectory, that is, the smallest convex polygon containing the trajectory. The second examines the velocity autocorrelation function of the tracer motion. The third uses Brownian dynamics calculations of motion in a corral to find the escape time as a function of barrier height and corral size. (Supported by NIII grant GM38133.)

Tu-Pos416

ASYMMETRIC KINETICS OF PORE OPENING AND CLOSING IN ELECTROPORATION. ((T.R. Gowrishankar, W. Chen and R.C. Lee)) The University of Chicago, IL 60637.

The molecular events underlying electroporation determine the kinetics of opening and closing of membrane pores. In order to obtain insight into these molecular events, electroporation current was measured and compared with the predictions of a theoretical model[1]. **Methods:** An isolated skeletal muscle cell from an English frog was mounted on a double vaseline gap voltage clamp. Channel blockers were used to block Na^+ and K^+ channels in order to measure only the electroporation component of transmembrane current. Measurements were made for a series of 8 msec pulses from -150 to -400 mV in steps of -10 mV. **Results:** The time constant of electroporation current during the pulse ranged from 0.26 to 0.65 msec compared to the current relaxation following the pulse which was between 2.1 and 7.3 msec for the range of transmembrane potentials studied. The diffusion coefficient of pores in radius space (D_p) was estimated from relaxation time constants and model simulations to be $5 \times 10^{-16}\ m^2/sec$. The opening and closing of membrane pores occurs as a result of the rotation of lipid molecules that form the pore walls. The asymmetry in the kinetics of electroporation during and after the pulse thus indicates an asymmetry in the time-scales of rotation of lipid molecules before and after electroporation. The estimated value of D_p is lower than the estimates for other membrane components. This suggests that certain pores are stable over a few msec after the pulse is turned off owing to a slower rotation of lipid molecules following electroporation resulting in a rectification of transmembrane current. [1]Freeman *et al.*, Biophys. J. 67:42. 1994.

Tu-Pos417

FLUORESCENCE STUDIES ON THE MOLECULAR ACTION OF AMPHOTERICIN B ON SUSCEPTIBLE AND RESISTANT FUNGAL CELLS ((M. P. Haynes, P. L.-G. Chong, H. R. Buckley & R. A. Pieringer)) Departments of Biochemistry and Microbiology & Immunology, Temple University School of Medicine, Philadelphia, PA 19140. (Spon. by J. H. Collins)

The molecular action of amphotericin B (AmB) on the cell membranes of both AmB-susceptible and resistant fungal cells was investigated through the use of the fluorescent membrane probe TMA-DPH. AmB, the most effective drug for the treatment of systemic fungal infections, is known to interact specifically with membrane sterols, especially ergosterol (the major sterol in fungal cells). Treatment of AmB-susceptible fungal cells with AmB induced a novel biphasic change in TMA-DPH fluorescence intensity over time. The initial decrease in fluorescence intensity is due to the binding of AmB to the fungal cell membrane as a result of energy transfer between AmB and TMA-DPH. The second phase of increasing fluorescence intensity is interpreted in terms of a combination of probe repartitioning and probe segregation as a result of the formation of membrane pores due to aggregation of AmB-ergosterol complexes. An AmB-resistant strain of *C. neoformans*, containing 94% of aberrant δ-8 double bonded ergosterol precursors and only 4% of ergosterol, exhibited the first phase of AmB binding, but not the second phase of increasing fluorescence intensity. This result suggests that AmB's antifungal activity lies in its ability to form membrane pores due to aggregation of AmB-ergosterol complexes. The AmB-induced biphasic fluorescence intensity profile may lead to further elucidation of the molecular action of AmB on fungal cells and may provide a sensitive method for screening the development of drug resistance in fungal cells (supported by AHA).

Tu-Pos418

TS28, A T-TUBULAR MARKER PROTEIN IN DEVELOPING AND ADULT SKELETAL MUSCLE, IS PHOSPHORYLATED BY PROTEIN KINASE C.
((C.A.E. Mason*, M.M. Rodriguez*· D. Mochly-Rosen+ and A.O. Jorgensen*))
*Department of Anatomy and Cell Biology, University of Toronto, Toronto, Ontario, M5S 1A8, CANADA and +Department of Molecular Pharmacology, Stanford University, School of Medicine, Stanford, CA. 94305-5332, U.S.A.

TS28 is a 28 kDa integral membrane protein localized to skeletal muscle T-tubules where it is first detected concurrently with the onset of de novo T-tubule formation in developing muscle. It has been suggested that TS28 may correspond to 1) a 28 kDa small GTP binding protein (Doucet, J.-P., Tuana, B.S. 1991. J. Biol. Chem. 266: 17613) and 2) a 28 kDa substrate of Protein kinase C (Salvatori, S. et al., Biochem. Biophys. Res. Commun. 196: 1073) previously identified in isolated transverse tubule membranes. To test these possibilities we have purified TS28 from skeletal muscle membranes by immunoaffinity purification and examined 1) its ability to bind [α-^{32}P] GTP in a blot overlay assay and 2) its potential to function as a substrate for Protein kinase C. Purified TS28 does not bind [α-^{32}P] GTP using a blot overlay assay. Initial studies show that TS28 is a substrate for exogenous Protein kinase C. Studies are in progress to determine whether TS28 is a substrate for a Protein kinase C intrinsic to T-tubules in skeletal muscle.
(Supported by MRC (A.O.J.) and by NIH (D.M.-R.).

Tu-Pos419

PLASMA MEMBRANE HETEROGENEITIES DURING CYTOKINESIS OF RBL-2H3 CELLS CHARACTERIZED USING TWO PHOTON EXCITED FLUORESCENCE MICROSCOPY ((Rebecca M. Williams and Watt W. Webb*)) Dept. of Physics and *School of Applied & Eng. Physics, Cornell University, Ithaca, NY 14853.

Though the molecular steps are becoming elucidated, the physical mechanism of cytokinesis is not yet understood. We report here studies of dividing RBL-2H3 cells using two-photon excited fluorescence microscopy. This technique enables three-dimensional resolution, access to a wide spectrum of dyes, and the opportunity for extended imaging on viable specimens. In dividing cells, located in the adhered culture using a vital DNA stain, several acyl-labeled, saturated plasma membrane probes exhibit drastic fluorescence enhancements that are localized to the cleavage furrow and coincident with furrow invagination. These order of magnitude fluorescence increases persist until cell division is complete. We obtain optical, three-dimensional images of mid-body structures that resemble those of electron dense material in TEM micrographs. Using fluorescent lipids of various types we are currently characterizing the physical properties of these distinctive regions. Whether these fluorescence enhancements are due to a complex folding that increases membrane volume or to a segregation of the lipid probes to specialized membrane domains is not yet known.

Supported by NSF (BIR9419978) and NIH (RR04224) at the Developmental Resource for Biophysical Imaging and Opto-Electronics.

Tu-Pos420

NEW ASPECTS ON MEMBRANE LIPID REGULATION IN *A. LAIDLAWII* AND *E. COLI*. ((G. Lindblom and L. Rilfors)) Department of Physical Chemistry, Umeå University, Umeå, SWEDEN.

The regulation of the membrane lipids of the cell wall-less *Acholeplasma laidlawii* (A-EF22) in response to the growth conditions has been extensively studied in our laboratory. It is shown that *A. laidlawii* can synthesize as many as eight membrane lipid classes (mainly **glucolipids**). A detailed determination of the structure of these lipids has been performed with 2D NMR spectroscopy. A new lipid is found (constituting up to 15 wt%) and the correct structures of three other lipids are established. It is worthy of note that **three** of the membrane lipids contain a **third acyl chain**.

The membrane lipids synthesized form a remarkable number of phases, covering the whole range of phase structures that can be formed by amphiphiles, i. e. from a *normal* micellar phase via lamellar, reversed cubic and hexagonal phases to a *reversed* micellar phase. The proportions of **all** these lipids are carefully **balanced** by *A. laidlawii* in relation to the prevailing growth conditions. The organism strives to maintain the proportion between bilayer- and nonbilayer-forming lipids within a certain range, resulting in a slightly negative curvature of the lipid monolayers in the membrane.

Wild-type *E. coli* cells also regulate the balance between bilayer- and nonbilayer forming **phospholipids** in relation to the growth temperature. The same physico-chemical model is working for both organisms. In this model the membrane lipid composition is always such that, at the growth temperature, the lipids form a bi-layer, which is above the gel to liquid crystalline phase transition temperature, and it is below a transition to a non-lamellar phase. It is concluded that the **packing** of the lipids in the bilayer plays a crucial role. The functional consequences for sthis will be discussed.

Tu-Pos421

VISCOELASTIC RELAXATION IN THE MEMBRANE OF THE AUDITORY OUTER HAIR CELL. ((David Ehrenstein and K. H. Iwasa)) NIDCD, NIH, Bethesda, MD 20892-0922.

The outer hair cell (OHC) in the mammalian ear has a unique membrane potential-dependent motility which is considered to be important for frequency discrimination (tuning). The OHC motile mechanism is located at the cell membrane and is strongly influenced by passive mechanical properties of the membrane. To improve our understanding of the motility, we studied the viscoelasticity of the membrane and found the time-scale at which a purely elastic description of the cell must be replaced by a viscoelastic description. We exposed cells to a hypo-osmotic solution for varying durations and then punctured them, to immediately release the osmotic stress. Using video records of the cells, we determined both the imposed strain and the strain after puncturing, when stress was reset to zero. The strain data were described by a simple rheological model consisting of two springs and a dashpot, and the fit to this model gave a time constant of 40 ± 19 s for the relaxation (reduction) of tension during prolonged strain. For time-scales much shorter or longer than this we would expect essentially elastic behavior. This relaxation process regulates the membrane tension of the cell, and since it has been shown that membrane tension has a regulatory role in the OHC's motility, this relaxation process may be part of an adaptation mechanism, with which the motility system of the OHC can adjust to changing conditions and maintain optimum membrane tension.

Tu-Pos422

THE ENERGY OF TETHER FORMATION FROM THE RED BLOOD CELL MEMBRANE ((W.C. Hwang and R.E. Waugh)) Department of Biophysics, School of Medicine and Dentistry, University of Rochester, Rochester, NY 14642.

The red blood cell membrane consists of the lipid bilayer and the underlying membrane skeleton. The lipid bilayer and the membrane skeleton are coupled together by specific molecular interactions. Defects in this association can result in decreased membrane stability and hemolytic anemia. The mechanical formation of bilayer cylinders (tethers) from the cell surface provides a way to measure the strength of this association. Evidence, from the distribution of membrane components after tether formation, and the solubility of tethers in detergent, indicates that tethers consist primarily of a bilayer membrane lacking both a membrane skeleton and associated integral proteins. The reversible work of separation was measured by measuring the force of tether formation under quasi-steady conditions. The tethering force was monitored by measuring the deflection of a pre-calibrated microcantilever, and the tether radius was calculated by measuring the displacement of the cell projection in the pipette. Two approaches were used to obtain the reversible work of separation. In the first approach, the steady state tethering forces were obtained at different tether growth rates, and then the tethering force at zero tether growth rate was obtained by extrapolation. In the second approach, the tether was held at constant length after being formed, and the steady state force was recorded. Both approaches yield independent, yet consistent results for reversible work of separation. The work of separation includes two main parts; the work of membrane bending and the work of separating the bilayer from the cell surface. We calculate a membrane bending stiffness of $\sim 1.9 \times 10^{-19}$ J and a reversible work of separation of ~ 0.2 mJ/m^2. The molecular origin of this separation energy is unknown at the present time, but remains the subject of future studies. (Supported under NIH grant No.'s HL 31524 and HL 18208.)

Tu-Pos423

GPI-ANCHORED PROTEINS AND GLYCOSPHINGOLIPIDS EXHIBIT TRANSIENT LATERAL CONFINEMENT TO SMALL DOMAINS: A SINGLE PARTICLE TRACKING STUDY. ((Erin D. Sheets* and Ken Jacobson†)) Departments of Chemistry* and Cell Biology & Anatomy†, University of North Carolina, Chapel Hill NC 27599.

Glycosylphosphatidylinositol (GPI)-anchored proteins have recently been proposed to be sequestered by caveolae, 50–75 nm diameter invaginations in the plasma membrane, for participation in events such as signal transduction. However, other biochemical work has suggested that these proteins are associated primarily with glycosphingolipids. To investigate the lateral distributions and mobilities of these two classes of molecules on live cells, we have used single particle tracking (SPT) to follow the movements of colloidal gold labelled Thy-1, a representative GPI-anchored protein, and GM1, a glycosphingolipid, on the surfaces of C3H 10T1/2 fibroblasts. The trajectories of particles observed for 6.6 s are classified into four categories—fast random diffusion, slow random diffusion, confined diffusion, and a stationary fraction. For both molecules, ~25% of the molecules underwent fast diffusion, 15–30% underwent slow diffusion, and ~10% were stationary on the time scale of the experiment. Approximately 37% of the Thy-1 and ~47% of the GM1 were transiently confined to membrane domains that were ~300 nm in diameter and significantly larger than caveolae. Thy-1 resides in the domains for ~8 s when observed for longer periods of time (60 s). The detergent Triton X-100 can selectively solubilize membrane-spanning proteins and phospholipids; thus, we have also used SPT to investigate the lateral mobilities on the detergent-inextractable cell membranes. Preliminary results show an increase in the percentages of immobile and confined Thy-1. The similarities between Thy-1 and GM1 suggest that lipid milieu determines the mobility and distribution of GPI-anchored proteins on cell surfaces. This work was supported by NIH grant 41402.

Tu-Pos424

STABILITY PROPERTIES OF ELEMENTARY DYNAMICAL MODELS OF INTEGRATED CELL MEMBRANE TRANSPORT SYSTEMS.
((Julio A. Hernández and Ernesto Cristina.)) Sec. Biofísica, Fac. Ciencias, Univ. de la República, 11200 Montevideo, Uruguay.

Some aspects of the dynamical behavior of cells are determined by the integrated functioning of diverse processes of transport across the plasma membrane. The models describing these phenomena consist in systems of differential equations governing the rate of change of the cell volume (V_c) ; the electrical potential across the membrane (V_m). and the intracellular ionic concentrations. Due to the complexity of these systems, the analysis of their stability properties is technically difficult, and the study is usually restricted to the steady-state analysis and to numerical simulations. Our purpose is to determine whether some dynamical properties of cells can be represented by systems of only two differential equations, more accessible to stability analysis.For this, we consider the particular cases of cells capable of maintaining their V_m (V_c), while modifying their V_c (V_m) and some intracellular ionic concentration in response to changes in intracellular or ambient parameters ("isoelectric" and "isovolumetric" cases). Since the active ionic transport is represented by explicit kinetic schemes, it is possible to study the sensitivity of the stability properties to the metabolic charge of the cell, represented by the ATP concentration (S). In the isoelectric case, the dependent variables are the V_c and one intracellular ionic concentration. For some of the examples studied here, the systems consistently describe the dynamics of short-term volume regulation induced by anisosmotic shocks, and exhibit strong neighborhood stability and little sensitivity to relatively important changes in S. In the isovolumetric case, the dependent variables are the V_m and one intracellular ionic concentration. Some examples exhibit complex stability poperties and a relatively high sensitivity to changes in S, and could represent the behavior of cells where changes in the V_m could constitute signals of their metabolic state.

Tu-Pos425

INCORPORATION OF SHORT-CHAIN FATTY ACIDS BY *ACHOLEPLASMA LAIDLAWII* MAY SUPPRESS GROWTH BY DISRUPTION OF MEMBRANE LIPID POLAR HEADGROUP DISTRIBUTION. ((X.-L. Cheng, R.N.A.H. Lewis and R.N. McElhaney*)) Dept. Biochemistry, Univ. Alberta, Edmonton, Canada, T6G 2H7.

The biosynthetic incorporation of short-chain linear saturated (but not other classes) of fatty acids results in the inhibition of growth of *Acholeplasma laidlawii* despite the fact that liquid-crystalline membrane lipids bilayers of moderate fluidity and at least minimal acceptable thickness are produced under these conditions. To investigate the molecular basis of such growth inhibition, the growth yields, lipid compositions and lipid physical properties of cells incorporating progressively increasing amounts of dodecanoic or tri-decanoic acids were studied. Normal cell growth was only observed when dodecanoyl and tri-decanoyl chains comprise no more than 60 and 90 mol % of the total lipid hydrocarbon chains, respectively. Short-chain saturated fatty acid incorporation was found to produce a marked elevation of monoglucosyl diacylglycerol (MGDG) and a marked decline in diglucosyl diacylglycerol (DGDG) and phosphatidylglycerol (PG) levels in the membrane. Although the increase in the higher-melting, reversed phase-preferring MGDG component could be viewed as compensatory in terms of both homeoviscous adaptation and nonlamellar/lamellar phase propensity, reductions in the levels of the lamellar phase-preferring DGDG and PG levels, and in anionic PG level, may have resulted in the formation of a membrane lipid bilayer with a lamellar phase propensity and surface charge density too low to support normal membrane function and cell growth.
(Supported by the Medical Research Council of Canada and the Alberta Heritage Foundation for Medical Research).

Tu-Pos426

CHOLESTEROL UPTAKE AND STIMULUS DEPENDENT TRANSLOCATION IN HUMAN PLATELET PLASMA MEMBRANE [[R.J. Schimmel & K. Boesze-Battaglia]] UMDNJ-SOM, Stratford, NJ 08084. [Spon. by G. Bailin]

Platelet membrane cholesterol content determines platelet responsiveness to aggregatory stimuli. A step in the aggregatory response involves the translocation of PS and PE from the inner to the outer membrane monolayer. The effect this translocation has on cholesterol distribution is the focus of this work. The uptake and transbilayer distribution of cholesterol was followed using NBD-cholesterol, cholestatrienol and cholesterol oxidase susceptibility. Cholestatrienol fluorescence quenching experiments showed cholesterol uptake to be a first order process with a $t_{1/2}$ of 39 min. The kinetics of cholestatrienol transbilayer distribution indicated a $t_{1/2}$ of 43 min. for movement of probe from the outer to the inner monolayer and a $t_{1/2}$ of 20 min. for movement from the inner to the outer monolayer. Once a steady state distribution of the fluorescent sterol probes had been reached, the effect of collagen and/or epinephrine on cholesterol distribution was determined. 10 mg/ml collagen resulted in a translocation of 25% of the outer membrane cholestatrienol. 10 uM epinephrine had no detectable effect on the transbilayer distribution of cholestatrienol, however, it potentiated the collagen response observed. Cholestatrienol and NBD-cholesterol were localized to plasma membrane relative to intracellular membrane cholesterol pools as determined by osmotic lysis and fluorescence quenching.

Tu-Pos427

MEMBRANE TOLERANCE AND CROSS TOLERANCE IN HEPATIC MITOCHONDRIAL MEMBRANES AFTER CHRONIC EXPOSURE TO ETHANOL OR NITROUS OXIDE ((I. Dey, E. D. Frank, E. Rubin, T.F. Taraschi, and N. Janes)) Dept. of Pathology and Dept. of Anesthesiology, Jefferson Medical College, Philadelphia, PA 19107

Long-term exposure of animals to ethanol causes adaptive alterations in the properties of most cellular membranes. This adaptation is characterized by an apparent homeostatic response to the fluidizing effects of ethanol administration *in vitro*. Yet, unknown is whether the adaptive response is peculiar to ethanol (perhaps induced by its metabolites, or metabolic imbalances associated with ethanol catabolism), or whether it is a ubiquitous consequence of chronic exposure to membrane fluidizing agents (organic solvents, anesthetics, etc.). That is, could membrane tolerance be broadly relevant to clinical tolerance to lipophilic drugs?

Nitrous oxide (N_2O), like ethanol, is a weak anesthetic that fluidizes membranes. Unlike ethanol, N_2O is not metabolized. Thereby, N_2O provides a purer paradigm for chronic exposure to membrane fluidizing agents. Rats were exposed to nitrous oxide (0.5 atm) or a Lieber-DeCarli ethanol diet (36% of calories) for 35 days. Hepatic mitochondrial membranes were isolated from the treated rats and littermate controls. The membranes were labeled with the EPR spin-label 5-doxylstearate (5-DS) and titrated with ethanol at 37°C. In the mitochondrial membranes obtained from both treatment paradigms 5-DS was more ordered and more resistant to the disordering effects of ethanol as compared to controls. *In vitro* administration of N_2O elicited a similar response. Thus, membrane tolerance is a common response to chronic exposure to (at least two) anesthetic agents. USPHS AA00163, AA07186, AA07215.

Tu-Pos428

REVERSIBLE PENETRATION OF GLUTATHIONE-S-TRANSFERASE INTO THE CELL PLASMA MEMBRANE REVEALED BY SITE DIRECTED PHOTOSENSITIZED LABELING. (N.Merezhinskaya, G.Kuijpers, H.Pollard, Y.Raviv)NIDDK,NIH,Bethesda MD.20892

The fluorescent lipid analogue 3,3'-Dioctadecyloxacarbocyanine (DiO) incorporated into biological membranes was used to induce photosensitized activation of the hydrophobic probe ^{125}Iodonaphthyl-azide (^{125}INA) in the membrane and thus selectively confine radiolabeling of proteins to the lipid bilayer. In order to distinguish quantitatively between integral and non-integral membrane proteins the ^{125}INA/protein molar ratio was measured on four integral membrane proteins and the values were compared to those obtained for four soluble proteins which interact with the membrane peripherally. The ^{125}INA/Pr values obtained for the integral proteins were 2-3 logs higher than the other class of proteins. This quantitative measure was used to identify in situ cytosolic proteins which penetrate into the membrane bilayer. When this approach was applied to bovine chromaffin cells,one labeled protein of 28KD was discovered in the cytosol which displayed an INA/protein value characteristic of integral membrane proteins. Purification and partial microsequencing of this protein revealed a high homology with the Rat alpha family GST.

SPECTROSCOPY - RAMAN

Tu-Pos429

Water in the Heme pocket: its effect on the Fe-His stretch in the resonance Raman spectra of Deoxymyoglobin.

J.F. Christian[1], M. Unno[1], J.T. Sage[1], S.G. Sligar[2], E. Chien[2], and P.M. Champion[1]
[1]Physics Department, Northeastern University, Boston, MA 02115; [2]Departments of Biochemistry and Chemistry, University of Illinois, Urbana, IL 61801.

The distal histidine(His-64) of deoxymyoglobin(Mb), which is located in the heme pocket, binds water in an aqueous solvent. Mutating His-64 to leucine(Leu) makes the heme pocket hydrophobic, i.e., it dehydrates the heme pocket. We examine the effect of water in the heme pocket on the Fe-His(93) mode in the resonance Raman spectra by comparing the solvent-induced shift, water versus 75% glycerol, of native Mb with the solvent-induced shift of the mutant (His64Leu). As illustrated in the figure, the solvent induces a larger shift in the native Mb. This indicates that the dehydration of the heme pocket substantially contributes to the observed glycerol-induced shift in native Mb. We also characterize the low-frequency resonance Raman spectra of the met, CN^--bound, and CO-bound forms of the mutant. Water does not bind to the heme in the met form of the mutant, unlike the met form of native myoglobin. This produces profound differences in the low-frequency region of the spectrum.

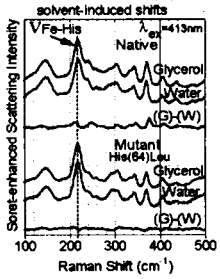

Tu-Pos430

CHARACTERIZATION OF PROTEIN-RETINOID INTERACTIONS BY VIBRATIONAL SPECTROSCOPY (L. SENAK, J.M. JU, D. MANOR, & R.H. CALLENDER)Department of Physics, The City College of the City University of New York, New York, N.Y. 10031

The nature of the binding interactions between retinal and many retinal binding proteins is not well understood. Two such proteins; cellular retinaldehyde binding protein (CRALBP) and cellular retinal binding protein (CRBP) have been isolated, complexed with 11-cis and all-trans retinal respectively, and probed using pre-resonance and difference Raman spectroscopy. To characterize the bonding between CRALBP and the carbonyl of 11-cis retinal, a difference experiment was performed using protein complexes with native 11-cis retinal and 11-cis retinal isotopically labeled with 13C at the 15 position. The difference spectrum has been compared to solution Raman spectra of 11-cis retinaldehyde, Schiff base, and protonated Schiff base in order to evaluate the retinoid CRALBP link. These spectra point to a Schiff base as the linkage between CRALBP an 11-cis retinal. The pre-resonance Raman spectrum of all-trans retinal complexed with CRBP has also been obtained, displaying a spectral shift in the position of the retinal carbonyl band that is typical of hydrogen bonding effects. This carbonyl red shift has been compared to hydrogen bonding interactions between the all-trans retinal carbonyl and a series of phenol derivatives, varying in proton donating ability by FT-IR spectroscopy, allowing quantitation of the hydrogen bond enthalpy. This technique quantitates the hydrogen bonding enthalpy between the carbonyl of the retinal and CRBP at 28.1 kJ/mol, which may be compared to a value of 22.4 kJ/mol for the same retinoid bound to retinol binding protein (RBP). Additionally the conformations of both 11-cis and all-trans retinoids complexed with CRALBP and CRBP are probed in these spectra.

Tu-Pos431

STRUCTURAL DIFFERENCES BETWEEN TWO MOLTEN GLOBULE FORMS OF α-LACTALBUMIN AS REVEALED BY VIBRATIONAL SPECTROSCOPY ((H.Zhong, R.Gilmanshin, R.Callender)) Department of Physics, City College of New York, New York, NY 10031

The molten globule state is considered to be an intermediate on protein folding pathway and the question arises whether the different forms of this state have similar structures. We compared two forms of molten globule state of α-lactalbumin by means of vibrational spectroscopy. The first one is the acid (A) form which is a well studied example of a molten globule state. The other form has one of the four disulfide bonds cleaved and Ca^{2+} ion removed (Apo-3SS). Not surprisingly, both forms show spectra very different from that of the native state. We found also differences between the two molten globules. The native form shows spectra in amide I' region with many sharp components, typical of the rigid compact proteins with various secondary structure elements. On the other hand, the A form has rather broad components which could hardly be resolved. The spectrum of the Apo-3SS form in neutral pH is rather similar to that of the A form but it differs by a sharp strong component at 1656 cm^{-1} which is usually attributed to the helical backbone conformation within the globular proteins. This is evidence that the Apo-3SS form comprises some relatively rigid subdomain formed by α-helices.

Tu-Pos432

DIFFERENCE RAMAN SPECTROSCOPY OF THE RECONSTITUTED RIBONUCLEASE S: EVIDENCE OF TWO DISTINCT AMIDE I COMPONENTS RESULTING FROM A SINGLE α-HELIX ((R.Gilmanshin, J.Van Beek, R.Callender)) Department of Physics, City College of New York, New York, NY 10031

Ribonuclease A can be reconstituted from its proteolitic fragments (RNAase S) - S-peptide (1-20 fragment of the RNAase) and S-protein. According to crystallographic analysis, residues from 3 to 13 of the S-peptide form an α-helix within the RNAase S complex. To decrease the influence of peptide's unordered part on our results, we also studied the complex with the pep01 analog which includes the first 15 residues of the S-peptide. Vibrational spectra of the both complexed peptides, obtained from Raman difference spectroscopy, include lines near 1644 and 1658 cm^{-1}. The 1658 cm^{-1} component is usually attributed to the helical part of globular proteins' structures while bands near 1640 cm^{-1} have been found previously for helix-forming polypeptides as well as for some destabilized helical proteins. Both isolated S-peptide and pep01 exhibit bands at 1642-1644 cm^{-1} whose intensities increase with increasing helicity. Another line in the dissolved peptides spectra (near 1672 cm^{-1}) is associated with the disordered moiety. No 1658 cm^{-1} component was found for the isolated peptides. Therefore, we assign both 1644 and 1658 cm^{-1} components of the complexed peptides spectra to the helical backbone pattern where the lower and higher frequency components are due to solvent exposed and screened hydrogen bonds, respectively.

Tu-Pos433

MOLECULAR MICROANALYSIS OF PATHOLOGICAL INCLUSIONS IN TISSUE BY LASER RAMAN MICROPROBE.

((J.A. Centeno,* F.G. Mullick, J.P. Pestaner)) Department of Environmental and Toxicologic Pathology, Armed Forces Institute of Pathology, Washington DC 20306

The identification of the chemical constituents and the evaluation of chemical structural changes of foreign inclusions in tissues may proceed in a variety of ways but generally can be classify into three methods: 1) histochemical/light microscopy methods, 2) ultrastructural methods (i.e., scanning electron microscopy, x-ray microanalysis) and 3) spectroscopic techniques. By employing histochemical and ultrastructural methods, it is frequently difficult to completely assess the identities of complex foreign materials in tissues, and only elemental composition can be obtained. Spectroscopic techniques including laser Raman microprobe (LRM), provide an accurate, fast and non-destructive identification by virtue of a molecule's characteristic spectrum of vibrational frequencies. Raman microprobe provides "fingerprint" information of organic species and allows for the *in situ* characterization of crystalline polymorphs of organic and inorganic inclusions that may be present in tissue sections. In this research, Raman microprobe has been used to obtain accurate identification of polymeric microparticles that were observed in tissues obtained form patients with known medical implants including metal fixation plates, Proplast-type implants, polymer-hip based implants and silicone-gel breast implants. In addition, the microspectroscopic identification of minerals and crystals from patients with crystal deposition diseases are discussed.

Tu-Pos434

SELFCONSISTENT DECOMPOSITION OF POLARIZED RAMAN AND FTIR SPECTRA OF MODEL PEPTIDES ((*Guido Sieler and Reinhard Schweitzer-Stenner*))
FB1 - Institut für Experimentelle Physik, Universität Bremen, 28359 Bremen, Germany

Monopeptides like N-Acetylglycine (AGL) and Glycyl-glycine are simple model systems for investigating the structural and physical properties of the peptide group. We have measured polarized Raman spectra of these substances with excitation wavelengths between 520 and 380 nm. From this we obtained the respective isotropic and anisotropic part of Raman scattering. In addition FTIR-spectra were recorded to assist the decomposition of the Raman spectra in the region between 1200 and 1800 cm^{-1} which are complicated due to the strong overlap between adjacent bands. Isotropic and anisotropic Raman spectra taken at different wavelengths and pH-values and FTIR spectra were consistently fitted in that the same band shapes, halfwidths and frequencies of corresponding bands were used for all data sets. The quality and the statistical significance of the fits were judged by their residuals and reduced χ^2-numbers. This strategy enabled us to obtain the reliable spectral parameters of even strongly overlapping bands. Thus we identified and assigned all Raman and IR-active bands in the spectral region above 1200 cm^{-1}, the major part or which result from $C_\alpha H_2$ wagging, twisting and bending modes. Moreover our results show that the amide I band of both substances are underlied by at least two subbands. In accordance with earlier results we interprete this as indicative of vibrational coupling with the sourrounding water molecules (1). From the depolarization ratios of the Raman bands we infer to which extent their Raman cross section is determined by the UV π->π^* transition of the peptide group. Generally our results demonstrate that non-resonant polarized Raman spectra can be exploited for a detailed vibrational analysis as well as for obtaining information about the type of the vibronic origin of the Raman cross section which normally requires experiments in the resonant (UV) region.

1. X.G. Chen, R. Schweitzer-Stenner, S. Krimm, N.G. Mirkin, S.A. Asher, JACS 116, 11141,1994.

SPECTROSCOPY - IR

Tu-Pos435

INFRARED VIBRATIONAL CIRCULAR DICHROISM OF CYCLOSPORIN *A* AND SEVERAL ANALOGS ((T.B. Freedman, S. Liu, F. Long E. Lee and L.A. Nafie)) Department of Chemistry, Syracuse University, Syracuse, NY 13244-4100 ((B.Z. Chowdry)) University of Greenwich, London, UK and ((H.H. Mantsch and A. Shaw)) Institute of Biodiagnostics, National Research Council, Winnipeg, Manitoba, Canada R3B 1Y6

Infrared vibrational circular dichroism (VCD) spectra have been measured in the OH, NH and C=O stretching regions for cyclosporin A (CsA) and three analogs, cyclosporin C, D and H (CsC, CsD, and CsH), in chloroform solution. CsA is a cyclic undecapeptide that functions as an immunosuppressive drug. Analogs C and D differ in the amino acid at residue 2 (Val and Thr, respectively) relative to that for CsA (Abu), whereas in analog H the absolute configuration of the amino acid at residue 11 is reversed from L-MeVal in CsA to D-MeVal. In the NH stretching region, intense negative VCD features are observed for CsA and CsD, indicative of strong hydrogen-bonded β-sheet and β-turn structures. Features in this region are weaker for CsH and CsC, indicative of altered intermolecular hydrogen-bonding interactions when the chiral center at residue 11 is inverted (CsH) or when an OH group is added at residue 2 (CsC). Similar spectral changes are seen in the C=O stretching region. *Ab initio* VCD calculations for fragments of these cyclosporin molecules have been carried out to strengthen the interpretation of the observed VCD spectra in terms of local conformational features.

Tu-Pos436

FT-IR STUDY OF TYROSINE PHOSPHORILATION. ((R.A.Gambetta*, M.Vivona, G.J.Nijmeijer, M.Schiatti, A.M.Villa, and S.M.Doglia)) Department of Physics, University of Milan, 20133 Milano (Italy), (*) Istituto Nazionale Tumori, 20133 Milano (Italy).

We have explored the possibility of monitoring tyrosine phosphorilation in solution and in intact living cells by FT-IR spectroscopy. The FT-IR spectra of tyrosine and phosphotyrosine, obtained in water solution by attenuated total reflection from 1700 to 800 cm^{-1}, display significant differences in the region of phosphates from 1150 to 950 cm^{-1} and in the region of tyrosine absorption from 1300 to 1200 cm^{-1}. These spectral differences have allowed us to monitor by FT-IR the dephosphorilation of phosphotyrosine at millimolar concentrations, catalysed in solution by alkaline phosphatases. Excellent agreement has been found between tyrosine and phosphotyrosine concentrations obtained by FT-IR and those evaluated by optical and fluorescence spectroscopy. Following these results, mouse NIH 3T3 fibroblasts, normal and expressing the highly phosphorilated product of the transfected *Erb*B2 human gene, have been studied under living conditions by attenuated total reflection. After subtraction of the water spectrum, high quality FT-IR spectra have been obtained for confluent cells with absorption intensities in the order of some milliabsorbances. Preliminary results indicate that the spectra of normal and transfected cells differ in the absorption region of phosphate stretching modes from 1150 to 1000 cm^{-1} as well as in the region of tyrosine ring deformations from 1300 to 1200 cm^{-1}.

Tu-Pos437

THE SELECTIVE ENHANCEMENT AND SUBSEQUENT SUBTRACTION OF ATMOSPHERIC WATER VAPOUR CONTRIBUTIONS FROM FTIR SPECTRA OF PROTEINS.((Stuart E. Reid and John E. Baenziger)) Department of Biochemistry, University of Ottawa, Ottawa, Ontario, Canada, K1H 8M5

The contributions from atmospheric water vapour distort resolution enhanced FTIR spectra of proteins and can interfere with the analysis of the secondary structure sensitive amide I band. We examine the effects of varying levels of water vapour on resolution enhanced FTIR spectra and present a simple, yet very sensitive method for detecting and subsequently subtracting extremely weak vapour contributions. Spectra are mildly deconvolved using both a narrow bandwidth parameter and little smoothing. Under these conditions, the intensities and shapes of the broad protein bands remain essentially unchanged, while the narrow water vapour contributions are enhanced in intensity by roughly 30 fold and distorted yielding, spectra dominated by very narrow vapour bands with a sinc function-like line shape indicative of over deconvolution. The characteristic shapes of the over deconvolved vapour bands are easily distinguished from both protein vibrations and the background noise, and can be subtracted from the spectra leading to an accurate determination of the correct subtraction coefficient. With the increased sensitivity of the method for detecting trace vapour contributions, it is shown that artifacts can be introduced into resolution enhanced FTIR spectra of proteins, even if the vapour contributions are too weak to be observed in the corresponding non-deconvolved absorbance spectra. The results demonstrate a clear requirement for the careful subtraction of vapour bands from all FTIR spectra before a detailed analysis of the amide I contour.

Tu-Pos438

TIME RESOLVED ANISOTROPY SPECTROSCOPY AND IMAGING THROUGH SCATTERING MEDIA USING MOST FAVORABLE FERMAT PHOTON PATHS. ((L. Yang, and J. M. Beechem)) Vanderbilt Univ., Dept. of Molecular Physiology & Biophysics, Nashville, TN 37232.

Time resolved optical tomography in the near infrared region has provided a new mechanism for clinical diagnosis of tissue structure and function. Light in the range 700 nm-900 nm can travel through human tissues without being absorbed but is strongly scattered. This scattered light can be described in part by diffusion processes. A portion of the scattered photons propagate through tissues along paths which are concentrated around the most favorable paths determined by the generalized Fermat principle.(Polishchuk & Alfano, Opt. Lett. **20**, 1937(1995)) Since these Fermat photons travel along well defined paths, they carry non-distorted imaging information concerning the location of structures within scattering media. The polarization and timing properties of Fermat photons differ from those of diffusive depolarized photons, and can be used to distinguish the two types. Time-resolved polarized single photon counting technique is utilized, with ~ 100 fsec excitation pulses at 780 nm using a Ti:Sapphire laser (Mira, Coherent Laser Group, CA). Detection utilizes a 6μm Hamamatsu R3890U microchannel plate photomultiplier yielding impulse response functions of < 35 psec FWHM. The time-resolved polarized technique allows one to separate the diffusion photons from Fermat photons and determine the intensity of Fermat photons with great accuracy. The result is a strong suppression of the diffusion background with the potential to image foreign objects embedded in tissue. (LY is supported by USPHS grant 5 T32 DK07563-07.)

Tu-Pos439

SPECIFIC RECOGNITION OF COILED COIL PROTEINS BY FTIR ANALYSIS. ((T. Heimburg*, J. Schünemann, K.Weber, and N.Geisler*)) Max-Planck-Institute for Biophysical Chemistry, 37077 Göttingen, Germany. (Spon. by J.Engel)

Intermediate filament (IF) proteins have a well defined three domain structure. The central domain forms a double stranded coiled coil (rod) with some 310 residues and represents the basic unit of the filament. The flanking terminal domains show a high cell type specific variablility both in sequence and in length.
Using Fourier transform infrared (FTIR) spectroscopy we analysed the spectra of the isolated domains and of the soluble tetramers and the filaments formed by type III IF-proteins. The amide I spectrum of the desmin rod is virtually identical to the spectra of other coiled coil proteins such as tropomyosin and the myosin rod. All these double stranded coiled coils reveal spectra distinctly different from classical α-helical spectra. The spectrum of coiled coils is a triplet of approximately equally strong bands. One band occurs at the normal α helix position, while the other two are found at lower wave numbers. The spectal shape can be rationalized using normal mode calculations (Reisdorf and Krimm, 1996). The unusually low wavenumbers of two of the bands require the assumption of very strong hydrogen bonding. Following a paper by Parrish and Blout (1972) we argue that bifurcated hydrogen bonds caused by simultaneous hydrogen bonding to an adjacent amino acid and to a solvent molecule account for this shift.
The aminoterminal head domain of desmin has a multicomponent spectrum with major fractions ß-sheet, ß-turns and random structure. The carboxyterminal domains of desmin and neurofilament proteins have very similar FTIR spectra and indicate mostly random structure. The spectrum of the protofilaments is very similar to the sum of the individual domain spectra. Polimerization of protofilaments into filaments induces only minor changes in the spectra.

Tu-Pos440

FTIR STUDIES ON THE SECONDARY STRUCTURAL CHANGES DURING THERMAL GELATION OF β-LACTOGLOBULIN ((J.J. Unruh, T.F. Kumosinski and Harold F. Farrell, Jr.)) ERRC, USDA, Philadelphia, PA 19118

High sensitivity Fourier Transform Infra-Red spectroscopy methodology has been developed to study the global secondary structural of globular proteins[1]. The methodology has been used to study the structural stability of β-lactoglobulin under thermal stress. The secondary structures of the A, B, and C genetic variants of *bovine* β-lactoglobulin were analyzed at pH 6.5 over the 25 to 75°C temperature range. Secondary structural changes were detected at 35-40°C and again at 60-70°C. These changes are in agreement with reported thermal calorimetry transitions. Global secondary structures were determined by nonlinear regression analysis of the amide I envelope (1700 - 1600 cm^{-1}). In general the amount of α-helix increased as temperature increased, at the expense sheet/extended and turn structure. How these reversible and nonreversable transitions relate to the gelation or aggregation of β-lactoglobulin will be discussed.

1. T.F. Kumosinski and J.J. Unruh. *Talanta*, accepted for publication 8/25/95.

Tu-Pos441

FAR-INFRARED SYNCHROTRON SPECTROSCOPY OF FUNCTIONALLY IMPORTANT LOW FREQUENCY MODES IN PROTEINS. ((A. Xie, Q. He, K. Hellingwerf, W.D. Hoff, E.M. Scheuring, B. Sclavi, M.R. Chance)). Dept. of Physiology and Biophysics, Albert Einstein College of Medicine, Bronx, NY 10461. Dept. of Microbiology, Univ. of Amsterdam, 1018 WS Amsterdam, The Netherlands.

Low frequency modes of proteins arise from (1) large effective masses, resulting from coupled motions of a large number of atoms, and (2) weak bonds, such as hydrogen bonds and salt bridges, which are important for the high-order structure of a protein. We study the structural origins, dynamic nature, and functional roles of low frequency modes of photoactive yellow protein, bacteriorhodopsin, and myoglobin, using far-infrared synchrotron spectroscopy (20 - 500 cm^{-1}), and model compound analysis with homologous amino acid polymers. All proteins examined exhibit broad band absorption with small ripples of narrow bands; while homologous polymers display a few well-defined bands above 60 cm^{-1}. One band around 110-150 cm^{-1} is found in poly-L-Ala, -Leu, and -Trp with dominant α-helical structures, and absent in poly-L-Gly, -Val, and -Phe lacking α-helical structures. Far-infrared difference spectroscopy is being applied to detect changes in collective modes of a protein from one state to another. Discussions will be presented concerning structural origins and biological importance of observed low frequency collective modes in proteins. This work was supported by grants from NIH RR01633, HL45989, and ONR N00014-95-I-0310.

Tu-Pos442

COMPARITIVE USE OF CALORIMETRY AND FTIR CH2-STRETCHING BAND ANALYSIS IN STUDYING CYTOCHROME B5 INTERACTIONS WITH LIPID. ((Robert W. Doebler, Harold M. Goldston, Jr., and Peter W. Holloway)) Dept. of Biochemistry, Univ. of Virginia Sch. Med., Charlottesville, VA. (Spon. by R. Taylor)

The infrared frequency shifts of the CH_2-stretching bands are commonly used to follow the gel to liquid-crystalline phase transition of phospholipid bilayers. The observed sensitivity of these vibrations in the region of the main phase transition has yielded a qualitative association with the enthalpic changes due to acyl chain melting as seen with differential scanning calorimetry (DSC). Although each technique appears to map the same general phenomenon, the precise interpretation of the FTIR CH_2-stretch information remains unclear. This study compares DSC and FTIR results from identical lipid systems. Previous calorimetric studies have shown that cytochrome b, bound to DMPC vesicles broadens the transition and prevents 14+1 lipids from undergoing the cooperative phase transition. In a similar analysis using FTIR, the first derivative of the CH_2-stretching profile yields a melting profile very similar to the heat capacity profiles produced by calorimetry, in which the melting curve broadens and the area beneath the curve decreases as protein concentration increases. In a contrasting example using a well-mixed binary lipid system of DMPG/DMPC (1:1), two melting peaks appear 2°C apart in the differentiated DMPG CH_2-profile, whereas only one peak is resolved using high-sensitivity calorimetry; the split peak resolved using FTIR is thought to be due to the known 1:1 racemic mixture of DMPG molecules. In another lipid mixture of POPE/POPS (1:1), the FTIR analysis clearly resolves a sharp peak at 25°C, indicative of highly cooperative melting of the POPE component, and a broader POPS melting profile at 17°C. Although differently shaped, the areas beneath the curves from FTIR analysis are equal in area, corresponding to equal molar lipid concentrations, whereas the areas beneath the DSC profiles are different due to varying enthalpic energies necessary for melting each lipid component.

Tu-Pos443

TWO DIMENSIONAL INFRARED CORRELATION SPECTROSCOPY OF THE MATURATION OF POORLY CRYSTALLINE HYDROXYAPATITE AT CONSTANT AND VARIABLE pH. ((Arne Gericke[1], Sergio J. Gadaleta[1], Joseph W. Brauner[1], Adele L. Boskey[2], and Richard Mendelsohn[1])) [1]Department of Chemistry, Rutgers University, Newark, N.J. 07102 and the [2]Hospital for Special Surgery, New York, N.Y. 10021

Recent publications from our laboratories report the FT-IR analysis of the ν_1, ν_3 phosphate region (900-1200 cm^{-1}) of poorly crystalline hydroxyapatite, the principle mineral phase in physiologically calcified tissue. The technique has been used to monitor the changes related to the maturation of poorly crystalline HA in both synthetic and biologic systems. One of the difficulties associated with analyzing spectra of poorly crystalline HA is that they are composed of several intrinsically overlapped bands which result in broad relatively featureless contours. To circumvent this problem a variety of techniques such as Fourier self-deconvolution, second derivative spectroscopy, and curve fitting have been used to elucidate the number and position of the underlying bands. However, each of the aforementioned techniques requires some degree of subjectivity in their respective applications. Recently, a generalized two-dimensional infrared (2D-IR) correlation method has been developed. This technique is capable of resolving the intrinsically overlapped bands in broad contours. The current work describes the use of 2D-IR for analysis of the ν_1, ν_3 phosphate region of maturing, poorly crystalline HA synthesized at constant and variable pH. Positions of the underlying bands elucidated by 2D-IR are compared with those from second derivative spectroscopy and Fourier self-deconvolution.

Tu-Pos444

CALCULATION OF VIBRATIONAL SPECTRA OF AMPHOTERIC SURFACTANTS. ((D. Grandbois, M. Trudel, and C. Chapados)) Département de chimie-biologie, Université du Québec à Trois-Rivières, Trois-Rivières, QC Canada G9A 5H7

Some amphoteric surfactants containing amino and carboxylic groups are of biological interests. While molecular spectroscopies are used more and more often to study the systems containing surfactants, the assignment of the bands used to probe the surfactant molecules is not completely done. To remedy the situation we have used a modified version of the computer program of Gribov and Dement'ev to calculate the ir and Raman spectra. The modified version that operates on an IBM RS6000 platform uses FORTRAN 90 as the programming language and is not limited by the number of atoms but only by the available memory of the computer. The molecular parameters of the molecule of interest which are obtained by Chem-X (Chemical Design, Inc.) are transported to the computer program where the position of the bands is calculated by the normal coordinate routines and the intensities by the electrooptical parameter routines. We have calculated the spectra of amines, carboxylic acids, and surfactants containing between 6 and 14 carbons. The comparison between experimental and calculated spectra is good. We will present the strategy used as well as the spectra obtained.

NUCLEIC ACID-PROTEIN COMPLEXES

Tu-Pos445

STRUCTURAL STUDIES OF A COMPLEX FORMED BY THE ROM PROTEIN AND A PAIR OF COMPLEMENTARY RNA STEM-LOOPS. ((A.J. Lee and D.M. Crothers)) Department of Chemistry, Yale University, New Haven, CT 06511. (Spon. by G. Brudvig)

Regulation of the replication for the Escherichia coli plasmid *ColE1* involves a plasmid encoded Rom protein and two RNA transcripts RNA I and RNA II, which function as antisense regulators of plasmid replication. Rom specifically recognizes an RNA loop-loop complex over standard A-form RNA and binds a bent helical RNA structure created by the interaction of the two stem-loops. Thus it negatively regulates the plasmid replication during the early stages of RNA I and RNA II interaction. Multidimensional heteronuclear magnetic resonance spectroscopy (NMR) was used for the initial analysis of the Rom-RNA complexes. The NMR data and the native gel electrophoretic analysis indicate that the RNA complex converts into duplex upon addition of the Rom protein.

Tu-Pos446

BINDING SITE IDENTIFICATION OF EUKARYOTIC PROTEIN SYNTHESIS INITIATION FACTOR EIF-4E USING A PHOTOAFFINITY ANALOG. ((D.E. Friedland[‡], C.H. Hagedorn[*], B.E. Haley[§] and D.J. Goss[‡])), [*]Dept. Of Medicine and Winship Cancer Center, Emory Univ. School of Medicine, Atlanta, GA 30322; [§]Dept. Of Medicinal Chem. And Pharmaceutics and the Markey Cancer Center, University of Kentucky Medical Center 40536; [‡]Chem. Dept., Hunter College , CUNY, NY, NY 10021.

Binding of eukaryotic initiation factors (eIF's) to the m^7(5')Gppp(5')N (where N indicates any nucleotide) cap structure at the 5' terminus of cellular mRNA represents the first committed step in the initiation phase of protein synthesis. Understanding the molecular basis for this recognition requires determination of the amino acids involved in the binding of the m^7G cap to eIF's. In order to investigate this, photoaffinity labeling with a cap analog [γ^{32}P]8N$_3$GTP was used in binding site studies of recombinant human cap binding protein ,eIF-4E. Competitive inhibition of this analog by m^7GTP and capped mRNA indicated probe specificity for interaction at the protein binding site. Aluminum (III)-chelate chromatography and reverse phase HPLC were used to isolate the photolabeled binding site peptide resulting from digestion of protein with modified trypsin. Subsequent amino acid sequencing results identified the amino acid sequence of the binding site peptide. In addition, sequencing results coupled with the inability to achieve trypsin digestion at a specific lysine indicate the individual residue which may be modified by [γ^{32}P]8N$_3$GTP.

Tu-Pos447

FLUORESCENCE AND CIRCULAR DICHROISM SPECTROSCOPIC CHARACTERIZATION OF WHEAT GERM PROTEIN SYNTHESIS INITIATION FACTOR EIF-4F AND ITS SUBUNIT P26 BINDING TO mRNA CAP ANALOGS. ((Y. Wang, T. Xiang, A. van Heerden[#], K.S. Browning[#], and D.J. Goss)) Dept. of Chem., Hunter College of CUNY, 695 Park Ave., NY, NY 10021; [#]Dept. of Chem., Univ. of Texas at Austin, Austin, TX 78712.

Recently the purified subunit p26, 26 kDa of wheat germ protein synthesis initiation factor eIF-4F has been obtained from *E. coli* expression of the cloned DNA. CD spectroscopy revealed 15% α-helix and 36% β sheet in p26 and 38% α-helix and 17% β sheet in eIF-4F. The binding of the 5'-terminal cap analog m^7GTP to p26 as a function of pH, temperature and ionic strength is described. The optimum binding pH was 8.0, ΔH and ΔS were 10.23 kcal/mol and 57.33 cal/mol°C, respectively. The environment of tryptophan residues in p26 and eIF-4F were monitored by using various quenchers. The results indicated the presence of negatively charged residues near the tryptophans which were surrounded by a hydrophobic environment in p26 and eIF-4F. The stopped-flow kinetics demonstrated the interaction of eIF-4F with m^7G cap followed a two-step mechanism. The rate constant and the activation energy for the second step were 121.7 s^{-1} and 4.55 kcal/mol, respectively.

Tu-Pos448

SPECTROSCOPIC STUDIES OF THE BINDING OF THE p28 AND P86 SUBUNITS OF WHEAT GERM INITIATION FACTOR, eIF-(iso)4F, TO eIF-4B AND TO mRNA. ((M.L. Balasta, M. Huang, Y. Wang, A. van Heerden[#], K.S. Browning[#] and D.J. Goss)) Chem. Dept., Hunter College (CUNY) New York, NY 10021; [#]Chem. Dept., Univ. of Texas at Austin, Austin, TX 78712.

Wheat germ protein synthesis initiation factor, eIF-(iso)4F, is a 110-kDa protein that is known to bind to mRNA and has exhibited ATP-dependent binding to oligoribonucleotides in the presence of eIF-4B and -4A. The p28 subunit of eIF-(iso)4F has been found to recognize and bind to the m^7G cap structure of mRNA, while the p86 subunit is believed to interact with other initiation factors and also with the mRNA. Direct fluorescence titration methods and circular dichroism spectroscopy was used to characterize the binding of the p28 and p86 subunits to eIF-4B, -4A and oligoribonucleotides. The oligoribonucleotide binding and CD spectra of several mutants of the p86 subunit were studied in order to further determine the role of the p86 subunit in protein-protein and protein-RNA interactions. Differences in alpha helical content have been observed among the mutants (by themselves or complexed with eIF-4B) and compared with p86. Equilibrium binding constants for the binary and ternary interactions involving p28, p86, eIF-4B and RNA indicate that initial binding of p86 or a p28:p86 complex with RNA enhances subsequent binding of eIF-4B to form the ternary complexes.